Università di Napoli Federico II

Dipartimento di Ingegneria Industriale

Ph.D Thesis

OPERATION OPTIMIZATION AND DYNAMIC SIMULATION OF COGENERATION SYSTEMS WITH THERMAL ENERGY STORAGE BASED ON AN INNOVATIVE OPERATION STRATEGY FOR RESIDENTIAL APPLICATIONS

Martina Caliano

Tutors

Prof. Nicola Bianco

Dr. Giorgio Graditi - ENEA

April 2017

Università di Napoli Federico II

Research Doctorate Program in Industrial Engineering

XXIX Cycle

Ph.D Thesis

OPERATION OPTIMIZATION AND DYNAMIC SIMULATION OF COGENERATION SYSTEMS WITH THERMAL ENERGY STORAGE BASED ON AN INNOVATIVE OPERATION STRATEGY FOR RESIDENTIAL APPLICATIONS

Doctorate Program Coordinator

Prof. Michele Grassi

Tutors

Prof. Nicola Bianco

Dr. Giorgio Graditi – ENEA

Candidate

Martina Caliano

To the memory of my grandmother, Maria,
a role model of strength
and determination.

To my parents, Antonio and Carmela,
for their unconditional love,
and for always being there for me.

To Francesco,
who more than anyone else
supported me in this path.

Contents

Acknowledgements

I am most grateful to the institutions where my educational pathway took place, the *Dipartimento di Ingegneria Industriale* (*DII*) of the *Università degli Studi di Napoli Federico II*, and the *ENEA Research Center of Portici*.

Special thanks to my tutors, *Prof. Nicola Bianco* (DII of the Università degli Studi di Napoli Federico II) and *Dr. Giorgio Graditi* (ENEA RC Portici), who gave me the opportunity to develop my doctorate project in these three years.

Finally, I am most grateful to *Dr. Luigi Mongibello* of the ENEA RC Portici, for his precious contribution on my research activity carried out during the doctorate program.

List of Figures

List of Tables

Preface

The ever increasing energy consumption of buildings, and of harmful CO_2 emission, which causes global warming, necessitate the urgent need of energy conservation. Moreover, because of relatively low combustion efficiency and no abatement measures, emission factors of various pollutants, especially the incomplete combustion products, from buildings are much higher than those in other sectors. For these reasons, energy efficiency in buildings is today a prime objective for energy policy at regional, national and international levels.

Polygeneration systems, by generating two or more energy products in a single integrated process, can offer potential benefits to humanity and environment, reducing greenhouse-gas emissions, increasing decentralization of energy supply at lower cost, improving energy security, and avoiding energy losses from electricity transmission and distribution networks. Therefore, in recent years such kind of systems has attracted much interest in building and residential sector applications.

However, to address sustainability issues properly, it is important to consider the complexity of polygeneration systems due to the interdependence between different energy products, different types of energy resources and energy conversion devices, as well as the inclusion of storage units. Therefore, polygeneration is mainly associated with generation optimization and related to decision making about production strategies of energy systems. The choice of the operational strategy to use has to be made taking into account the objectives to be achieved, the available devices, and the considered time-period, and often it can strongly depend on local energy policies in terms of costs of energy resources, and provided incentives.

This thesis presents a novel approach for improving, from the economical point of view, the operation of polygeneration systems, represented by residential natural gas fuelled Combined Heat and Power (CHP) systems. Optimization problems are formulated to find the optimized operation schedule of the CHP systems prime mover, aimed at the maximization of the economic savings obtained from the CHP systems with respect to the separate generation of electricity and heat. The

sustainability of such approach is evaluated by means of environmental impact assessments, and its effectiveness is demonstrated through a dynamic simulation.

Keywords: Cogeneration systems, Operation schedule optimization, Heat dumping, Economic and primary energy savings, Pollutant emission, Dynamic simulation.

Martina Caliano,
April 2017

Nomenclature

AC	annual cost (€)
AS	annual savings (€)
c	cost (€/m^3) – (€/kWh) in Eq. (2.1)
C	heat storage capacity (kWh)
CF	annual cash flow (€)
c_p	specific heat (J/kg/K)
E	energy (kWh)
E'	energy (kWh)
EH	equivalent hours (h)
EPR	electric power ratio
F	fuel energy (kWh) in Eq. (2.1)
FF	objective function
f	fraction of electric power
g	selling price (€/kWh) in Eq. (2.1)
i	summation index (yr) in Eq. (3.10)
I	investment cost (€)
*I**	investment cost net of the cost of the heat storage system(€)
l	correction factor for the calculation of the reference electric efficiency for separate generation
m	mass (kg)
NPV	net present value (€)
P	power (kW)
PES	primary energy saving (toe/yr)
r	discount rate
R	revenues (€)
SV	economic value of the electricity sent to the grid (€)
t	period (h) in Eq. (2.1)
T	temperature (°C)
TC	cost of the heat storage system (€)

TPR	thermal power ratio
TV	economic value of the electricity taken from the grid (€)
V	volume of hot water in the heat storage tank (m^3)
X	generic energy vector
Δ	difference operator
η	efficiency
μ	emission factor (g/kWh)
ρ	density (kg/m^3)

Subscripts

AB	auxiliary boiler
c	cold
CHP	combined heat and power
D	dumping
dumped	referred to the dumped thermal energy
el	electric
electricity	electricity
f	fuel
FL	full-load
h	hot
HTF	heat transfer fluid
HW	hot water
in	inlet
max	maximum
mean	average
min	minimum
NG	natural gas
out	outlet
p	generic pollutant
PL	partial-load
PM	prime mover
ref	reference

sc	self-consumed
sent	referred to the electricity sent to the grid
taken	referred to the electricity taken from the grid
TES	thermal energy storage
th	thermal
user	referred to the energy demand
w	water
WC	white certificates

Superscripts

*	non-dimensional
CHP	combined heat and power
E	energy
SG	separate generation
X	generic energy vector
PM	prime mover

Acronyms

AB	auxiliary boiler
AH	ambient heating
BAT	best available technology
CHP	combined heat and power
D	dumping
DHW	domestic hot water
ED	electricity driven
GHG	greenhouse gas
HD	heat driven
HTF	heat transfer fluid
HX	heat exchanger
ICE	internal combustion engine
MT	microturbine
NG	natural gas

NPV	net present value
PL	partial-load
PM	prime mover
SG	separate generation
TES	thermal energy storage
TOE	tons of equivalent oil

"We are the first generation to feel the impact of climate change and the last generation that can do something about it"

Chapter 1. Introduction

1.1. Motivation and Background

Environmental degradation due to greenhouse gas emissions is one of the major threats to the world today. Since Kyoto Protocol, central and local governments have paid great attention to the issue of greenhouse gas emissions, which are mainly caused by fossil energy consumption, and the Conference of the Parties on climate changes (COP 21) has further emphasized the need for urgency in addressing climate change. Pollutants emission from combustion devices and power plants are considered to be the most responsible causes of the global warming. According to the IEA's report "CO_2 Emissions from Fuel Combustion Highlights 2016" [1], in 2014 global CO_2 emissions reached 32.4 $GtCO_2$, having an increase of 0.8% over 2013 levels. Climate scientists have observed that the atmospheric concentration of carbon dioxide (CO_2) have been increasing significantly over the past century, compared to the pre-industrial era level of about 280 parts per million (ppm). In 2015, the average concentration of CO_2 (399 ppm) was about 40% higher than in the mid-1800s, with an average growth of 2 ppm/year in the last ten years. Significant increases have also occurred in the levels of methane (CH_4) and nitrous oxide (N_2O) [1]. The Fifth Assessment Report from the Intergovernmental Panel on Climate Change [2] states that human influence on the climate system is clear. Among the many human activities that produce greenhouse gases, the use of energy represents by far the largest source of emissions, estimated to be roughly two-thirds of all anthropogenic greenhouse-gas emissions, as shown in Figure 1.1.

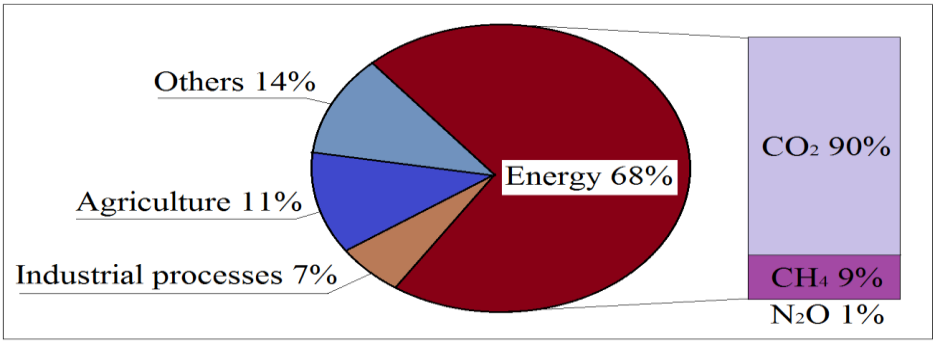

Figure 1.1. Estimated shares of global anthropogenic GHG [1].

Increasing production of greenhouse-gas emission is especially due to increasing demand for energy, which comes from worldwide economic growth and development. Global total primary energy supply increased by almost 150% between 1971 and 2014, still mainly relying on fossil fuels [2]. Figure 1.2 shows the world primary energy supply divided into fossil fuel and non fossil fuel energy supply, in 1971 and 2014.

Figure 1.3 shows the primary energy demand predicted in 2035 by the IEA's World Energy Outlook 2013 [3] and the share of global energy demand growth in the period 2011-2035. This scenario forecasts that the global energy demand will grow significantly to 2035, especially in emerging economies, that will account for more than 90% of global net energy demand growth.

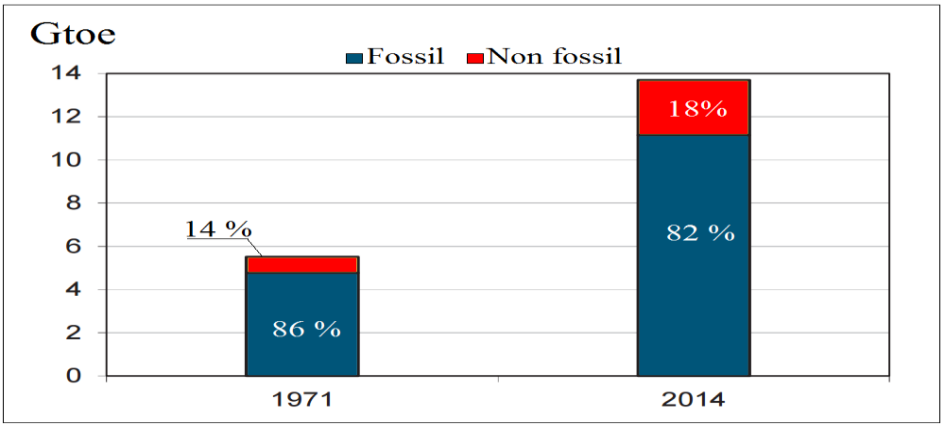

Figure 1.2. World primary energy supply [1].

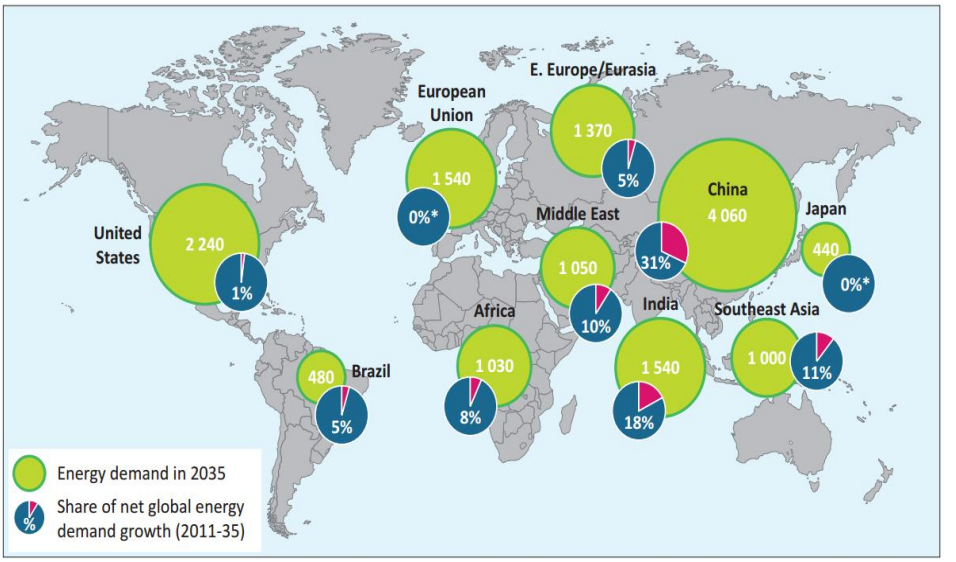

Figure 1.3. Primary energy demand predicted in selected regions in 2035 and the share of global growth in the New Policies Scenario in the period 2011-2035 (Mtoe) [3].

The ever increasing demand of energy, and harmful CO_2 emission, which causes global warming, necessitate the urgent need of energy conservation [4]. One of the most energy-consuming sector is the building one. Particularly, the energy consumption of residential and commercial buildings in developed countries are continuously increasing more rapidly. Moreover, growth in population, increasing demand for building services and comfort levels, assure the upward trend in energy demand will continue in the future [5]. The climate and health impacts of greenhouse gases are most affected by consumption in the building sector that contributes significantly, not only to ambient and household air pollution, but also to temporal trends in energy use. Because of relatively low combustion efficiency and no abatement measures, emission factors of various pollutants, especially the incomplete combustion products, from buildings are much higher than those in other sectors [6]. For these reasons, energy efficiency in buildings is today a prime objective for energy policy at regional, national and international levels, and advanced technologies to mitigate global warming and increase the efficiency of energy systems are being proposed and tested in many countries [7].

Among these technologies, polygeneration systems offer potential benefits to humanity and environment, reducing greenhouse-gas emissions, increasing decentralization of energy supply at lower cost, improving energy security, and avoiding energy losses from electricity transmission and distribution networks [8]. Polygeneration is the simultaneous generation of two or more energy products in a single integrated process [9,10]. A possible pathways of polygeneration systems is shown in Figure 1.4. By providing additional options for energy outputs, polygeneration can provide increased opportunities to minimize primary energy consumption, maximize exergy efficiency, and reduce greenhouse gas emissions [11-18]. The utilization of polygeneration technology can achieve significant energy savings in the case when both power and heat are used. Therefore, the overall efficiency of power plants is determined mainly by the utilization of the thermal energy. Energy efficiency plays an essential role in supplying energy demands in a sustainable, reliable, and economic way, especially when fossil fuels are used. Different storage facilities can provide a buffer for temporal imbalance for different energy products. Thermal storage especially makes it possible to operate polygeneration plants at the most fuel-efficient load [19,20].

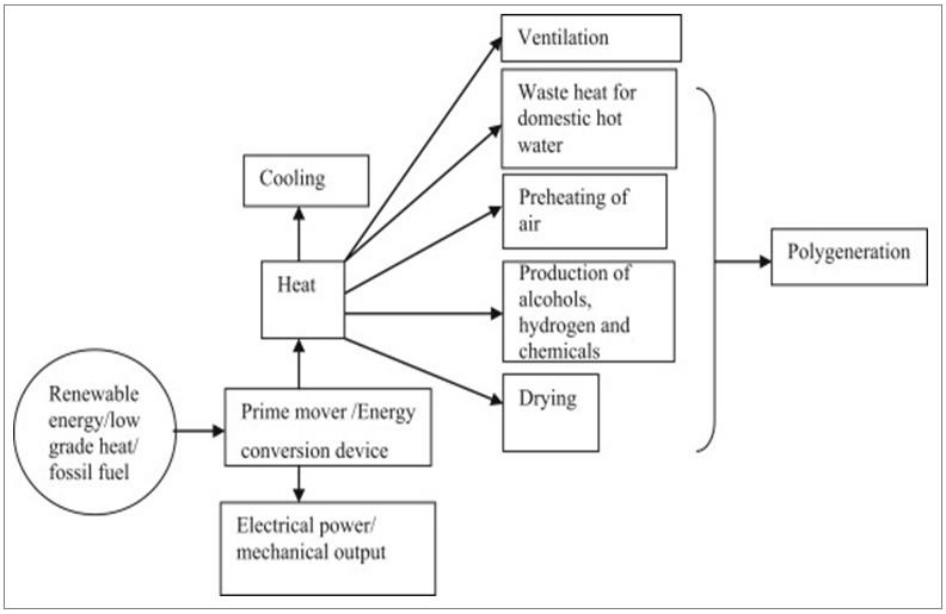

Figure 1.4. Possible pathways of polygeneration systems [9].

To address sustainability issues properly, it is important to consider that polygeneration systems are more complicated than power-only systems because of interdependence between different energy products. For this reason, polygeneration is mainly associated with generation optimization and related to decision making about production strategies of energy systems [21-29]. In such systems, production strategies should be centered around the impacts of energy production and energy consumption on the environment, and are designed and implemented through different levels of production planning over a time horizon (day, week, month, or year), including long-term strategic planning, medium-term tactical planning and short-term operational planning. In general, long-term planning determines capacity investments and types of production technologies to invest in, medium-term planning determines the allocation of fuel and emission allowance as well maintenance schedules of the system, and short-term planning (scheduling) is associated with unit commitment, economic dispatch of committed plants, and bidding strategies in the market.

1.2. Aims and originality

The aim of this thesis is to provide a novel approach for improving the operation of residential natural gas fuelled CHP systems from the economical point of view, based on the possibility to dump part of the cogenerators heat generation, while operating with a heat-driven full-load operation mode. This approach differs from the usual ones used in the cogenerative field as it allows the prime mover of the CHP systems to operate also when its thermal energy generation is higher than the sum of the user thermal demand and the thermal energy required to fill a thermal energy storage system, included to store the exceeding heat for a later use.

In order to evaluate the effectiveness of such operation strategy, its effects on the operation of CHP systems are evaluated by comparing them to the ones obtained when the CHP systems operate following two typical operation strategies for cogenerator, or rather a heat-driven full-load operation strategy without heat dumping, and a partial-load one.

The CHP systems under consideration are composed of a prime mover, generating electricity and heat, a thermal energy storage system, and an auxiliary

boiler, providing for electricity and heat to a multi-apartment housing situated in Italy.

Firstly, the effects of the heat dumping are evaluated on the operation of four residential micro-CHP systems, differing from one another on the prime mover technology, and are compared to the ones obtained considering the CHP systems operating according to the typical heat-driven full-load operation strategy without heat dumping. For both operation strategies, an optimization problem is formulated to find the optimized operation schedule of the CHP systems prime mover that maximize the revenues for the CHP systems with respect to the separate generation of electricity and heat, by taking into account of the natural gas and electricity tariffs, and the Italian incentives for high efficiency cogeneration.

In order to evaluate the effects of the variation of the thermal energy storage system maximum capacity, and of the auxiliary boiler efficiency on the optimized results, six sizes of the storage, and two values for the boiler efficiency are considered, respectively.

To evaluate the environmental impact of the two operation strategies, a model is proposed for evaluating the annual global emissions of CO_2 and the annual local emissions of NO_X and CO of the CHP systems by means of emission factors, and the pollutants emission obtained in each case are compared to the ones of the separate generation of electricity and heat.

To demonstrate the practical feasibility of the novel operation strategy, the dynamic simulation of the CHP system operating according to the heat dumping and no-dumping full-load operation strategies is conducted by means of the commercial software TRNSYS 17. For the purpose, the simulation of two optimized cases, one for each operation strategy, that present nearly the same operation hours and economic savings are carried out, and the choice of the two configurations is made considering a compromise between the economic savings and the size of the tank.

To generalize the effectiveness of the novel operation strategy for heat-driven residential natural gas-fired CHP systems, the effects on the operation of a CHP system of the novel operation strategy with heat dumping are compared with the ones relative to the case in which the CHP system operates following the heat-

driven strategy allowing load partialization. To optimize the operation schedule of the prime mover, for both cases, an optimization problem is formulated aimed at the maximization of the economic savings that can be obtain with respect to a separate generation system of electricity and heat, and the evaluation of the annual global emissions of CO_2 and the annual local emissions of NO_X and CO of the CHP systems operating according to the two operation strategies are compared to each other and to the ones of the separate generation. Also in this case, the variation of the storage system maximum capacity is considered.

The three operation strategies analyzed are implemented in a home-made numerical code, written in Matlab environment, and the heuristic algorithm patternsearch is used to perform the economic optimization of the systems.

Lastly, being the market price of a CHP system strongly dependent on the prime mover technology and size, and lacking in Italy, at the moment, a well-established market for residential CHP systems, an economic analysis is carried out to evaluate, for each analyzed case, the feasible investment cost for the purchase and the maintenance of the CHP system. The economic analysis results, combined with the environmental and the energetic ones, allow to assess which of the operation strategies considered provides the best compromise in terms of higher economic savings, reduced environmental impact, and reduced dimensions of the storage tank.

1.3. Organization of the thesis

After the present Introduction (Chapter 1) and before the Conclusions (Chapter 6), the thesis is articulated in the following chapters:

- In Chapter 2, a comprehensive review on performance improvement and optimization of polygeneration systems is presented, focusing the attention on the use of polygeneration systems in the residential sector.
- In Chapter 3, a novel approach for improving the operation of residential micro-CHP systems from the economical point of view is proposed, and compared to a typical heat-driven full-load operation strategy without heat dumping.

- In Chapter 4, the dynamic simulation of a residential micro-CHP system operating according to the operation strategies presented in Chapter 3 is performed to demonstrate the effectiveness of the heat dumping.
- In Chapter 5, the novel operation strategy with heat dumping is compared to a typical heat-driven operation strategy allowing load partialization, with the aim to generalize the effectiveness of the novel operation strategy for heat-driven residential natural gas-fired CHP systems.

References

[1] IEA, CO2 Emissions from Fuel Combustion Highlights, October 2016. Available: https://www.iea.org/publications/freepublications/publication/CO2EmissionsfromFuelCombustion_Highlights_2016.pdf

[2] IPCC, Climate Change 2013, The Physical Science Basis. Available: http://www.climatechange2013.org/images/report/WG1AR5_ALL_FINAL.pdf

[3] IEA, World Energy Outlook 2013, November 2013. Available: http://www.iea.org/publications/freepublications/publication/WEO2013.pdf

[4] S. D. Rezaei, S. Shannigrahi, S. Ramakrishna. A review of conventional, advanced, and smart glazing technologies and materials for improving indoor environment. Solar Energy Materials and Solar Cells. Volume 159 (2017), pp. 26–51.

[5] L. Pérez-Lombard, J. Ortiz, C. Pout. A review on buildings energy consumption information. Energy and Buildings. Volume 40 (2008), pp. 394−398.

[6] R. Kannan, N. Strachan. Modelling the UK residential energy sector under long-term decarbonisation scenarios: comparison between energy systems and sectoral modelling approaches. Applied Energy, 86 (2009), pp. 416–428.

[7] Q. Wang, B. Su, J. Sun, P. Zhou, D. Zhou. Measurement and decomposition of energy-saving and emissions reduction performance in Chinese cities. Applied Energy 151 (2015) 85–92.

[8] AD. Hawkes, MA. Leach. Cost-effective operating strategy for residential micro-combined heat and power. Energy. Volume 32 (2007), pp. 711-723.

[9] S. Murugan, B. Horák. A review of micro combined heat and power systems for residential applications. Renewable and Sustainable Energy Reviews. Volume 64, (2016), pp. 144–162.

[10] L.M. Serra, M.A. Lozano, J. Ramos, A.V. Ensinas, S.A. Nebra. Polygeneration and efficient use of natural resources. Energy. Volume 34 (2009), pp. 575-586.

[11] P. Mancarella. MES (multi-energy systems): an overview of concepts and evaluation models. Energy. Volume 65 (2013), pp. 1-17.

[12] P. Ahmadi, I. Dincer, M.A. Rosen. Thermoeconomic multi-objective optimization of a novel biomass-based integrated energy system. Energy. Volume 68 (2014), pp. 985-970.

[13] P. Ahmadi, I. Dincer, M.A. Rosen. Thermoeconomic multi-objective evolutionary-based optimization of a new multigeneration energy system. Energy Conversion Management. Volume 76 (2013), pp. 282-300.

[14] P. Ahmadi, M.A. Rosen, I. Dincer. Multi-objective exergy-based optimization of a polygeneration energy system using evolutionary algorithm. Energy. Volume 46 (2012), pp. 21-31.

[15] M. Ozturk, I. Dincer. Thermodynamic analysus of a solar-based multi-generation system with hydrogen production. Applied Thermal Engineering. Applied Thermal Engineering. Volume 51 (2013), pp. 1235-1244.

[16] M. Ozturk, I. Dincer. Thermodynamic assessment of an integrated sola power tower and coal gasification system for multi-generation purposes. Energy Conversion Management. Volume 76 (2013), pp. 1061-1072.

[17] C. Rubio-Maya, J. Uche, A. Martinez. Sequential optimization of a polygeneration plant. Energy Conversion Management. Volume 52 (2011), pp. 2861-2869.

[18] D. Djuric Ilic, E. Dotzauer, L. Trygg. District heating and ethanol production through polygeneration in Stockholm. Applied Energy. Volume 91 (2012), pp. 214-221.

[19] R. Rong, Lahdelma, P.B. Luh. Lagrangian relaxation based algorithm for trigeneration planning with storages. European Journal of Operational Research. Volume 188 (2008), pp. 240−257.

[20] M.L. Ferrari, M. Pascenti, A. Sorce, A. Traverso, A.F. Massardo. Real-time tool for management of smart polygeneration grids including thermal storage. Applied Energy. Volume 130 (2014), pp. 670−678.

[21] E. Cadorna, A. Piacentino. A methodology for sizing a trigeneration plant in mediterranean areas. Applied Thermal Engineering. Volume 23 (2003), pp.1665–80.

[22] P.J. Mago, N. Fumo, L.M. Chamra. Performance analysis of CCHP and CHP systems operating following the thermal and electric load. International Journal of Energy Research. Volume 33 (2009), pp. 852–864.

[23] E. Cardona, A. Piacentino, F. Cardona. Matching economical, energetic and environmental benefits: an analysis for hybrid CHCP-heat pump systems. Energy Conversion and Management. Volume 47 (2006), pp. 3530–3542.

[24] G. Chicco, P. Mancarella. From cogeneration to trigeneration: profitable alternatives in a competitive market. Energy Conversion, IEEE Trans, 21 (2006), pp. 265–272.

[25] N. Fumo, P.J. Mago, A.D. Smith. Analysis of combined cooling, heating, and power systems operating following the electric load and following the thermal load strategies with no electricity export. Journal of Power and Energy. Volume 225 (2011), pp. 1016–1025.

[26] A.K. Hueffed, P.J. Mago. Influence of prime mover size and operational strategy on the performance of combined cooling, heating, and power systems under different cost structures. Journal of Power and Energy. Volume 224 (2010), pp. 591–605.

[27] K.C. Kavvadias, A.P. Tosios, Z.B. Maroulis. Design of a combined heating, cooling and power system: Sizing, operation strategy selection and parametric analysis. Energy Conversion and Management. Volume 51 (2010), pp. 833–845.

[28] P.J. Mago, L.M. Chamra. Analysis and optimization of CCHP systems based on energy, economical, and environmental considerations. Energy and Buildings. Volume 41 (2009), pp. 1099–1106.

[29] J.J. Wang, Y.Y. Jing, C.-F. Zhang, Z.(John) Zhai. Performance comparison of combined cooling heating and power system in different operation modes. Applied Energy. Volume 88 (2011), pp. 4621–4631.

"Energy efficiency is the only energy resource possessed by all countries"

Chapter 2. Review on performance improvement and optimization of polygeneration systems

2.1. Introduction

Traditional power plants convert about 30% of the fuel's available energy into electric power [1]. The majority of the fuel energy content is lost at the generation facility through waste heat. Further energy losses occur in the transmission and distribution of electric power to individual users. Inefficiencies and environmental issue associated with conventional power plants provide the thrust for developments in "on-site" and "near-site" power generation. Polygeneration systems have the potential to increase resource energy efficiency, to reduce air pollutant emissions dramatically, and to reduce energy cost to consumers by the simultaneous generation of different energy products, at or close to the point of use [2-7]. Polygeneration can be seen as a generalization of Combined Heat and Power (CHP) generation, in which in addition to the simultaneous generation of electricity and useful heat, a few or more processes, such as generation of domestic hot water, cooling, etc, are carried out in a single plant [8-9].

Polygeneration systems usually involve a prime mover, such as Sterling engine, reciprocating engine, steam engine, gas turbine and micro-gas turbine, and organic Rankine cycle, and an energy conversion device. Moreover, renewable energy systems, such biomass, solar, wind and fuel cells can also be incorporated. A polygeneration system may not only consist of generation facilities, but also non-generation components. Generation facilities include polygeneration plants and

plants for separate provision of different energy products, such as traditional condensing power plants, heat plants (boilers), and cooling plants (chillers), whereas non-generation components include various bilateral contracts and demand side management components for different energy products, used in order to shift demands from peak hours to off-peak hours.

According to the EPA's Catalog of CHP technologies [1], and the IEA's information paper on Combined heat & power and emissions trading [10], CHP systems produce both electric and usable thermal energy on-site or near-site, converting 75-85% of the fuel source into useful energy. If more useful energy products can be derived from the excess heat (e.g., cooling energy), the overall energy efficiency of polygeneration can be improved further [11-12]. Figure 2.1 shows the efficiency advantage of CHP compared with conventional central station power generation and onsite boilers. When considering both thermal and electrical processes together, CHP typically requires only ¾ the primary energy separate heat and power systems require [1].

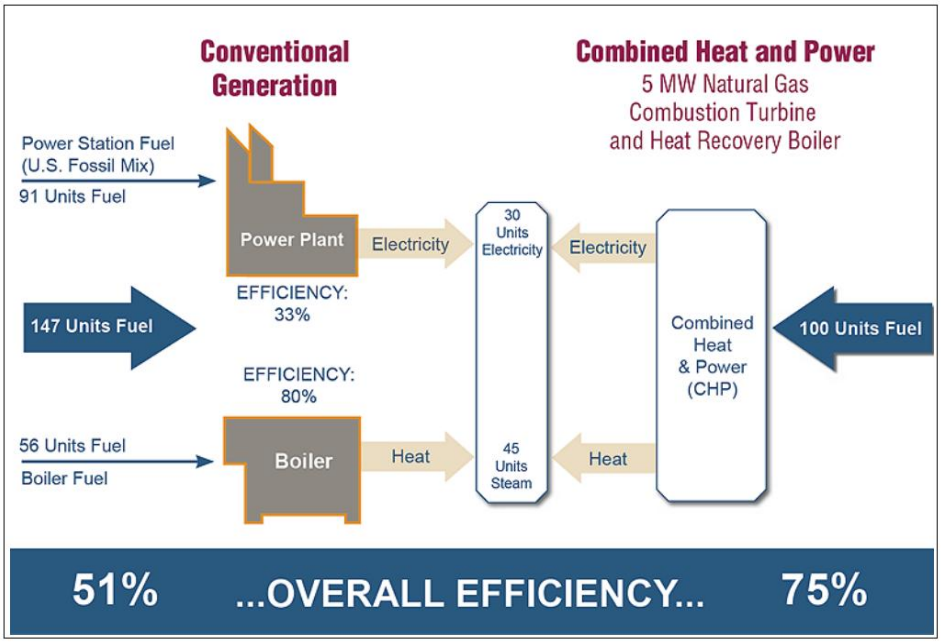

Figure 2.1. CHP versus conventional generation [1].

The application of polygeneration systems has also a great potential to reduce CO_2 emissions. IEA [13] estimates that in Europe, CHP system have been responsible for 15% of greenhouse gas emission reduction (57 Mt) between 1990 and 2005, and that by 2030, CHP systems have the potential to reduce CO_2 emissions arising from new generation to more than 10% (950 Mt/year). However, there are many barriers to the spread of these systems. One of which is the lack of a plan and evaluation method for the final decision-making about system selection, taking into account the optimal design and operation planning. Earlier on, building energy supply systems have been selected mainly on the cost-benefit analysis.

The economic benefit is an important factor to consider when deciding whether to install a polygeneration system or determining the system capacity and operational strategy. The factors that affect the economic benefits are various, e.g. equipment cost and efficiency, electricity and fuel cost, building electric and thermal loads, etc, and since these factors vary widely case by case, it is not straightforward to estimate economic savings for the system implementation. Additionally, the metric used to assess economic performance is different according to the different energy policy in different regions. The building thermal loads are significantly affected by local climate conditions, therefore, for the same system, the economic benefits could vary widely depending on the location where the system is installed [14-24]. The payback period of polygeneration systems can be evaluated in order to demonstrate the economic feasibility of such systems [22,25-28]. However, a simple payback period assessment, which includes operating costs and capital costs, may result in a longer payback period than a more conventional reference system, without taking into account the potential environmental and performance benefits of the system. In such context, it is clear that, in order to address sustainability issues properly, it is important to conduct comprehensive analyses, and that optimal design and operation of polygeneration systems are becoming important issues.

This chapter provides a comprehensive review on performance improvement and optimization of polygeneration systems. The performance improvement and performance evaluation of polygeneration systems are discussed in Section 2.2, whereas the optimization in such systems design and operation is presented in

Section 2.3. A literature review on the main current research on the polygeneration systems used in the residential sector is presented in Section 2.4. Lastly, the actual global status and the prospects of the spread of polygeneration systems are discussed in Section 2.5.

2.2. Performance improvement and performance evaluation of polygeneration systems

The energetic and exergetic performances of polygeneration systems are of interests of many researchers, for both theoretical and existing systems, as their evaluation allows for comparison with other methods for energy generation. Polygeneration systems performance evaluation is a necessary process to attain economically and environmentally feasible solutions in such systems design and operation. Without proper performance evaluations, in fact, improvement in the system design and operation cannot be quantified. Popular approaches for comprehensive analysis include combination of energy savings and/or energy efficiency, economic, emissions, and exergetic analyses [29-44].

Both first- and second-law thermodynamic analyses are fundamental tools to evaluate energy systems performance, so that several polygeneration system performance evaluations using the first and second law of thermodynamics have been presented in the literature.

Energy analysis is the most common method for evaluating the performance of polygeneration systems, either for primary energy usage, or energy efficiency, and can be used to compare different types of polygeneration systems, different operation strategies, or a polygeneration system against a reference system or other alternative energy system. Many authors have conducted studies on energy efficiency, stating that often energy efficiency benefits tend to translate to economic benefits, stressing the importance of the user demand on the system performances, and analyzing different configurations of the systems [45-48]. Others have conducted studies focused on energy savings by evaluating the potential of different technologies in terms of both energy performance and emissions reduction [49-61].

To provide a measure of not only the energy used by a polygeneration system, but also of the quality of energy provided and consumed, and of the amount of

availability destroyed within the system, exergy analysis can be conducted. Khaliq et al. [62] assert that exergy analysis is beneficial over energy analysis, allowing to determine the true magnitudes of losses and their causes and locations, and to improve the overall system and component performances. Many authors have calculate the exergy efficiency of a given or proposed system, also comparing it with energy efficiency and exergy efficiency of another polygeration system or an alternative system [54,62-64]. Others have found the relative contribution of individual components or subsystems to the overall exergy destruction [54,65,66].

Several case studies based on field tests have been conducted to evaluate polygeneration systems performance [67-69]. However, even if the systems performance can be accurately evaluated using actual measurements, on field tests have several limitations: costly data acquisition system need to be installed; year-round field measurements cannot be easily obtained; and each study is limited to a specific system. On the other hand, computer-based simulations can be used to predict system performance.

Many studies have been focused on polygeneration system performance evaluation using transient simulation models and different dynamic simulation tools [70-72], demonstrating that a validated transient simulation of polygeneration systems can provide accurate performance evaluation with relatively simple implementation, time-efficient yearly-simulation using statistical yearly weather data, and straightforward modifications for different sizes and type of polygeneration system components in different climate conditions.

2.3. Optimization of polygeneration systems

A polygeneration system is more complicated than a power-only system due to interdependence between different energy products, and because production scheduling need to be done in coordination through different production, storage and auxiliary facilities in the system. Moreover, there are different technical, legal (such as the capacity, efficiency and self-consumption percentage of polygeneration installations), and social considerations that need to be respected in practice. To promote polygeneration technology for building applications, the eligibility criteria for introducing technology needs to be modified or carefully designed because it is

not easy for a micro- and small-scale polygeneration plant to operate as efficiently as a large-scale plant. Furthermore, the system operates in a dynamic environment full of uncertainty.

For these reasons, optimization in polygeneration systems design and operational strategy is one of the key element to improve energy efficiency and to reduce overall cost and greenhouse gas emissions [73].

2.3.1. Optimization in polygeneration design

Design of polygeneration systems involves a selection process of the system components type and size, which have to take into consideration the efficiency of individual components, the system operating strategy, and the building energy demand, so that the system can balance cost savings, real energy savings based on primary consumption, and net emission of pollutants [14].

The prime movers or power generation units are the main components of polygeneration systems, therefore they have to be carefully selected to guarantee the desired performance of the system. Among them, reciprocating internal combustion engines, steam turbines and combustion turbines, micro-turbines, fuel cells, and Stirling engine, whose advantages and drawbacks related to the polygeneration systems designing are often discussed in literature [74-76].

Wu and Wang [74] state that the prime mover characteristics, such as its efficiency, capacity range, and power-to-heat ratio, are important factor to determine the optimal size and type of the prime mover for different applications. Once the type of a prime mover is selected, it is important to determine a rational capacity to maximize availability of the prime mover. For the purpose, it is necessary to take into account the systems' annual operation strategies, defined by considering the variation of electric and thermal energy demands, and the deviations of electricity and fuel price throughout the year [73]. This problem can be dealt by using an optimization programming technique.

Many authors have demonstrated that sizes of prime movers can be effectively determined using mixed-integer linear programming (MILP), such as [77], others have developed optimal sizing methods using mixed-integer non linear programming (MINLP) [78,79].

2.3.2. Optimal operating strategy of polygeneration systems

Polygeneration systems can be controlled by several possible operation strategies. The most common presented in literature are:

- electricity-driven (*ED*);

- heat-driven (*HD*);

- base load operation.

When a system operates under the *ED* strategy, the power generation units generate all the electricity following the electric demand, and the waste heat is used to satisfy the building's thermal load. If the recovered heat is not sufficient to satisfy the thermal load, auxiliary boilers can be used to integrate the system heat generation. When the recovered heat is higher than the building's heat demand, the excess can be stored or discarded.

When a system operates under the *HD* strategy, the system follows the building's thermal load, while the electricity generated by the power generation units is used to satisfy part or all the building's electric demand. In this case, if the electricity generation is lower than the electric requirements, additional electricity has to be purchase from the external grid. On the other hand, if the electricity produced is more than the amount needed by the building, the excess electricity can be stored or sold back to the grid, if it is possible.

When the system follows the *base load operation*, it covers only a constant amount of the electrical load: it is possible that part of the electricity has to be imported by the external grid to complete satisfy the electric demand, and auxiliary boilers are used if the recovered heat form the power generation units is not sufficient to satisfy the heat demand.

Many authors have evaluated the effect of the above operation strategies, by comparing them to each other [14,30,44,49,80-84], and to new operation strategies [57,80,81,85-87].

Although these mentioned operation strategies are the most used in polygeneration systems, they may not guarantee the best performance of the systems, being the system operation subjected not only to the variation of load demands, but also to the fuel prices [77]. For this reason, an optimal operation of a

polygeneration system can be effectively determined using mathematical optimization techniques, such as genetic algorithms, linear programming and stochastic optimization, with the objective of minimizing the operational cost, primary energy consumption and/or greenhouse gas emissions.

An optimization problem can be formulated as shown in equation (2.1) to minimize the total operational cost of a polygeneration system while satisfying the total energy demand.

$$Minimize \sum_{t=1}^{n} \left\{ c_{el}(t) E_{el,taken}(t) + c_{f,PM}(t) F_{PM}(t) + c_{f,AB}(t) F_{AB}(t) - g_{el,sent}(t) E_{el,sent}(t) \right\} \quad (2.1)$$

where variables $E_{el,taken}(t)$, $F_{PM}(t)$ and $F_{AB}(t)$ represent the electric energy taken from the electrical grid, the fuel energy for the prime movers, and the fuel energy to operate the auxiliary boilers in time period *t*. $c_{el}(t)$ represents the cost of the purchasing electricity, $c_{f,PM}(t)$ represents the cost of the fuel used to feed the prime movers, and $c_{f,AB}(t)$ represents the cost of the fuel used in the auxiliary boilers. $E_{el,sent}(t)$ represents the electricity sold back to the grid in the period *t*, and $g_{el,sent}(t)$ the selling price of electricity. Along with the objective function, presented in equation (2.1), a set of constraints are formulated to specify conditions for the decision variables that require to be satisfied. The constraints are determined based on the equipment characteristics, energy flow relationship, and the operational limitations [88].

The effectiveness of using mathematical optimization techniques to determine optimized operations of polygeneration systems has been widely demonstrated in literature. Many authors have conducted single objective analyses to optimize separately economically or environmentally the system operation [51,77,89-96], others have conducted multi-objective analyses to optimize the system in terms of energy and environmental benefits simultaneously [97-104].

A key role for the optimal operation of polygeneration systems is played by thermal energy storage (TES) systems. They are often used for managing the peak energy demand for better performance and economy, and according to Haeseldonckx et al. [105], their use prolongs the CHP unit operation and allows to power generation units to operate more continuously, by reducing the CO_2 emissions to about a third of the reference case without storage.

Different studies tried to assess the benefits of using a TES system, some of which focused on the operational role of TES that enables more steady and extended operation of CHP units, others deal with the storage aimed at shifting operation to the commercially most profitable hours [79,106,107].

2.4. Polygeneration systems in residential sector

According to the IEA [108], the residential sector has wide margins for enhancing energy savings, and reducing the primary energy consumption. Generally, in residential houses and apartments, energy demand for lighting, air conditioning, home appliances, entertainment devices, and in some cases also space heating and hot water, is covered by electricity taken from the electrical energy network; in other cases, heat is provided to residential buildings by natural gas or biomass or electric boilers for space heating and hot water supply. Hence, energy consumption in residential buildings is significant, worldwide, and even though it has achieved a reduction in the Italian residential sector, in 2014 it was still at around 26 Mtep, as shown in the ENEA's annual report on energy efficiency [109].

Residential electricity, heating and hot water demands continuously vary with daily and seasonal cycles, therefore a heating system has to satisfy the maximum required demand of a house, but has also to be flexible enough to operate on low demand. Moreover, the energy demand of a house or residential building is a function of the building type, size, materials used for construction, occupancy, and location [110,111]. Therefore, energy savings in the residential buildings can be achieved by incorporating energy performance measures, and/or by improving of energy efficiency in new buildings, by introducing proper insulation materials and energy efficient technologies for heating cooling and lighting in the new buildings [111].

Installing some types of polygeneration systems has been identified as one of the efficient methods to meet these objectives.

2.4.1. Small and micro CHP and CCHP for residential buildings

Small and micro cogenerative and trigenerative systems are, certainly, the most popular polygeneration systems in the residential sector. They offer potential

benefits to humanity and environment by reducing green house gas emissions, improving energy security, reducing and, in some cases, avoiding energy losses from electricity transmission and distribution networks, and potentially reducing energy cost to end users [7]. For these reasons, small and micro units represent an important topic of interest today, and during the last three decades they have been focused on by many researchers [112-114].

The micro units used in residential buildings are usually based on internal combustion engines (ICE), micro-gas turbines (MGT), micro Rankine cycle (MRC) and Stirling engine (SE), with a capacity ranging between 5 to 100 kW_{el} [115-119], and, especially in new buildings, they can also be based on renewable energy sources such as solar, wind and biomass [110]. Figure 2.2. a) and Figure 2.2. b) show the electric and thermal efficiency respectively, as a function of the electric power for various prime mover used for CHP systems. Figure 2.3 illustrates the possible routes of using different energy sources and devices for a micro-CHP system in residential building.

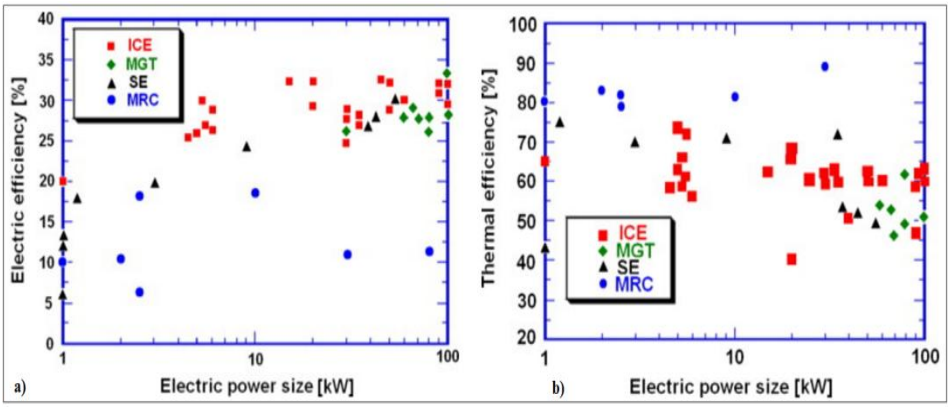

Figure 2.2. a) Electric and b) thermal efficiency for various prime mover technologies [116].

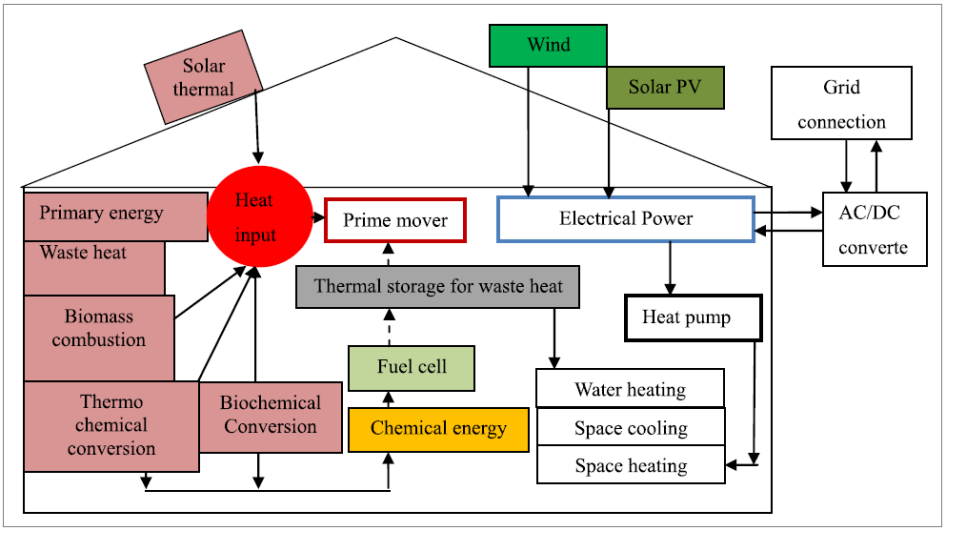

Figure 2.3. Possible options for micro-CHP from various sources in a residential building [110].

2.4.2. Literature review on polygeneration systems used in the residential sector

A huge number of recent works have addressed the effectiveness of multi-generation system applications in the residential sector, focusing on calculating characteristics, such as rated capacity, control methods, and others, and implementing simulation and optimization models. Various studies have been reported on the modeling and optimization of micro-CHP and micro-CCHP systems focusing on different designs, scenarios and operational modes [120-126], aimed at the estimation and maximization of the environmental benefits in terms of CO_2 emission reduction and primary energy savings [127], or reduction and minimization of the operating costs [6,128].

Barbieri et al. [129,130] minimized the costs of heat-driven micro-CHP systems for a single-family house in Italy considering different sizes of the heat storage system by means of a genetic optimization algorithm. Rosato et al. [131] analyzed the feasibility of a micro-CHP system for an Italian residential application by dynamic simulations. Kopanos et al. [132] developed a mixed integer linear programming framework for the economic optimization of the energy production plan of a micro-CHP based residential microgrid in the UK considering power and heat interchange. Shaneb et al. [133] developed a generic optimal online linear

programming model with the objective of minimizing the daily operation costs of a micro-CHP system in the UK, considering three different simulation scenarios. Hawkes and Leach [7] evaluated the economic effectiveness of three micro-combined heat and power technologies by implementing different operating strategies, in the UK residential sector.

Fubara et al. [134] minimized separately the costs and the primary energy consumptions of a distributed energy supply system by means of the GAMS solver, both at the building level and the overall energy supply network level, considering different micro-CHP systems fed by natural gas applied to a case study in the UK residential sector. Wakui and Yokoyama [135] performed the energy-saving optimization of the size of a residential cogeneration system in Japan with power interchange operation by means of a mixed integer linear programming model.

Ren et al. [79] developed a mixed integer nonlinear programming model in order to evaluated the optimal size of a micro-CHP system for a residential customer in Japan from the economic point of view.

Hong et al. [136] analyzed both the electricity-driven operation mode and the heat-driven one in order to find out the optimal implementation strategy of a fuel-cell based cogeneration system in terms of primary energy savings, costs and CO_2 emissions for a case study in South Korea. Arsalis et al. [137] formulated and applied an improved operational strategy different from the electricity-driven and the heat-driven ones to a fuel-cell-based micro-CHP system for single-family households in Denmark. Angrisani et al. [138] performed dynamic simulations to optimize the operation of a micro-CHP system providing thermal and electrical energy to two end users connected between them through a district heating micro-grid in a load sharing approach, considering two different geographical locations in Italy. In another work, Angrisani et al. [139] evaluated and compared pollutants emissions of a residential micro-CHP system with those of a conventional system, in Italy, considering different climatic conditions and control modes.

Other studies have analyzed the advantages related to the use of thermal energy storage systems in CHP and CCHP plants for residential building applications [72,140-149]. Lozano et al. [150] developed an optimization model, using mixed integer linear programming, to determine the design of CHCP systems with thermal

storage. The optimization model was applied to design a system providing energy services for a set of building consisting of 5000 apartments, in Spain. Streckiene et al. [151] evaluated the optimal size of a CHP plant with thermal storage under German spot market conditions by means of a commercial software. They based the economic feasibility analysis of the CHP-plant on the net present value (NPV) and the payback period. Haeseldonckx et al. [105] studied the impact of thermal storage on the operational behavior of residential CHP facilities. They point out that using a thermal storage device prolongs the yearly operation time of the CHP plant, allows a continuous operation and causes a reduction in CO_2 emissions. Ferreira et al. [152] performed the economic optimization of a micro-CHP system driven by the heat demand of a residential building located in Portugal by using the Box's method as optimization algorithm. They also analyzed the optimal size of the heat storage tank connected to the system. Katulic et al. [153] proposed an innovative method for the optimization from the economic viewpoint of the heat storage tank capacity of a cogeneration system in Croatia, considering different heat-driven operational modes. Bianchi et al. [116] analyzed the energy benefits and profitability of micro-CHP systems with thermal energy storage system in meeting energy demands in domestic dwellings. Their analysis revealed that a micro-CHP unit with an appropriate sized thermal storage system can cover the overall thermal energy demand for a building while saving 15-45% of primary energy, depending on the technology considered. A proper system sizing of the prime mover and thermal storage, and consumption of electrical energy play important roles in the economic viability of the systems. In such condition, single family houses can allow micro-CHP systems up to 5 kWel, with a marginal cost that will range between 2000 and 3500 €/kW_{el}.

2.5. Global status and prospects of the spread of polygeneration systems

As discussed in Section 2.1, the polygeneration systems are a reliable and cost-effective technology that can offer a great contribution for meeting the global heat and electricity demand, contributing to reduce the greenhouse gas emissions and encouraging the use of renewable energy sources.

IEA [1] reported in 2007 that CHP systems produce approximately 9% of global power generation, with a global capacity of about 330 GW_{el}, and that although the benefits of using this technology are well known, and despite some countries have been able to promote their dissemination through targeted energy policies, many countries have been much less successful. Figure 2.4 shows the share of CHP systems in different nations. From this figure, it is clear that only few countries have successfully expanded the use of CHP to between 30-50% of total power generation, meaning that CHP plays only a marginal part in the electricity and heat generation of the countries presented in Figure 2.4 [3].

According to the IEA [1], the G8+5 countries, consisting of G8 (group of eight) nations including Canada, France, Germany, Italy, Japan, Russia, the United Kingdom and the United States, and 5 nations of the leading emerging economy including Brazil, China, India, Mexico and South Africa, have the potential to raise their CHP systems capacity over 820 GW_{el} in 2030. The IEA's scenario states that, if suitable policy regimes are introduced based on best-practice CHP policies, by 2030, the CHP share of G8+5 countries electricity generation could rise from 9-10% to 24%.

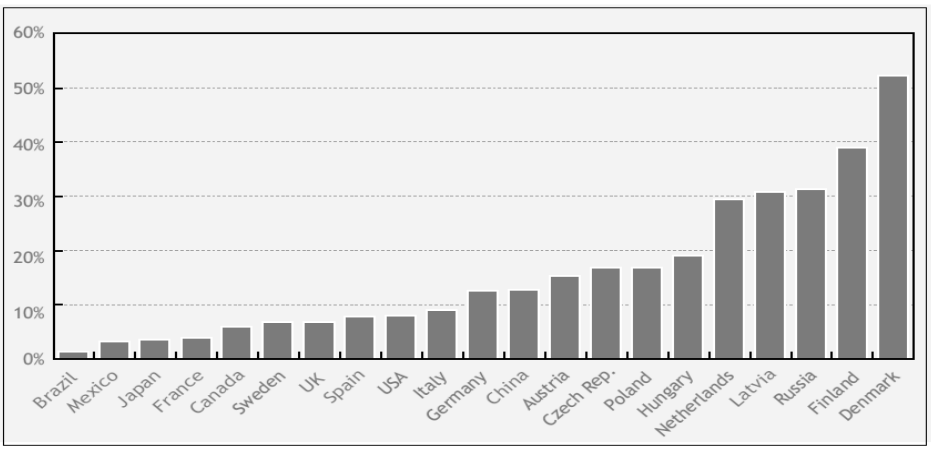

Figure 2.4. CHP share of national power production [12].

References

[1] EPA, Catalog of CHP technologies, March 2015. Available: https://www.epa.gov/sites/production/files/2015-07/documents/catalog_of_chp_technologies.pdf

[2] H. Cho, A.D. Smith, P. Mago. Combined cooling, heating and power: A review of performance improvement and optimization. Applied Energy. Volume 136 (2014), pp. 168-185.

[3] D.W. Wu, R.Z. Wang. Combined cooling, heating and power: a review. Pro Energy Combustion Sci. Volume 32 (2006), pp. 459-495.

[4] J. Xu, J. Sui, B. Li, M. Yang. Research, development and the prospect of combined cooling, heating, and power systems. Energy. Volume 35 (2010), pp. 4361-4367.

[5] A.D. Peacock, M. Newborough. Impact of micro-CHP systems on domestic sector CO2 emissions. Applied Thermal Engineering. Volume 25 (2005), pp. 2653-2676.

[6] A.D. Hawkes, M.A. Leach. Solid oxide fuel cell systems for residential micro-combined heat and power in the UK: Key economic drivers. Journal of Power Sources. Volume 149 (2005), pp. 72−83.

[7] A.D. Hawkes, M.A. Leach. Cost-effective operating strategy for residential micro-combined heat and power. Energy. Volume 32 (2007), pp. 711−723.

[8] A.Rong, R. Lahdelma. Role of polygeneration in sustainable energy system development challenges and opportunities from optimization viewpoints. Renewable and Sustainable Energy Reviews. Volume 53 (2016), pp. 363–372.

[9] S. Murugan, B. Horák. Tri and Polygeneration systems – A review. Renewable and Sustainable Energy Reviews. Volume 60 (2016), pp1032–1051.

[10] IEA, Combined heat & power and emissions trading: options for policy makers, July 2008. Available: http://www.iea.org/publications/freepublications/publication/chp_ets.pdf

[11] G. Chicco, P. Mancarella. Trigeneration primary energy saving evaluation for energy planning and policy development. Energy Policy. Volume 35 (2007), pp. 6132−6144.

[12] G. Chicco, P. Mancarella. Distributed multi-generation: a comprehensive view. Renewable and Sustainable Energy Reviews. Volume 13 (2009), pp. 535−551.

[13] IEA, Combined Heat and Power: evaluating the benefits of greater global investment, February 2008. Available: https://www.iea.org/publications/freepublications/publication/chp_report.pdf

[14] P.J. Mago, N. Fumo, L.M. Chamra. Performance analysis of CCHP and CHP systems operating following the thermal and electric load. International Journal of Energy Research. Volume 33 (2009), pp. 852–864.

[15] A.D. Smith, P.J. Mago. Effects of load-following operational methods on combined heat and power system efficiency. Applied Energy. Volume 115 (2014), pp. 337–351.

[16] H. Cho, P.J. Mago, R. Luck, L.M. Chamra. Evaluation of CCHP systems performance based on operational cost, primary energy consumption, and carbon dioxide emission by utilizing an optimal operation scheme. Applied Energy, 86 (2009), pp. 2540–2549.

[17] M. Hu, H. Cho. A probability constrained multi-objective optimization model for CCHP system operation decision support. Applied Energy, 116 (2014), pp. 230–242.

[18] S.G. Tichi, M.M. Ardehali, M.E. Nazari. Examination of energy price policies in Iran for optimal configuration of CHP and CCHP systems based on particle swarm optimization algorithm. Energy Policy. Volume 38 (2010), pp. 6240–6250.

[19] W. Jiang-Jiang, Z. Chun-Fa, J. You-Yin. Multi-criteria analysis of combined cooling, heating and power systems in different climate zones in China. Applied Energy. Volume 87 (2010), pp. 1247–1259.

[20] H. Ren, W. Zhou, W. Gao. Optimal option of distributed energy systems for building complexes in different climate zones in China. Applied Energy. Volume 91 (2012), pp. 156–165.

[21] Y. Li, Y. Xia. DES/CCHP: The best utilization mode of natural gas for China's low carbon economy. Energy Policy. Volume 53 (2013), pp. 477–483.

[22] M. Ebrahimi, A. Keshavarz. Sizing the prime mover of a residential micro-combined cooling heating and power (CCHP) system by multi-criteria sizing method for different climates. Energy. Volume 54 (2013), pp. 291–301.

[23] M. Ebrahimi, A. Keshavarz. Prime mover selection for a residential micro-CCHP by using two multi-criteria decision-making methods. Energy and Buildings. Volume 55 (2012), pp. 322–331.

[24] M. Ebrahimi, A. Keshavarz. Climate impact on the prime mover size and design of a CCHP system for the residential building. Energy and Buildings. Volume 54 (2012), pp. 283–289.

[25] Z.G. Sun. Energy efficiency and economic feasibility analysis of cogeneration system driven by gas engine. Energy and Buildings. Volume 40 (2008), pp. 126–130.

[26] D. Xu, M. Qu. Energy, environmental, and economic evaluation of a CCHP system for a data center based on operational data. Energy and Buildings. Volume 67 (2013), pp. 176–186.

[27] B. Jabbari, N. Tahouni, A. Ataei, M.H. Panjeshahi. Design and optimization of CCHP system incorporated into kraft process, using Pinch Analysis with pressure drop consideration. Applied Thermal Engineering. Volume 61 (2013), pp. 88–97.

[28] M. Medrano, J. Brouwer, V. McDonell, J. Mauzey, S. Samuelsen. Integration of distributed generation systems into generic types of commercial buildings in California. Energy and Buildings. Volume 40 (2008), pp. 537–548.

[29] Y.Y. Jing, H. Bai, J.J. Wang. A fuzzy multi-criteria decision-making model for CCHP systems driven by different energy sources. Energy Policy. Volume 42 (2012), pp. 286–296.

[30] G. Chicco, P. Mancarella. From cogeneration to trigeneration: profitable alternatives in a competitive market. Energy Converter, IEEE Trans. Volume 21 (2006), pp. 265–272.

[31] H. Cho, P.J. Mago, R. Luck, L.M. Chamra. Evaluation of CCHP systems performance based on operational cost, primary energy consumption, and carbon dioxide emission by utilizing an optimal operation scheme. Applied Energy. Volume 86 (2009), pp. 2540–2549.

[32] K.J. Chua, W.M. Yang, T.Z. Wong, C.A. Ho. Integrating renewable energy technologies to support building trigeneration – a multi-criteria analysis. Renewable Energy. Volume 41 (2012), pp. 358–367.

[33] H. Ghaebi, M. Amidpour, S. Karimkashi, O. Rezayan. Energy, exergy and thermoeconomic analysis of a combined cooling, heating and power (CCHP) system with gas turbine prime mover. International Journal of Energy Research. Volume 35 (2011), pp. 697–709.

[34] Y. Huangfu, J.Y. Wu, R.Z. Wang, X.Q. Kong, B.H. Wei. Evaluation and analysis of novel micro-scale combined cooling, heating and power (MCCHP) system. Energy Conversion and Management. Volume 48 (2007), pp. 1703–1709.

[35] B. Jabbari, N. Tahouni, A. Ataei, M.H. Panjeshahi. Design and optimization of CCHP system incorporated into kraft process, using Pinch Analysis with pressure drop consideration. Applied Thermal Engineering. Volume 61 (2013), pp. 88–97.

[36] L. Gao, H. Wu, H. Jin, M. Yang. System study of combined cooling, heating and power system for eco-industrial parks. International Journal of Energy Research. Volume 32 (2008), pp. 1107–1118.

[37] M. Badami, A. Portoraro, G. Ruscica. Analysis of trigeneration plants: engine with liquid desiccant cooling and micro gas turbine with absorption chiller. International Journal of Energy Research. Volume 36 (2012), pp. 579–589.

[38] M. Badami, A. Portoraro. Performance analysis of an innovative small-scale trigeneration plant with liquid desiccant cooling system. Energy and Buildings. Volume 41 (2009), pp. 1195–1204.

[39] M. Liu, Y. Shi, F. Fang. A new operation strategy for CCHP systems with hybrid chillers. Applied Energy. Volume 95 (2012), pp. 164–173.

[40] F.A. Al-Sulaiman, F. Hamdullahpur, I. Dincer. Performance comparison of three trigeneration systems using organic rankine cycles. Energy. Volume 36 (2011), pp. 5741–5754.

[41] E.T. Calva, M.P. Núñez, M.A.R. Toral. Thermal integration of trigeneration systems. Applied Thermal Engineering. Volume 25 (2005), pp. 973–984.

[42] G. Chicco, P. Mancarella. Assessment of the greenhouse gas emissions from cogeneration and trigeneration systems. Part I: Models and indicators. Energy. Volume 33 (2008), pp. 410–417.

[43] H. Ghaebi, M.H. Saidi, P. Ahmadi. Exergoeconomic optimization of a trigeneration system for heating, cooling and power production purpose based on TRR method and using evolutionary algorithm. Applied Thermal Engineering. Volume 36 (2012), pp. 113–125.

[44] E. Cardona, A. Piacentino, F. Cardona. Matching economical, energetic and environmental benefits: an analysis for hybrid CHCP-heat pump systems. Energy Conversion and Management. Volume 47 (2006), pp. 3530–3542.

[45] S. Behboodi Kalhori, H. Rabiei, Z. Mansoori. Mashad trigeneration potential – an opportunity for CO_2 abatement in Iran. Energy Conversion and Management. Volume 60 (2012), pp. 106–114.

[46] L. Fu, X.L. Zhao, S.G. Zhang, Y. Jiang, H. Li, W.W. Yang. Laboratory research on combined cooling, heating and power (CCHP) systems. Energy Conversion and Management. Volume 50 (2009), pp. 977–982.

[47] F. Calise, M.D. d'Accadia, L. Vanoli. Design and dynamic simulation of a novel solar trigeneration system based on hybrid photovoltaic/thermal collectors (PVT). Energy Conversion and Management. Volume 60 (2012), pp. 214–225.

[48] F.A. Al-Sulaiman, F. Hamdullahpur, I. Dincer. Performance assessment of a novel system using parabolic trough solar collectors for combined cooling, heating, and power production. Renewable Energy. Volume 48 (2012), pp. 161–172.

[49] E. Cardona, A. Piacentino. A methodology for sizing a trigeneration plant in mediterranean areas. Applied Thermal Engineering. Volume 23 (2003), pp. 1665–1680.

[50] P. Mancarella, G. Chicco. Assessment of the greenhouse gas emissions from cogeneration and trigeneration systems. Part II: analysis techniques and application cases. Energy. Volume 33 (2008), pp. 418–430.

[51] H. Li, L. Fu, K. Geng, Y. Jiang. Energy utilization evaluation of CCHP systems. Energy and Buildings. Volume 38 (2006), pp. 253–257.

[52] P.J. Mago, N. Fumo, L.M. Chamra. Performance analysis of CCHP and CHP systems operating following the thermal and electric load. International Journal of Energy Research. Volume 33 (2009), pp. 852–864.

[53] P.J. Mago, A.K. Hueffed. Evaluation of a turbine driven CCHP system for large office buildings under different operating strategies. Energy and Buildings. Volume 42 (2010), pp. 1628–1636.

[54] D.B. Espirito Santo. Energy and exergy efficiency of a building internal combustion engine trigeneration system under two different operational strategies. Energy and Buildings. Volume 53 (2012), pp. 28–38.

[55] G. Angrisani, A. Rosato, C. Roselli, M. Sasso, S. Sibilio. Experimental results of a micro-trigeneration installation. Applied Thermal Engineering. Volume 38 (2012), pp. 78–90.

[56] M. Ebrahimi, A. Keshavarz, A. Jamali. Energy and exergy analyses of a microsteam CCHP cycle for a residential building. Energy and Buildings. Volume 45 (2012), pp. 202–210.

[57] Q. Gu, H. Ren, W. Gao, J. Ren. Integrated assessment of combined cooling heating and power systems under different design and management options for residential buildings in Shanghai. Energy and Buildings. Volume 51 (2012), pp. 143–152.

[58] J. Harrod, P.J. Mago, R. Luck. Sizing analysis of a combined cooling, heating, and power system for a small office building using a wood waste biomass-fired Stirling engine. International Journal of Energy Research. Volume 36 (2012), pp. 64–74.

[59] X.Q. Kong, R.Z. Wang, X.H. Huang. Energy efficiency and economic feasibility of CCHP driven by stirling engine. Energy Conversion and Management. Volume 45 (2004), pp. 1433–1442.

[60] C. Cuviella-Suárez, A. Colmenar-Santos, M. Castro-Gil. Tri-generation system to couple production to demand in a combined cycle. Energy. Volume 40 (2012), pp. 271–290.

[61] Y.Y. Jing, H. Bai, J.J. Wang, L. Liu. Life cycle assessment of a solar combined cooling heating and power system in different operation strategies. Applied Energy. Volume 92 (2012), pp. 843–853.

[62] A.Khaliq, I. Dincer. Energetic and exergetic performance analyses of a combined heat and power plant with absorption inlet cooling and evaporative after-cooling. Energy. Volume 36 (2011), pp. 2662–2670.

[63] A.Fontalvo,H. Pinzon, J. Duarte, A. Bula, A.G. Quiroga, R.V. Padilla. Exergy analysis of a combined power and cooling cycle. Applied Thermal Engineering. Volume 60 (2013), pp. 164–71.

[64] P. Ahmadi, I. Dincer, M.A. Rosen. Exergo-environmental analysis of an integrated organic Rankine cycle for trigeneration. Energy Conversion and Management. Volume 64 (2012), pp. 447–453.

[65] F.A. Al-Sulaiman, I. Dincer, F. Hamdullahpur. Exergy modeling of a new solar driven trigeneration system. Solar Energy. Volume 85 (2011), pp. 2228–2243.

[66] F.A. Al-Sulaiman, F. Hamdullahpur, I. Dincer. Greenhouse gas emission and exergy assessments of an integrated organic Rankine cycle with a biomass combustor for combined cooling, heating and power production. Applied Thermal Engineering. Volume 31 (2011), pp. 439–446.

[67] A.D. Peacock, M. Newborough. Impact of micro-CHP systems on domestic sector CO_2 emissions. Applied Thermal Engineering. Volume 25 (2005), pp. 2653–2676.

[68] M. De Paepe, P. D'Herdt, D. Mertens. Micro-CHP systems for residential applications. Energy Conversion and Management. Volume 47 (2006), pp. 3435–3446.

[69] V. Kuhn, J. Klemeš, I. Bulatov. MicroCHP: overview of selected technologies, products and field test results. Applied Thermal Engineering. Volume 28 (2008), pp. 2039–2048.

[70] V. Dorer, A. Weber. Energy and CO_2 emissions performance assessment of residential micro-cogeneration systems with dynamic whole-building simulation programs. Energy Conversion and Management. Volume 50 (2009), pp. 648–657.

[71] A.Hawkes, M. Leach. Impacts of temporal precision in optimization modeling of micro-Combined Heat and Power. Energy. Volume 30 (2005), pp. 1759–1779.

[72] M. Caliano, N. Bianco, G. Graditi, L. Mongibello. Economic optimization of a residential micro-CHP system considering different operation strategies. Applied Thermal Engineering. Volume 101 (2016), pp. 592-600.

[73] H. Cho, A.D. Smith, P. Mago. Combined cooling, heating and power: A review of performance improvement and optimization. Applied Energy. Volume 136 (2014), pp. 168-185.

[74] D.W. Wu, R.Z. Wang. Combined cooling, heating and power: a review. Progress in Energy and Combustion Science. Volume 32 (2006), pp. 459–95.

[75] Educogen. The European educational tool on cogeneration; 2001.

[76] WADE (World Alliance of Decentralized Energy). Guide to Decentralized Energy Technologies; 2003.

[77] R. Yokoyama, Y. Matsumoto, K. Ito. Optimal sizing of a gas turbine cogeneration plant in consideration of its operational strategy. Journal of Engineering for Gas Turbines and Power. Volume 116 (1994), pp. 116-132.

[78] L. Weiding, Z. Beihong. An optimal sizing method for cogeneration plants. Energy and Buildings. Volume 38 (2006), pp. 189–195.

[79] H. Ren, W. Gao, Y. Ruan. Optimal sizing for residential CHP system. Applied Thermal Engineering. Volume 28 (2008), pp. 514–23.

[80] K.C. Kavvadias, A.P. Tosios, Z.B. Maroulis. Design of a combined heating, cooling and power system: Sizing, operation strategy selection and parametric analysis. Energy Conversion and Management. Volume 51 (2010), pp. 833–845.

[81] P.J. Mago, L.M. Chamra. Analysis and optimization of CCHP systems based on energy, economical, and environmental considerations. Energy and Buildings. Volume 41 (2009), pp. 1099–1106.

[82] J.J. Wang, Y.Y. Jing, C.-F. Zhang, Z.(John) Zhai. Performance comparison of combined cooling heating and power system in different operation modes. Applied Energy. Volume 88 (2011), pp. 4621–4631.

[83] Y.Y. Jing, H. Bai, J.J. Wang. Multi-objective optimization design and operation strategy analysis of BCHP system based on life cycle assessment. Energy. Volume 37 (2012), pp. 405–416.

[84] N. Fumo, P.J. Mago, L.M. Chamra. Emission operational strategy for combined cooling, heating, and power systems. Applied Energy. Volume 86 (2009), pp. 2344–2350.

[85] M. Liu, Y. Shi, F. Fang. A new operation strategy for CCHP systems with hybrid chillers. Applied Energy. Volume 95 (2012), pp. 164–173.

[86] J. Wang, Z.(John) Zhai, Y. Jing, X. Zhang, C. Zhang. Sensitivity analysis of optimal model on building cooling heating and power system. Applied Energy. Volume 88 (2011), pp. 5143–5152.

[87] G. Chicco, P. Mancarella. Matrix modelling of small-scale trigeneration systems and application to operational optimization. Energy. Volume 34 (2009), pp. 261–273.

[88] J. Wang, Z.(John) Zhai, Y. Jing, C. Zhang. Optimization design of BCHP system to maximize to save energy and reduce environmental impact. Energy. Volume 35 (2010), pp. 3388–3398.

[89] J. Wang, Z. (John) Zhai, Y. Jing, C. Zhang. Optimization design of BCHP system to maximize to save energy and reduce environmental impact. Energy. Volume 35 (2010), pp. 3388–3398.

[90] A.Rong, R. Lahdelma. An efficient linear programming model and optimization algorithm for trigeneration. Applied Energy. Volume 82 (2005), pp. 40–63.

[91] J.J. Wang, Y.Y. Jing, C.F. Zhang. Optimization of capacity and operation for CCHP system by genetic algorithm. Applied Energy. Volume 87 (2010), pp. 1325–1335.

[92] H. Cho, R. Luck, S.D. Eksioglu, L.M. Chamra. Cost-optimized real-time operation of CHP systems. Energy and Buildings. Volume 41 (2009), pp. 445–451.

[93] H. Cho, P.J. Mago, R. Luck, L.M. Chamra. Evaluation of CCHP systems performance based on operational cost, primary energy consumption, and carbon dioxide emission by utilizing an optimal operation scheme. Applied Energy. Volume 86 (2009), pp. 2540–2549.

[94] M. Hu, H. Cho. A probability constrained multi-objective optimization model for CCHP system operation decision support. Applied Energy. Volume 116 (2014), pp. 230–242.

[95] M.A. Lozano, M. Carvalho, L.M. Serra. Operational strategy and marginal costs in simple trigeneration systems. Energy. Volume 34 (2009), pp. 2001–2008.

[96] E. Thorin, H. Brand, C. Weber. Long-term optimization of cogeneration systems in a competitive market environment. Applied Energy. Volume 81 (2005), pp. 152–169.

[97] H.S. Gholamhossein Abdollahi. Application of the multi-objective optimization and risk analysis for the sizing of a residential small-scale CCHP system. Energy and Buildings. Volume 60 (2013), pp. 330–344.

[98] S. Bracco, G. Dentici, S. Siri. Economic and environmental optimization model for the design and the operation of a combined heat and power distributed generation system in an urban area. Energy. Volume 55 (2013), pp. 1014–1024.

[99] B. Shi, L.X. Yan, W. Wu. Multi-objective optimization for combined heat and power economic dispatch with power transmission loss and emission reduction. Energy. Volume 56 (2013), pp. 135–143.

[100] C.Z. Li, Y.M. Shi, X.H. Huang. Sensitivity analysis of energy demands on performance of CCHP system. Energy Conversion and Management. Volume 49 (2008), pp. 3491–3497.

[101] A. Smith, R. Luck, P.J. Mago. Analysis of a combined cooling, heating, and power system model under different operating strategies with input and model data uncertainty. Energy and Buildings. Volume 42 (2010), pp. 2231–2240.

[102] C.Z. Li, Y.M. Shi, S. Liu, Z. Zheng, Y. Liu. Uncertain programming of building cooling heating and power (BCHP) system based on Monte-Carlo method. Energy and Buildings. Volume 42 (2010), pp. 1369–1375.

[103] M. Liu, Y. Shi, F. Fang. Optimal power flow and PGU capacity of CCHP systems using a matrix modeling approach. Applied Energy. Volume 102 (2013), pp. 794–802.

[104] R.J. Flores, B.P. Shaffer, J. Brouwer. Dynamic distributed generation dispatch strategy for lowering the cost of building energy. Applied Energy. Volume 123 (2014), pp. 196–208.

[105] D. Haeseldonckx, L. Peeters, L. Helsen, W. D'haeseleer. The impact of thermal storage on the operational behaviour of residential CHP facilities and the overall CO2 emissions. Renewable and Sustainable Energy Reviews. Volume 11 (2007), pp. 1227–1243.

[106] G.P. Henze, B. Biffar, D. Kohn, M.P. Becker. Optimal design and operation of a thermal storage system for a chilled water plant serving pharmaceutical buildings. Energy and Buildings. Volume 40 (2008), pp. 1004–1019.

[107] Y. Li, X. Wang, D. Li, Y. Ding. A trigeneration system based on compressed air and thermal energy storage. Applied Energy. Volume 99 (2012), pp. 316–323.

[108] IEA, Energy Efficiency Policy Recommendations, 2011. Available: https://www.iea.org/publications/freepublications/publication/25recom_2011.pdf

[109] ENEA, Annual energy efficiency report, June 2016. Available: http://www.enea.it/it/pubblicazioni/pdf-volumi/raee-2016-versione-integrale.pdf

[110] A. Alexandros, E.S. Fraga, D.j.L. Brett. Options for residential building services design using fuel cell based microCHP and the potential for heat integration. Applied Energy. Volume 138 (2015), pp. 685–694.

[111] A. Alexandros, E.S. Fraga, D.j.L. Brett. Modelling and optimization in terms of CO2 emissions of a solid oxide fuel cell based micro-chp system in a four bedroom house in London. Energy Procedia. Volume 42 (2013), pp. 201–209.

[112] S. Li, J.Y. Wu. Theoretical research of a silica gel–water adsorption chiller in a micro combined cooling, heating and power (CCHP) system. Applied Energy. Volume 86 (2009), pp. 958–967.

[113] M. Ebrahimi, A. Keshavarz, A. Jamali. Energy and exergy analyses of a micro-steam CCHP cycle for a residential building. Energy and Buildings. Volume 45(2012), pp. 202–210.

[114] M. Ebrahimi, A. Keshavarz.Prime mover selection for a residential micro-CCHP by using two multi-criteria decision-making methods. Energy and Buildings. Volume 55 (2012), pp. 322–331.

[115] M.A. Meybodi, M. Behnia. Impact of carbon tax on internal combustion engine size selection in a medium scale CHP system. Applied Energy. Volume 88 (2011), pp. 5153−5163.

[116] M. Bianchi, A. De Pascale, P.R. Spina. Guidelines for residential micro-CHP systems design. Applied Energy. Volume 97 (2012), pp. 673−685.

[117] A. Parente, C. Galletti, J. Riccardi, M. Schiavetti, L. Tognotti. Experimental and numerical investigation of a micro-CHP flameless unit. Applied Energy. Volume 89 (2012), pp. 203−214.

[118] R. Mikalsen, Y.D. Wang, A.P. Roskilly. A comparison of miller and otto cycle natural gas engines for small scale CHP applications. Applied Energy. Volume 86 (2009), pp. 922−927.

[119] F. Caresana, C. Brandoni, P. Feliciotti, C.M. Bartolini. Energy and economic analysis of an ICE-based variable speed-operated micro-cogenerator. Applied Energy. Volume 88 (2011), pp. 659−671.

[120] P. Ghadimi, S. Kara, B. Kornfeld. The optimal selection of on-site CHP systems through integrated sizing and operational strategy. Applied Energy. Volume 126 (2014), pp. 38–46.

[121] A. De Pascale, C. Ferrari, F.M. Melino, M. Morini, M. Pinelli. Integration between a thermophotovoltaic generator and an Organic Rankine Cycle. Applied Energy. Volume 97 (2012), pp. 695–703.

[122] D. Tempesti, G. Manfrida, D. Fiaschi. Thermodynamic analysis of two micro CHP systems operating with geothermal and solar energy. Applied Energy. Volume 97 (2012), pp. 609–617.

[123] K. Qiu, A.C.S. Hayden. Integrated thermoelectric and organic Rankine cycles for micro-CHP systems. Applied Energy. Volume 97 (2012), pp. 667–672.

[124] Hayden. Implementation of a TPV integrated boiler for micro-CHP in residential buildings. Applied Energy. Volume 134 (2014), pp. 143–149.

[125] J.Y. Wu, J.L. Wang, S. Li, R.Z. Wang. Experimental and simulative investigation of a micro-CCHP system with thermal management controller. Energy. Volume 68 (2014), pp. 444–453.

[126] A. Rosato, S. Sibilio. Performance assessment of a micro-cogeneration system under realistic operating conditions. Energy Conversion and Management. Volume 70 (2013), pp. 149–162.

[127] S. Sepehr, M. M. Aghaei, S. Shahabeddin. Selecting the prime movers and nominal powers in combined heat and power systems. Applied Thermal Engineering. Volume 28 (2008), pp. 1177–1188.

[128] M.A. Ehyaei, P. Ahmadi, F. Atabic, M.R. Heibatic, M. Khorshidvand. Feasibility study of applying internal combustion engines in residential buildings by exergy, economic and environmental analysis. Energy and Buildings. Volume 55 (2012), pp. 405–413.

[129] E.S. Barbieri, F. Melino, M. Morini. Influence of the thermal energy storage on the profitability of micro_CHP systems for residential building applications. Applied Energy. Volume 97 (2012), pp. 714–722.

[130] E.S. Barbieri, P.R. Spina, M. Venturini. Analysis of innovative micro-CHP systems to meet household energy demands. Applied Energy. Volume 97 (2012), pp. 723–733.

[131] A.Rosato, S. Sibilio, G. Ciampi. Dynamic performance assessment of a building integrated cogeneration system for an Italian residential application. Energy and Buildings. Volume 64 (2013), pp. 343–358.

[132] G.M. Kopanos, M.C. Georgiadis, E.N. Pistikopoulos. Energy production planning of a network of micro combined heat and power generators. Applied Energy. Volume 102 (2013), pp. 1522–1534.

[133] O.A. Shaneb, P.C. Taylor, G. Coates. Optimal online operation of residential micro-CHP systems using linear programming. Energy and Buildings. Volume 44 (2012), pp. 17–25.

[134] T.C. Fubara, F. Cecelja, A. Yang. Modelling and selection of micro-CHP systems for domestic energy supply: the dimension of network-wide primary energy consumption. Applied Energy. Volume 114 (2014), pp. 327–334.

[135] T. Wakui, R. Yokoyama. Optimal sizing of residential gas engine cogeneration system for power interchange operation from energy-saving viewpoint. Energy. Volume 36 (2011), pp. 3816–3824.

[136] T. Hong, D. Kim, C. Koo, J. Kim. Framework for establishing the optimal implementation strategy of a fuel-cell-based combined heat and power system: focused on multi-family housing complex. Applied Energy. Volume 127 (2014), pp. 11–24.

[137] A. Arsalis, M.P. Nielsen, S.K. Kaer. Application of an improved operational strategy on a PBI fuel cell-based residential system for Danish single-family households. Applied Thermal Engineering. Volume 50 (2013), pp. 704–713.

[138] G. Angrisani, M. Canelli, A. Rosato, C. Roselli, M. Sasso, S. Sibilio. Load sharing with a local thermal network fed by a microcogenerator: thermo-economic optimization by means of dynamic simulations. Applied Thermal Engineering. Volume 71 (2014), pp. 628–635.

[139] G. Angrisani, A. Rosato, C. Roselli, M. Sasso, S. Sibilio, A. Unich. Influence of climatic conditions and control logic on NOx and CO emissions of a micro-cogeneration unit serving an Italian residential building. Applied Thermal Engineering. Volume 71 (2014), pp. 858–871.

[140] A. Arteconi, N.J. Hewitt, F. Polonara. State of the art of thermal storage for demand-side management. Applied Energy. Volume 93 (2012), pp. 371–389.

[141] A. Fragaki, A.N. Andersen, D. Toke. Exploration of economical sizing of gas engine and thermal store for combined heat and power plants in the UK. Energy. Volume 33 (2008), pp. 1659–1670.

[142] Z. Bogdan, D. Kopjar. Improvement of the cogeneration plant economy by using heat accumulator. Energy. Volume 31 (2006), pp. 2285–2292.

[143] G. Pagliarini, S. Rainieri. Modeling of a thermal energy storage system coupled with combined heat and power generation for the heating requirements of a University Campus. Applied Thermal Engineering. Volume 30 (2010), pp. 1255–1261.

[144] A. Fragaki, A.N. Andersen. Conditions for aggregation of CHP plants in the UK electricity market and exploration of plant size. Applied Energy. Volume 88 (2011), pp. 3930–3940.

[145] A. Christidis, C. Koch, L. Pottel, G. Tsatsaronis. The contribution of heat storage to the profitable operation of combined heat and power plants in liberalized electricity markets. Energy. Volume 41 (2012), pp. 75–82.

[146] A. Chesi, G. Ferrara, L. Ferrari, S. Magnani, F. Tarani. Influence of the heat storage size on the plant performance in a Smart User case study. Applied Energy. Volume 112 (2013), pp. 1454–1465.

[147] G. Diaz, B. Moreno. Valuation under uncertain energy prices and load demands of micro-CHP plants supplemented by optimally switched thermal energy storage. Applied Energy. Volume 177 (2016), pp. 553–569.

[148] L. Mongibello, N. Bianco, M. Caliano, G. Graditi. Influence of heat dumping on the operation of residential micro-CHP systems. Applied Energy. Volume 160 (2015), pp. 206–220.

[149] L. Yongliang, X. Wang, L. Dacheng, Y. Ding. A trigeneration system based on compressed air and thermal energy storage. Applied Energy. Volume 99 (2012), pp. 316–323.

[150] M.A. Lozano, J.C. Ramos, L.M. Serra. Cost optimization of the design of CHCP (combined heat, cooling and power) systems under legal constraints. Energy. Volume 35 (2010), pp. 794–805.

[151] G. Streckiene, V. Martinaitis, A.N. Andersen, J. Katz. Feasibility of CHP-plants with thermal stores in the German spot market. Applied Energy. Volume 86 (2009), pp. 2308–2316.

[152] A.C.M. Ferreira, M.L. Nunes, S.F.C.F. Teixeira, C.P. Leão, Â.M. Silva, J.C.F. Teixeira, et al. An economic perspective on the optimization of a small-scale cogeneration system for the Portuguese scenario. Energy. Volume 45 (2012), pp. 436–444.

[153] S. Katulic, M. Cehil, Z. Bogdan. A novel method for finding the optimal heat storage tank capacity for a cogeneration power plant. Applied Thermal Engineering. Volume 65 (2014), pp. 530–538.

[154] IEA, Tracking industrial energy efficiency and CO_2 emissions, June 2007. Available: https://www.iea.org/publications/freepublications/publication/tracking_emissions.pdf

[155] IEA, Cogeneration and district energy, 2009. Available: https://www.iea.org/publications/freepublications/publication/CHPbrochure09.pdf

"Without a good strategy, it is easy to fall into the common trap of having people busy with all kinds of activities, but achieving few measurable results"

Chapter 3. A new operation strategy for residential CHP systems

3.1. Introduction

In this chapter, a novel approach for improving the operation of residential micro-CHP systems from the economical point of view is proposed. Such approach relies with the possibility to dump part of the heat generated by cogenerators operating with a heat-driven operation strategy.

The effects of the heat dumping are shown on the operation of four residential micro-CHP systems, each composed of a prime mover (PM), generating electricity and heat, a thermal energy storage system (TES) and an auxiliary boiler (AB). The micro-CHP systems differ from one another on the prime mover technology, while the same user is considered, or rather a multi-apartment housing situated in Italy. As concerns the prime movers, four natural gas fuelled commercial prime movers are considered, two internal combustion engine (ICE1 and ICE2) and two microurbines (MT1 and MT2), characterized by different electric and thermal powers. For each micro-CHP system, two different heat-driven operation strategies, one with heat dumping and one without, are implemented by means of an home-made numerical code developed in Matlab environment, and in both cases, the economic optimization of the operation is performed by using the patternsearch algorithm.

An economic analysis is also performed to evaluate, for each considered case, the feasible investment cost for the purchase and the maintenance of the micro-CHP systems, by fixing two values of the payback period. Moreover, the effects of the

variation of the thermal energy storage system maximum capacity, and of the auxiliary boiler efficiency on the optimized results are analyzed.

The major results of the analysis presented in the following, show that, for all the analyzed micro-CHP systems, an optimized application of heat dumping in the system operation allows to considerably reduce the size of the thermal energy storage system with respect to the heat-driven operation strategy without heat dumping.

In the following, the analyzed cases, in terms of energetic system and user, are presented in Section 3.2. The operation strategies are presented in Section 3.3, whereas the methodologies used for the optimization, and the evaluation of local and global pollutants emission are presented in Section 3.4. Results of the optimization process obtained considering conventional and high efficiency auxiliary boilers, the economic analysis, and the pollutants emission obtained for each case, are presented and discussed in Section 3.5.

3.2. Analyzed cases

In the following, the details of the energetic system and of the user are presented in Sections 3.2.1 and 3.2.2, respectively.

3.2.1. Energetic system

Figure 3.1 shows a simplified layout of the micro-CHP plants. In each analyzed case, the prime mover is considered interconnected to the external electrical grid, to the internal electric network relative to the user, and to a thermal energy storage system consisting in an insulated tank for Domestic Hot Water (DHW) storage. In turn, the TES system is connected to the heat distribution network of the user, and to a natural gas fuelled auxiliary boiler. The electrical energy generated by the prime mover is sent either to the user, or, in case of zero electric energy consumption, to the external grid, or to both of them in case of a surplus of generation with respect to the electricity demand. Otherwise, if the electricity demand is higher than the electric power provided by the prime mover, electricity is taken from the external grid.

The TES system allows to accumulate thermal energy for a later use when the thermal demand is lower than the prime mover heat generation, while the auxiliary boiler is included in order to fulfill thermal energy demands higher than the sum of the prime mover heat generation and the heat accumulated in the storage system.

As concerns the prime movers, they are natural gas fuelled commercial prime movers, whose main characteristics are shown in Table 3.1. It is assumed that they follow a heat-driven control logic, and that operate in ON/OFF mode, recognized to be a very effective mode for micro-CHP systems applications like the present one [1-3], for avoiding the decrease of the electrical efficiency at partial load operation, and the large augmentation of hazardous emissions at district level that may occur with load modulation [4,5]. The four prime movers are analyzed separately, and for each of them, different values of the TES maximum capacity is considered. Defining the maximum TES equivalent hours as the ratio between the TES maximum capacity and the prime mover thermal power, six values of the TES equivalent hours are analyzed, ranging from zero, representing the limit case without storage, to four. Moreover, two values for the auxiliary boiler efficiency are considered, namely 0.8 and 0.95, representing the efficiency of the average available technologies and the one relative to the best available technologies (BATs), respectively.

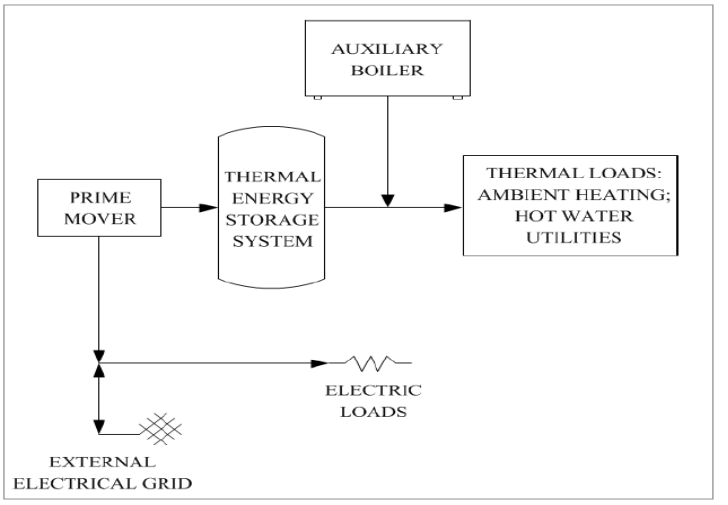

Figure 3.1. Layout of the micro-CHP plants.

Table 3.1. Prime movers characteristics.

Prime mover	P_{el} (kW)	P_{th} (kW)	η_{el} (%)	η_{th} (%)
MT1	15	37.0	22.7	56.0
ICE1	20	47.5	28.6	67.9
MT2	30	60.0	26.0	52.0
ICE2	50	100.0	30.0	60.0

3.2.2. User

The user is represented by a residential building with 50 apartments located in the Italian climatic zone E, characterized by a total surface area of 5000 m^2 and a shape factor *S/V* of 0.5 m^{-1}.

The yearly thermal energy demand relative to the ambient heating is evaluated with reference to the Italian limits for the energy performance of buildings [6], and it is equal to 68 kWh/m^2/yr, while the yearly thermal demand for the hot water utilities is evaluated with reference to [7], and it is equal to 15 kWh/m^2/yr. The yearly electric energy demand relative to the electric appliances is 18 kWh/m^2/yr, while the electricity demand for the air conditioning in the warm season is considered equal to 7 kWh/m^2/yr [1].

The total yearly thermal energy demand for DHW is equally distributed among all days of the year, and the daily demand for DHW is distributed among the day hours by means of the hourly profile of Figure 3.2. The yearly thermal energy demand relative to the ambient heating is distributed among the months, the days and the hours of the cold season by means of the profiles reported in Figures 3.3 and 3.4, showing the hourly thermal demand profile relative to the ambient heating, and the total thermal demand for each month of the cold season, this last including both the ambient heating demand and the DHW one, respectively. For each month, the total demand relative to ambient heating is considered uniformly distributed among its days.

The electric loads are evaluated using a similar procedure. Figure 3.5 shows the non-dimensional hourly demand profile relative to the electric equipment not including the devices for the air conditioning in the warm season, whereas Figure 3.6 shows the one relative to the air conditioning in the warm season.

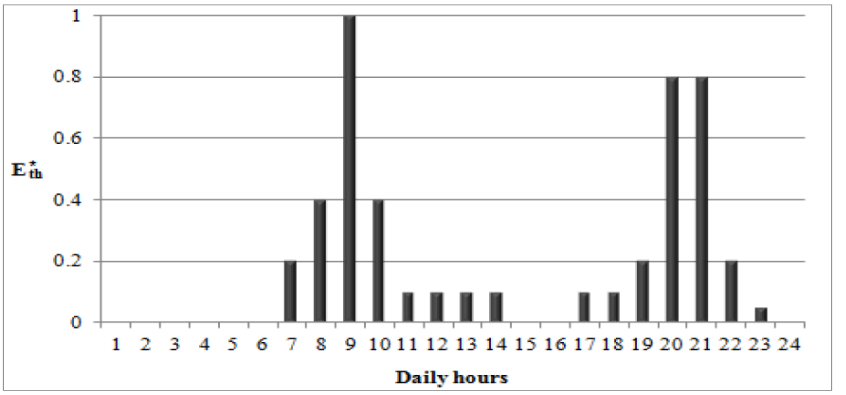

Figure 3.2. Non-dimensional hourly thermal demand profile relative to DHW.

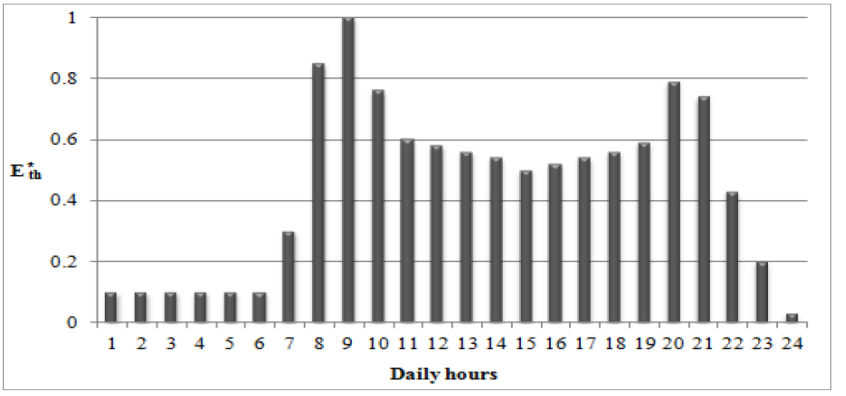

Figure 3.3. Non-dimensional hourly thermal demand profile relative to ambient heating in the cold season.

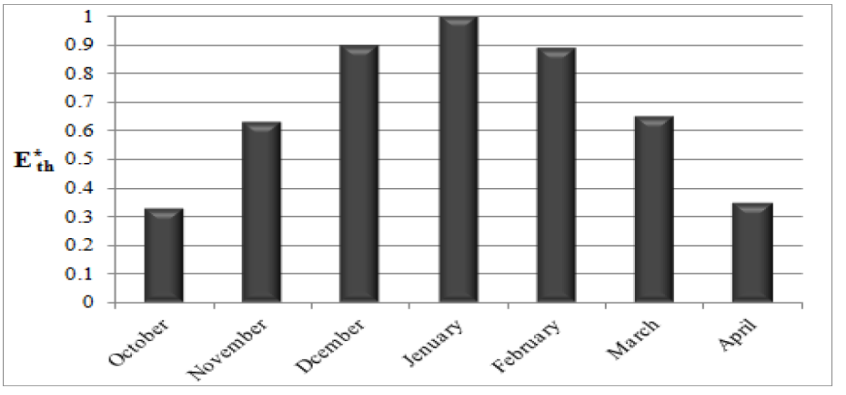

Figure 3.4. Non-dimensional monthly total thermal demand profile in the cold season.

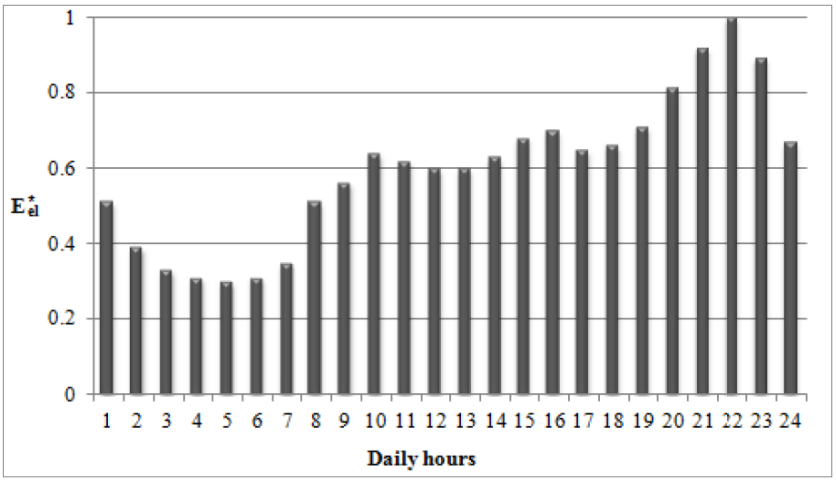

Figure 3.5. Non-dimensional hourly electric demand profile relative to the equipment.

The load profile relative to the equipment is supposed to be the same for each day of the year, whereas the electric loads relative to the air conditioning are considered only during the summer months of June, July and August. As for the electric load profiles, once the yearly electricity demand is know, the non-dimensional load profiles permit to calculate the hourly demand of electricity for each day of the year.

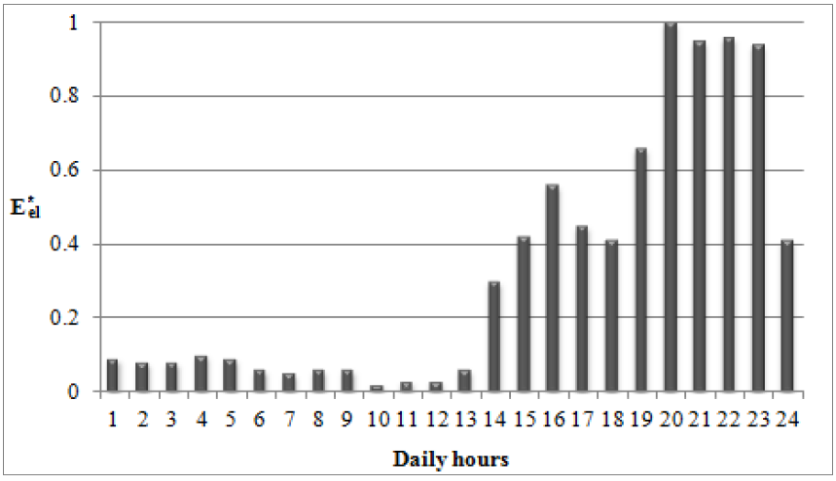

Figure 3.6. Non-dimensional hourly electric demand profile relative to air conditioning.

3.3. Operation strategies

The prime movers operation is considered limited to the cold season from October 15th to April 15th, whereas the thermal and the electrical demands relative to the remaining part of the year is covered by the separate generation.

For each analyzed configuration of the micro-CHP system, two different operation strategies are implemented. For a given time step, in one case the prime mover operates only if its thermal energy generation in an hour, at full load, ($E_{th,PM}$) is lower than or equal to the sum of the user thermal demand ($E_{th,user}$) in the same hour and the energy required to fill the TES, this last evaluated as the difference of the TES maximum capacity ($C_{TES,max}$) and the current one (C_{TES}), otherwise the prime mover is switched off. In the second case, the prime mover can operate also when its thermal generation is higher than the sum of the user demand and the energy required to fill the TES. In other words, with the first operation strategy, to which we will refer in the following as *operation 1*, the prime mover operates only if there is not heat surplus; whereas with the second one, to which we will refer in the following as *operation 2*, there is the possibility to dump part of the heat surplus generated by the prime mover.

Figure 3.7 shows the block diagrams relative to the two heat-driven operation strategies of the prime mover. In detail, the block diagram relative to the case with heat dumping (*operation 2*) is obtained by including the blocks in the dashed rectangle, whereas the one relative to the case without heat dumping (*operation 1*) is obtained by excluding the blocks in the dashed rectangle. So that, in the latter case, the prime mover is switched on only if the following relation holds:

$$E_{th,PM} \leq E_{th,user} + \left(C_{TES,\max} - C_{TES}\right) \tag{3.1}$$

Finally, in all analyzed cases it is assumed that the prime mover can be switched on at most two times a day, in order to limit the number of the prime movers warm-up period, which limit their efficiency.

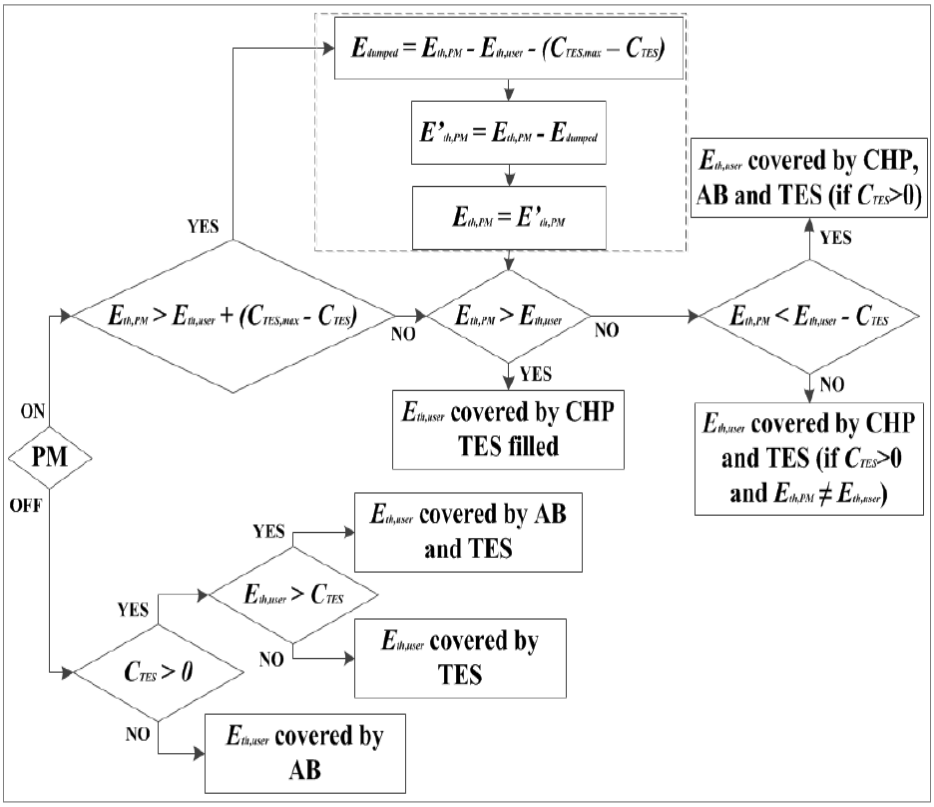

Figure 3.7. block diagram relative to the prime mover operation strategy with (and without) heat dumping.

3.4. Methodologies

The formulation of the optimization problem, and the model used for evaluating the local and global pollutants emission of the micro-CHP systems and of the separate generation are presented in Sections 3.4.1 and 3.4.2, respectively.

3.4.1. Optimization

The operation strategies are implemented by means of a home-made numerical code written in Matlab, realized in order to establish, for each micro-CHP system configuration, the optimal operation schedule of the prime mover that maximizes the revenues for the energy cogeneration with respect to the Separate Generation (SG). To this purpose, the code takes into account the natural gas and electricity

costs evaluated according to [8] as a function of the climatic zone, the consumption ranges and, as regards the electricity cost, also as a function of the installed electrical power, and the Italian incentives for high efficiency cogeneration. For the analyzed cases, the Italian incentives consist in a reduction of the excise duty on the fraction of the natural gas used for the electricity generation by means of CHP systems, advantages related to the possibility of releasing the electricity generated by the CHP system but not immediately consumed in the external grid for a later use on a yearly basis, and the possibility to obtain tradable white certificates, whose quantity depends on the TOE (tons of oil equivalent) saved through plant operation [9-14].

The schedule optimization is performed by means of the Matlab patternsearch optimization algorithm, and the variable of the optimization process are represented by the prime mover ON/OFF periods. In detail, considering the assumption that the prime mover can be switched on at most two times a day, each day is considered divided into 5 periods consisting in a certain number of hours, corresponding to the sequence OFF-ON-OFF-ON-OFF. Thus, for each day of operation, the optimization variables are represented by the first four periods relative to the above sequence, since the last one is dependent on the first four, and it can be derived as their complement to 24.

The objective function that is minimized in the optimization problem resolution is given by:

$$FF = \Delta CF = -(\Delta AC_{NG} + \Delta AC_{electricity}) - R_{WC} \tag{3.2}$$

where ΔCF represents the difference between the annual cash flow relative to separate generation and the one relative to combined generation, ΔAC_{NG} is the difference between the annual cost of the natural gas consumed in separate generation and the one relative to combined generation that includes the gas consumed by the auxiliary boiler not covered by the reduction of the excise duty, $\Delta AC_{electricity}$ is the difference between the annual cost of electricity in separate generation and the one relative to combined generation, and R_{WC} are the revenues relative to the white certificates. The parameters presented in equation (3.2) are evaluated over an entire year, and the Italian incentives for high efficiency cogeneration are accounted for in the evaluation of ΔAC_{NG} and $\Delta AC_{electricity}$.

An iterative procedure, in which each months is optimized separately, is adopted to limit the number of parameters to be optimized simultaneously. In detail, once fixed an initial condition, i.e. an initial operation schedule for the entire operation period of the prime mover, the operation periods relative to October are optimized considering the operation periods relative to the other months fixed and equal to the initial ones. Then, November is optimized by using the optimized operation periods relative to October, and the initial operation periods for the remaining months, and so on. After that the operation periods of April are optimized, the optimization process restarts from October and the updated operation schedule is used. The iterative procedure stops after the optimization of the operation periods of April if convergence of results is reached.

Several initial conditions are tested aimed at minimizing the simulations duration. Finally, the initial condition adopted for the prime movers with lower power (MT1 and ICE1) prescribes in all simulations that the first four periods of all days of the colder months, namely December, January and February consist of two OFF periods of 3 hours and two ON periods of 9 hours, while in the other months the initial condition prescribes that the first four periods of all days consists of the same number of hours fixed to 6. Relatively to the prime movers with higher power (MT2 and ICE2), a similar approach is adopted, with the difference that the ON periods consist of 6 hours and 3 hours in the colder months and in the other ones, respectively.

The maximum number of iterations relative to the patternsearch algorithm is found out by means of a sensitivity analysis, and it is fixed to 1000 in all simulations, and the runs are performed on a computer workstation having an eight cores processor with a clock frequency ranging from 3.1 GHz to 3.8 GHz, and a random access memory (RAM) of 64 GB. Each run takes about 48 hours to finish.

The main inputs of the optimization code are the characteristics of prime mover and auxiliary boiler, the maximum capacity of the heat storage system, the user thermal and electrical hourly demands, the tariffs of electricity and natural gas, the incentives for cogeneration, and the initial operation schedule.

The main outputs are represented by the optimized ON/OFF sequence relative to each simulated day, the dumped thermal energy relative to each simulated hour, the

hourly consumption and the cost of electricity taken from the grid and of natural gas both for cogeneration and separate generation, the amount of incentives relative to cogeneration, and the pollutants emission on local and global scale.

3.4.2. Evaluation of local and global pollutants emission

Being all the prime movers considered in this study fed by natural gas, only CO_2, CO, and NO_X emissions are estimated, and the comparison between the pollutants emission of the analyzed micro-CHP systems, and the ones relative to the separate generation of heat and electricity, both on local and global scale, is accomplished by means of the emission factors [4,5]. In the following, the details of the model are presented.

For an energy generator based on the combustion of a certain fuel, the mass of the generic pollutant *p*, emitted for the generation of a generic energy vector *X*, is calculated as follows:

$$m_p^X = \mu_p^X \cdot X \tag{3.3}$$

where μ_p^X is the emission factor, expressed in g/kWh, that depends on the pollutant, the energy vector, and also on the generator equipment, operation and maintenance state.

In each analyzed case, the total emission including the ones of the prime mover, the auxiliary boiler, and of the centralized power plant generating the fraction of the user electricity demand not covered by the prime mover, and for that taken from the grid, are compared to the ones relative to the separate generation of the same amounts of heat and electricity generated by the auxiliary boiler and the centralized power plant, respectively.

As concerns the separate generation system, two scenarios are considered: the first, in which the separate generation of heat and electricity is made by means of a conventional natural gas boiler, and a mix of conventional technologies for the power generation in Italy, respectively; the second, in which the separate generation system consists in the best available technologies, namely a high efficiency boiler for heat generation, and a natural gas fuelled combined cycle power plant for the electricity one. Table 3.2 presents the emission factors and the efficiencies of the

separate generation of heat, whereas Table 3.3 the emission factors and the efficiencies of the separate generation of electricity.

Table 3.4. shows the emission factors of the considered prime movers at full load operation. By assuming the complete combustion of the fuel, the CO_2 emission factor of the prime movers is evaluated as a function of the carbon content of natural gas, its lower heating value, and prime mover efficiencies, while the emission factors relative to CO and NO_X are fixed by considering the ones reported in the references [4,5,15]. For the internal combustion engines, it is assumed that they are provided by a catalytic filter.

Table 3.2. Emission factors and efficiencies for separate generation of heat.

Reference technology	**Heat generation (g/kWh$_{th}$)**			
	$\mu_{NO_X}^{E_{th}}$	$\mu_{CO}^{E_{th}}$	$\mu_{CO_2}^{E_{th}}$	η_{th} (%)
Conventional	0.19	0.03	253	80
BAT	0.05	0.02	210	95

Table 3.3. Emission factors and efficiencies for separate generation of electricity.

Reference technology	**Electricity generation(g/kWh$_{el}$)**			
	$\mu_{NO_X}^{E_{el}}$	$\mu_{CO}^{E_{el}}$	$\mu_{CO_2}^{E_{el}}$	η_{el} (%)
Conventional	0.50	0.30	700	40
BAT	0.10	0.20	363	55

Table 3.4. Emission factors of the prime movers.

Prime mover	$\mu_{NO_X}^{E_{el}}$ **(g/kWh$_{el}$)**	$\mu_{CO}^{E_{el}}$ **(g/kWh$_{el}$)**	$\mu_{CO_2}^{E_{el}}$ **(g/kWh$_{el}$)**
MT1	0.1	0.550	890
ICE1	1.5	1	706
MT2	0.1	0.550	777
ICE2	1.5	1	673

The global and local emissions are evaluated by using a hourly-based model. In detail, in each analyzed case, the global emission of the micro-CHP system and the ones of the two separate generation are evaluated as follows, respectively:

$$m_p^{CHP} = \mu_p^{E_{el},PM} \cdot E_{el,PM} + \mu_p^{E_{th},SG} \cdot E_{th,AB} + \mu_p^{E_{el},SG} \cdot E_{el,taken} \quad (3.4)$$

$$m_p^{SG} = \mu_p^{E_{el},SG} \cdot E_{el,PM} + \mu_p^{E_{th},SG} \cdot E_{th,PM} + \mu_p^{E_{th},SG} \cdot E_{th,AB} + \mu_p^{E_{el},SG} \cdot E_{el,taken} \quad (3.5)$$

As to the local emissions, they do not include the emissions due to the electricity generation by centralized power stations, because they are usually located far enough from urban districts, for that reason they are evaluated as follows:

$$m_p^{CHP} = \mu_p^{E_{el},PM} \cdot E_{el,PM} + \mu_p^{E_{th},SG} \cdot E_{th,AB} \quad (3.6)$$

$$m_p^{SG} = \mu_p^{E_{th},SG} \cdot E_{th,PM} + \mu_p^{E_{th},SG} \cdot E_{th,AB} \quad (3.7)$$

3.5. Results

In this section, the results of the economic optimization of the several analyzed cases are presented and discussed. The following data refer to the operation period of the prime movers that goes from October 15th 2013 to April 15th 2014, and the tariffs used to evaluate the annual cost of natural gas and electricity, and to estimate the incentives for cogeneration are relative to the period that goes from September 1st 2013 to August 31st 2014 [8].

In detail, the results relative to the cases with conventional auxiliary boilers are presented in Section 3.5.1, whereas the results of the cases with high efficiency auxiliary boilers are presented in Section 3.5.2. The economic analysis conducted in order to evaluate, for each analyzed case, the feasible investment cost relative to the purchase of the micro-CHP system, and its results are presented in Section 3.5.3. Finally, the pollutants emission modelling results are shown in Section 3.5.4.

3.5.1. Conventional auxiliary boilers

Figure 3.8 shows for both operation strategies the total operation hours of the prime movers as a function of the maximum TES equivalent hours ($EH_{TES,max}$), in the cases with conventional boilers (η_{AB}=0.8).

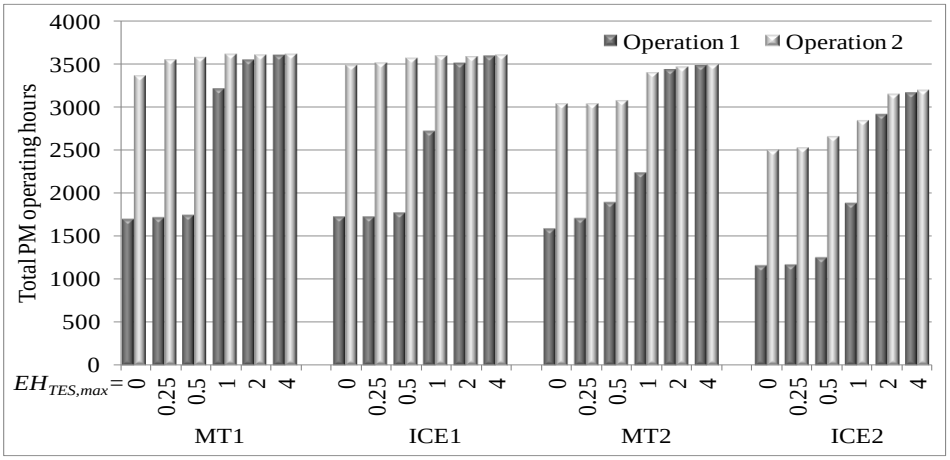

Figure 3.8. Total operation hours of the prime movers as a function of the maximum TES equivalent hours for both the operation strategies with η_{AB}=0.8.

Being the user the same for all the analyzed micro-CHP systems, for each value of the TES equivalent hours, the prime mover ICE2 presents the lowest working hours as compared to the others prime movers, as it is characterized by the highest power.

As concerns the operation without heat dumping (*operation 1*), for all prime movers the operation hours increase with the increase in the maximum TES equivalent hours, allowing the TES systems to store the exceeding heat generated by the prime movers for a later use. Nevertheless, there is a very low variation of prime movers operation hours for $EH_{TES,max}$ from 0 to 0.5, except for MT2 that, in the above interval, presents a more noticeable increase in operation hours with the increase in the maximum TES equivalent hours, while in general for $EH_{TES,max}$ from 0.5 to 1, and from 1 to 2, there is a marked augmentation of operation hours. As it was to be expected, the longest operation is obtained in all cases when $EH_{TES,max}$ is equal to 4. However, the operation hours when $EH_{TES,max}$ is equal to 2 are nearly equal to the ones at $EH_{TES,max}$ equal to 4, except for ICE2 that presents a more marked difference between them.

Relatively to the operation with heat dumping (*operation 2*), at low $EH_{TES,max}$, for all prime movers the operation hours are much higher than in the corresponding cases without heat dumping, especially for the prime movers with the lowest

powers, namely MT1 and ICE1, that in some cases present operation hours higher than double the corresponding ones relative to *operation 1*. This is essentially because, at low $EH_{TES,max}$ and without heat dumping, the constraint expressed by equation (3.1) is very limiting. Moreover, at high values of $EH_{TES,max}$, for all prime movers the total operation hours approach the corresponding value relative to *operation 1*. This is due to the fact that at high values of $EH_{TES,max}$, i.e. at high values of $C_{TES,max}$, the right term in equation (3.1) is generally lower with respect to the cases with smaller values of $EH_{TES,max}$, thus minimizing heat dumping. In practice, at high values of $EH_{TES,max}$, namely with very large heat storage tanks, the micro-CHP systems are enough flexible to maximize the prime movers operation without heat dumping. Furthermore, in all cases the operation hours present an asymptotic behavior at higher storage sizes, and the asymptotic values do not correspond to the maximum prime movers capacities in terms of percentage of the total heat demand covered. This is explained considering that in some hours it is more convenient to generate heat by means of the auxiliary boiler and to purchase electricity from the grid, because the economic value of the electricity generated by the prime movers is too low. As a result of the heat dumping, low-power prime movers MT1 and ICE1 present a low variation of the total operation hours at the different values of $EH_{TES,max}$, especially in the cases with $EH_{TES,max}$ equal to 1, 2 and 4, where the total operation hours assume practically the same value.

Figures 3.9 and 3.10 show for both operation strategies the percentage of the annual electricity demand and of the annual total thermal demand including ambient heating and DHW covered by the prime movers for each value of $EH_{TES,max}$, respectively. It can be noticed that the trends in Figure 3.10 are slightly different from those in Figure 3.8, as the dumped thermal energy is not included.

Figure 3.11 shows the total heat dumped from the micro-CHP systems, represented by the prime movers, for each value of $EH_{TES,max}$ relative to *operation 2*. For all systems, the dumped heat is higher at low $EH_{TES,max}$ and approaches zero at larger heat storage systems. However, even at low storage sizes, the values of the dumped heat are all quite low as compared to the total prime mover thermal energy generation.

Figure 3.12 shows for both operation strategies the natural gas annual consumption of the micro-CHP systems for each value of $EH_{TES,max}$. In each case, the value of the natural gas annual consumption are calculated as the sum of the natural gas consumed by the prime mover and the natural gas consumed by the auxiliary boiler, including the consumption in the six months in which the prime mover is inactive.

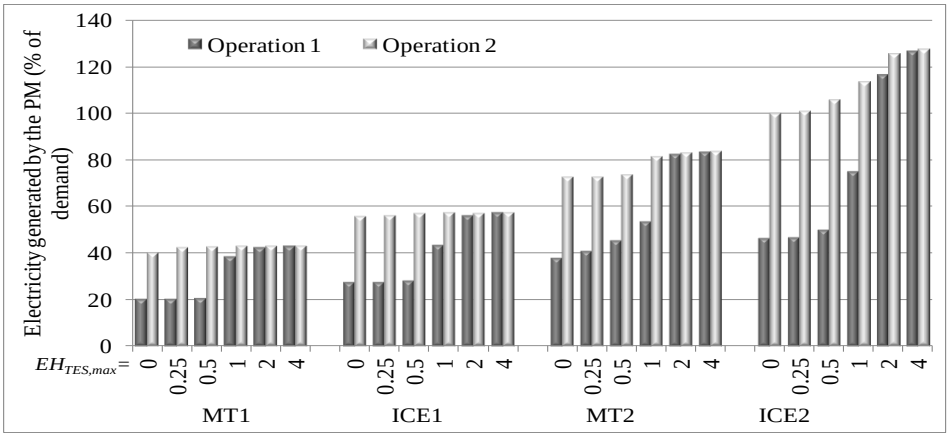

Figure 3.9. Electricity generated by the prime movers as a function of the maximum TES equivalent hours for both the operation strategies with η_{AB}=0.8.

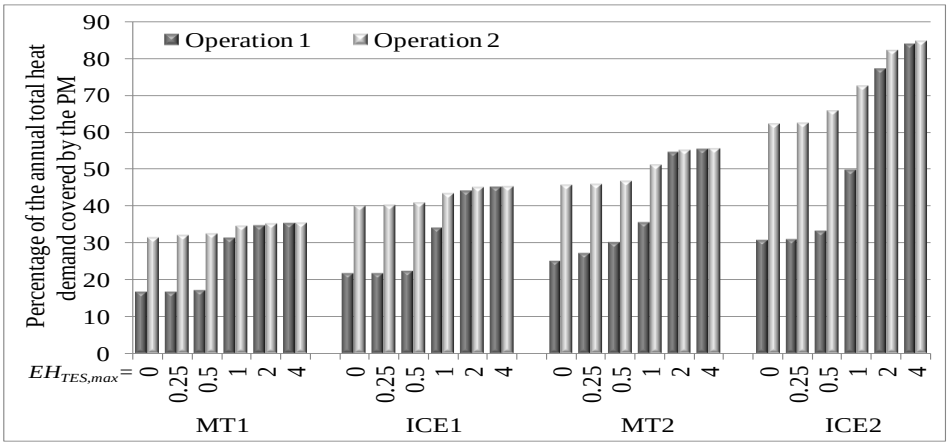

Figure 3.10. Percentage of the annual total heat demand (ambient heating + DHW) covered by the prime movers as a function of the maximum TES equivalent hours for both the operation strategies with η_{AB}=0.8.

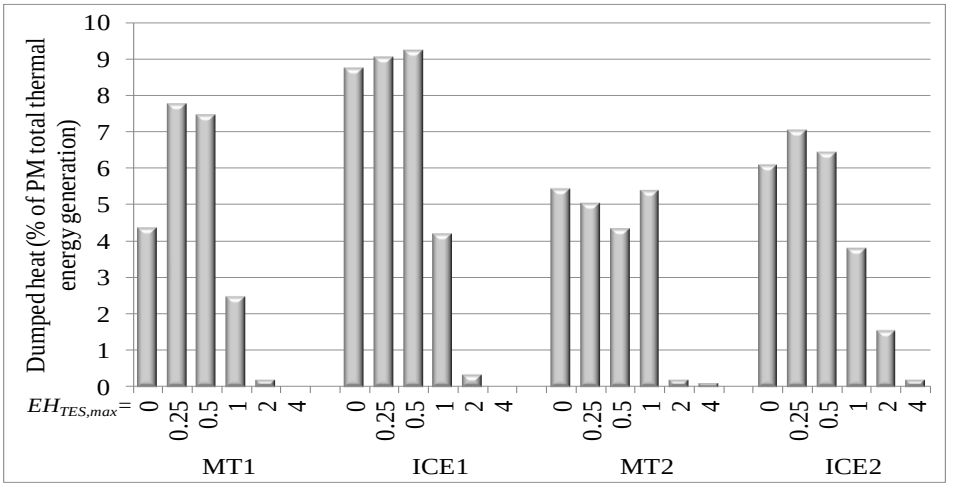

Figure 3.11. Dumped heat with η_{AB}=0.8.

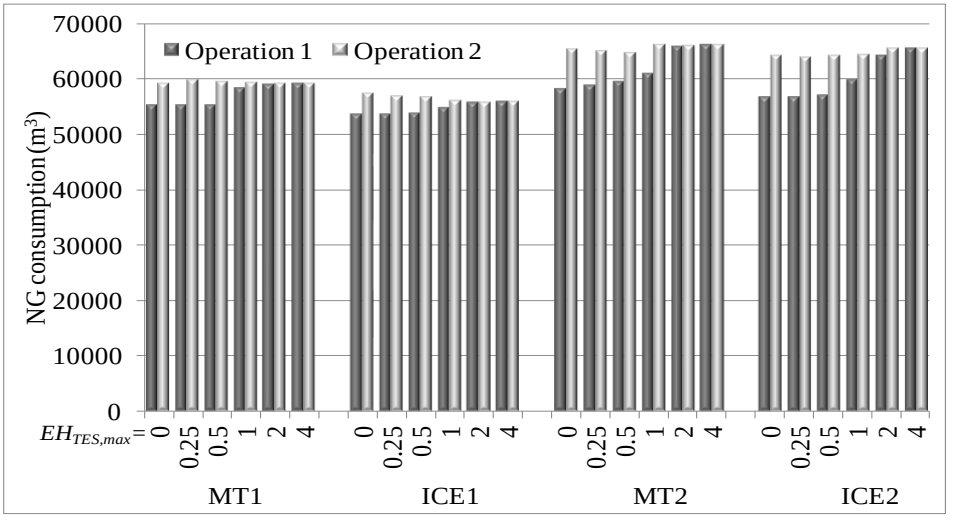

Figure 3.12. Natural gas annual consumption with η_{AB}=0.8.

The natural gas annual consumptions relative to the prime mover and the auxiliary boiler in the cases relative to *operation 2* are depicted in Figure 3.13. Besides the prime movers thermal powers and the thermal demand that is the same in all analyzed cases, for each micro-CHP system and for each storage size the natural gas total consumption depends on the prime mover total operation hours, on

the prime mover thermal efficiency, and on the efficiency of the auxiliary boiler that has to fulfill the fraction of the heat demand not covered by the prime mover. For all micro-CHP systems, the natural gas consumptions relative to *operation 2* at low $EH_{TES,max}$ are higher than the corresponding ones resulting from *operation 1*, and this is clearly due to the much higher prime movers operation hours. Moreover, for both operation strategies and for each value of $EH_{TES,max}$, the lowest natural gas annual consumption is the one relative to the micro-CHP system with ICE1, characterized by the highest thermal efficiency. It is followed by the micro-CHP system with MT1 as prime mover. This can be explained considering that, even if MT1 thermal efficiency is lower than the one of ICE2, its thermal generation is much lower than the one of ICE2, and thus for the micro-CHP system with MT1 great part of the thermal demand is satisfied by the auxiliary boiler characterized by a thermal efficiency of 0.8, that is much higher than the ones of the prime movers. The highest consumption is obtained by the micro-CHP system with MT2, that is the prime mover with the lowest thermal efficiency. These considerations are also valid for the results relative to *operation 2*, because in the cases where the dumped heat is not null, it yet represents a low fraction of the total thermal energy generation.

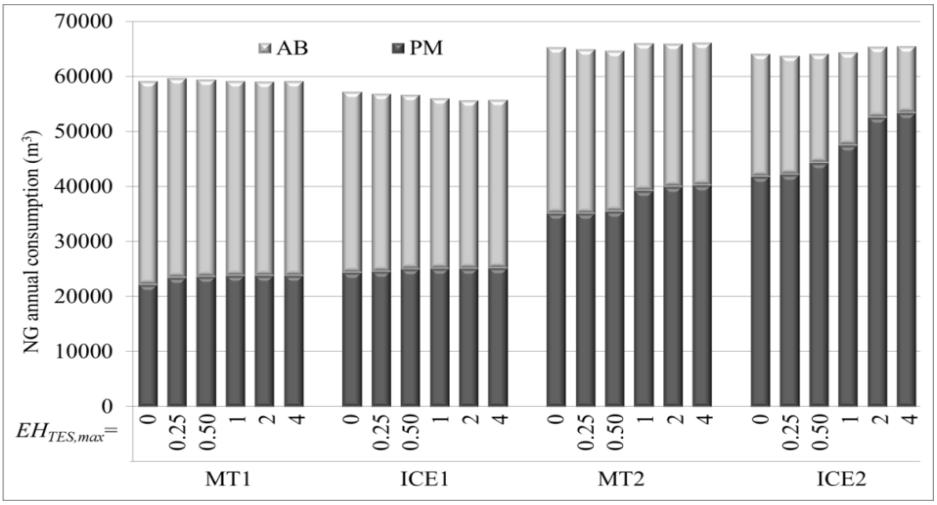

Figure 3.13. Natural gas annual consumptions of prime movers and auxiliary boilers relative to *operation 2* with η_{AB}=0.8.

In each analyzed case, the primary energy saving (PES) expressed in equivalent oil tons per year is calculated as follows:

$$PES = \frac{E_{el,PM}}{\eta_{el,ref}} + \frac{\left(E_{th,PM} - E_{th,dumped}\right)}{\eta_{th,ref}} - E_f \tag{3.8}$$

where $E_{el,PM}$ and $E_{th,PM}$ are the annual total electric and thermal energy generation of the prime mover, respectively; E_{dumped} is the total thermal energy dumped; E_f is the energy relative to the total annual natural gas consumed by the prime mover, evaluated by means of the natural gas lower heat value; and $\eta_{el,ref}$ and $\eta_{th,ref}$ are the reference efficiencies for the separate generation of electricity and heat in Italy [13,14], respectively. The reference efficiency for the separate generation of electricity is considered equal to the average efficiency relative to the electricity generation in Italy, evaluated as 0.46**l*, where *l* is a correction factor that depends on the avoided losses and on the percentage of electricity self-consumed, while the reference efficiency for the separate generation of heat is fixed to 0.90.

The primary energy savings relative to the micro-CHP systems for both operation strategies and for all values of $EH_{TES,max}$ are reported in Figure 3.14. The heat dumping in *operation 2* permits to obtain higher primary energy savings than those relative to *operation 1*, especially for the internal combustion engines that are the prime movers with the highest thermal efficiencies.

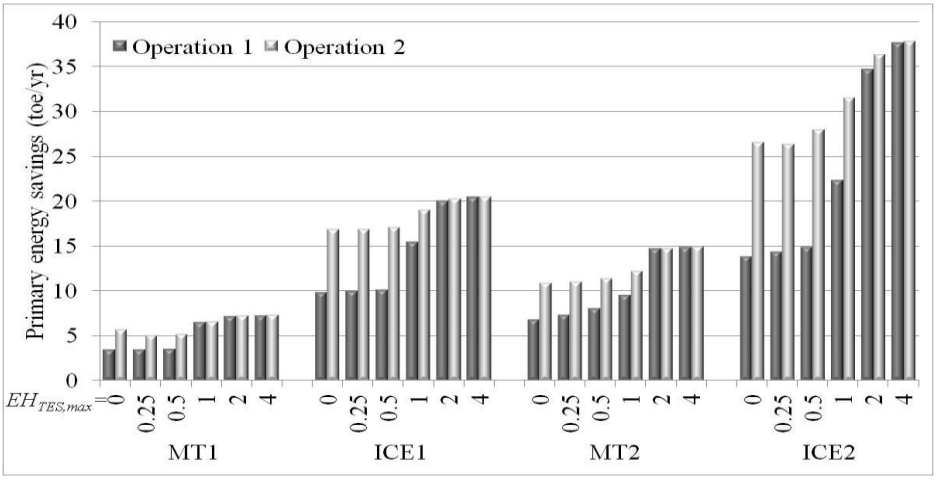

Figure 3.14. Primary energy savings relative to the micro-CHP systems with η_{AB}=0.8.

The micro-CHP systems annual economic savings with respect to the separate generation of electricity and heat are reported in Figure 3.15 for both operation strategies and for all values of $EH_{TES,max}$. The micro-CHP systems that present the highest economic savings are the ones relative to the internal combustion engines ICE1 and ICE2, due essentially to the their higher efficiencies. For all systems, at low $EH_{TES,max}$ the economic savings relative to *operation 2* are much higher than the ones relative to *operation 1*, due essentially to the much higher total operation hours of prime movers that occur when the heat dumping is allowed. For all micro-CHP systems, the maximum economic savings are obtained at the maximum value of $EH_{TES,max}$. At this value, the two different operation strategies present about the same economic savings, and this is because they have about the same operation hours.

Considering the results relative to *operation 1*, for the micro-CHP systems with ICE1, MT2 and ICE2, there is a sensible difference between the economic savings at $EH_{TES,max}$ equal to 2 and those relative to smaller values of $EH_{TES,max}$, while the economic savings at $EH_{TES,max}$ equal to 4 are slightly higher than the ones at $EH_{TES,max}$ equal to 2. Differently, for the micro-CHP system relative to MT1, the economic savings relative to $EH_{TES,max}$ equal to 1, 2 and 4 are very close to each other.

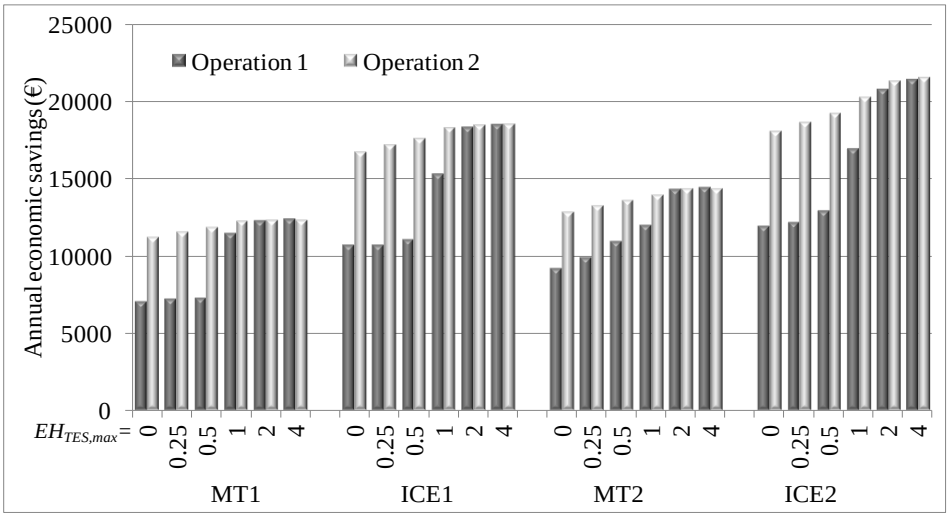

Figure 3.15. Annual economic savings relative to the micro-CHP systems with η_{AB}=0.8.

As to the results relative to *operation 2*, namely the operation strategy with heat dumping, it can be observed that for the micro-CHP systems with ICE1, MT2 and ICE2 about the same economic savings obtained in *operation 1* at $EH_{TES,max}$ equal to 2 are achieved at $EH_{TES,max}$ equal to 1 with slightly lower primary energy savings, as can be seen in Figure 3.14. Similar considerations can be made as regards the micro-CHP system with MT1, that in *operation 2* at $EH_{TES,max}$ equal to 0.25 and 0.5 presents economic savings even higher than those relative to *operation 1* at $EH_{TES,max}$ equal to 1.

Figure 3.16 shows for all micro-CHP systems the difference between the natural gas annual cost in separate generation and the one in combined generation (ΔAC_{NG}), and the difference between the electricity annual cost in separate generation and the one in combined generation ($\Delta AC_{electricity}$) for each value of $EH_{TES,max}$, with and without incentives, resulting from the implementation of *operation 2*.

In the majority of cases the value of ΔAC_{NG} is negative even with the tax reduction, meaning that the cost of natural gas in combined generation is higher than the one in separate generation. The only prime mover that presents for some values of $EH_{TES,max}$ a lower cost than the one in separate generation is ICE1. This is explained by considering that it is the prime mover with the highest thermal efficiency, and that the cases that present a positive ΔAC_{NG} are the ones with the highest prime mover operating hours and with the lowest dumped heat.

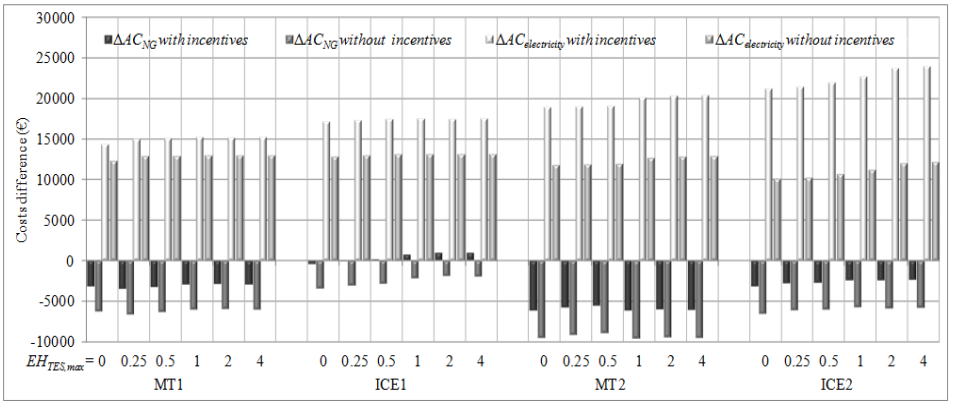

Figure 3.16. Difference between the natural gas annual cost in separate generation and the one in combined generation, and between the electricity annual cost in separate generation and the one in combined generation, with and without incentives, relative to *operation 2* with η_{AB}=0.8.

As concerns the differences of the electricity total costs, the values without incentives is evaluated considering only the electricity generated by the prime movers and self-consumed, while the values with incentives take also account of the value of the electricity released to the grid and not immediately consumed. It can be noticed that the ratios between the costs difference relative to the self-consumed electricity and the ones with incentives are higher for the prime movers with lower power. This result, considering that the mean cost of the self-consumed electricity is higher than the mean value of the generated electricity that is released to the grid, implies that the prime movers with lower power permit a better exploitation of the electricity generation, since they are less bounded by the constraints imposed by operational strategy. Finally, by considering the differences of the electricity total costs with incentives, it follows that the economic savings of micro-CHP systems are due to the fact that, in addition to thermal energy, the prime movers also generate electricity, that is fully recognized in the calculation of the incentives.

3.5.2. High efficiency auxiliary boilers

In the following, the results obtained considering the auxiliary boilers belonging to the best available technologies, with efficiency equal to 0.95 are presented.

Figure 3.17 shows for both operation strategies the total operation hours of the prime movers as a function of the maximum TES equivalent hours.

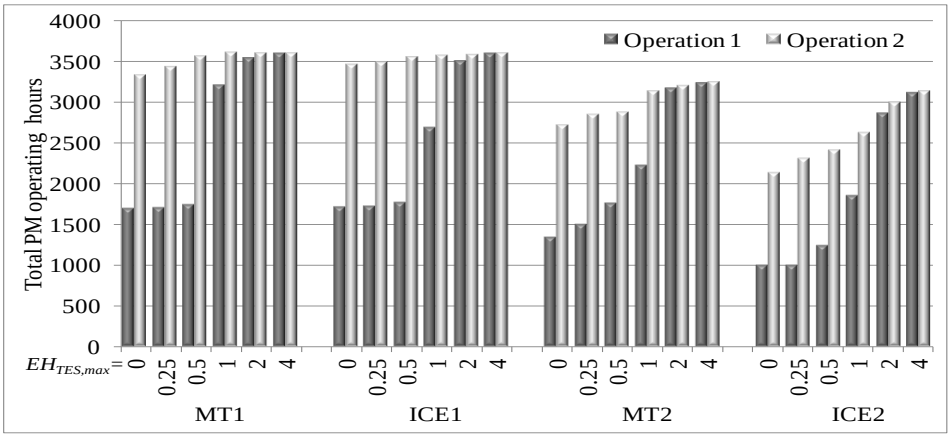

Figure 3.17. Total operation hours of the prime movers as a function of the maximum TES equivalent hours for both operation strategies with η_{AB}=0.95.

For both operation strategies, the prime movers with lower powers, MT1 and ICE1, present about the same total operation hours as in the case with η_{AB} equal to 0.8, while the operation hours of prime movers with higher powers, MT2 and ICE2, for all values of $EH_{TES,max}$ are in general lower than the corresponding ones relative to η_{AB} equal to 0.8. This last finding indicates that, for both operation strategies implemented on a hourly basis, the prime movers with higher powers are more sensitive to the cost reduction of the heat generated by the auxiliary boilers. Analogous considerations can be made for the dumped heat shown in Figure 3.18.

Figure 3.19 shows for each value of $EH_{TES,max}$ the natural gas annual consumptions of prime movers and auxiliary boilers with η_{AB} equal to 0.95 relative to *operation 2*. For all micro-CHP systems there is a general reduction of natural gas consumptions as compared to the cases with η_{AB} equal to 0.8, that for the micro-CHP systems with MT1 and ICE1 is essentially due to the higher efficiency of boilers, while for the ones with MT2 and ICE2 it is also due to the lower prime movers total operating hours.

The annual economic savings obtained by the micro-CHP systems with respect to the separate generation of electricity and heat relative to the cases with η_{AB} equal to 0.95 are reported in Figure 3.20 for both operation strategies and for all values of $EH_{TES,max}$.

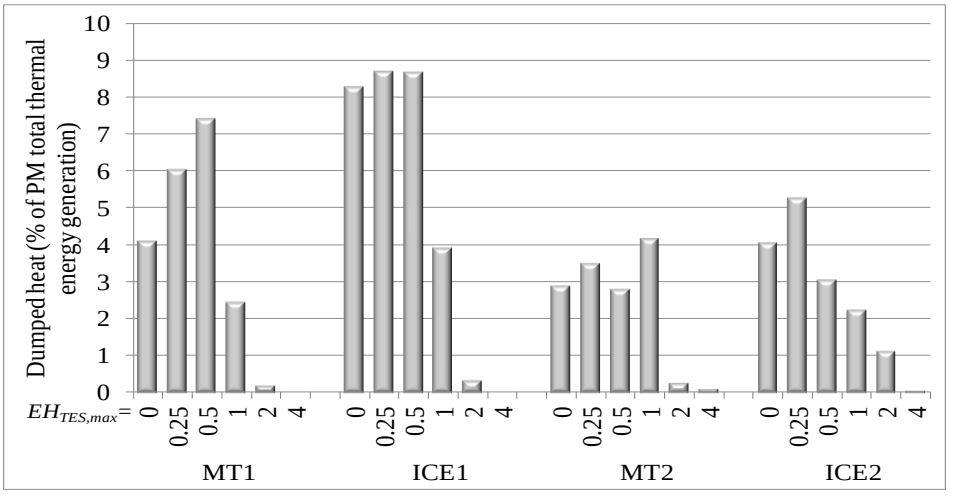

Figure 3.18. Dumped heat with η_{AB}=0.95.

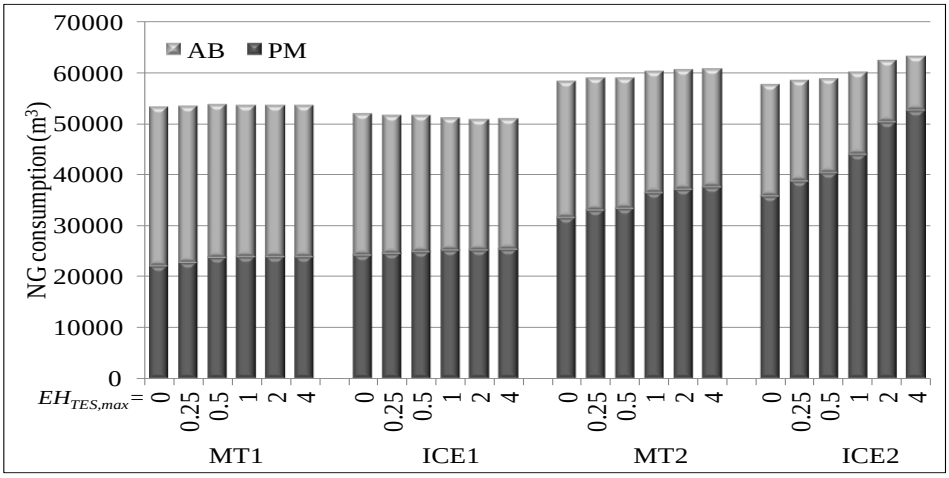

Figure 3.19. Natural gas annual consumptions of prime movers and auxiliary boilers with η_{AB}=0.95 relative to *operation 2*.

Comparing the results in Figure 3.20 with the ones relative to η_{AB} equal to 0.8 shown in Figure 3.15, it can be noticed that in this case there is a general reduction of the annual economic savings: for the systems with MT1 and ICE1 this is essentially due to the much lower natural gas consumption in the separate generation of heat; for the ones with MT2 and ICE2 it is also due to the lower prime movers total operating hours. For all systems, at low $EH_{TES,max}$ also in this case the

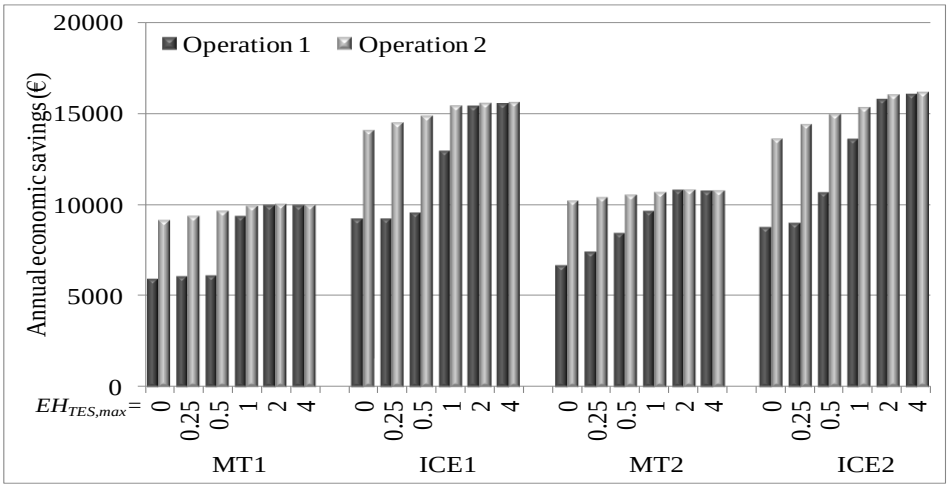

Figure 3.20. Annual economic savings relative to the micro-CHP systems with η_{AB}=0.95.

economic savings relative to *operation 2* are much higher than the ones relative to *operation 1*, and the micro-CHP systems that present the higher economic savings are the ones relative to the internal combustion engines, ICE1 and ICE2. Furthermore, considering in Figure 3.20 the results relative to the micro-CHP systems with ICE1 and ICE2, it can be noticed that for both operation strategies the economic savings of the two systems at the same values of $EH_{TES,max}$ do not differ significantly, and that for some small values of $EH_{TES,max}$ the economic savings relative to the system with ICE1 are even higher than the one with ICE2, that has twice the power of ICE1.

Figure 3.21 shows for all micro-CHP systems the difference between the natural gas annual cost in separate generation and the one in combined generation, and the difference between the electricity annual cost in separate generation and the one in combined generation for each value of $EH_{TES,max}$, with and without incentives, resulting from the implementation of *operation 2* and with η_{AB} equal to 0.95. In this case ΔAC_{NG} is always negative, that is a consequence of the higher reduction of natural gas consumption in separate generation.

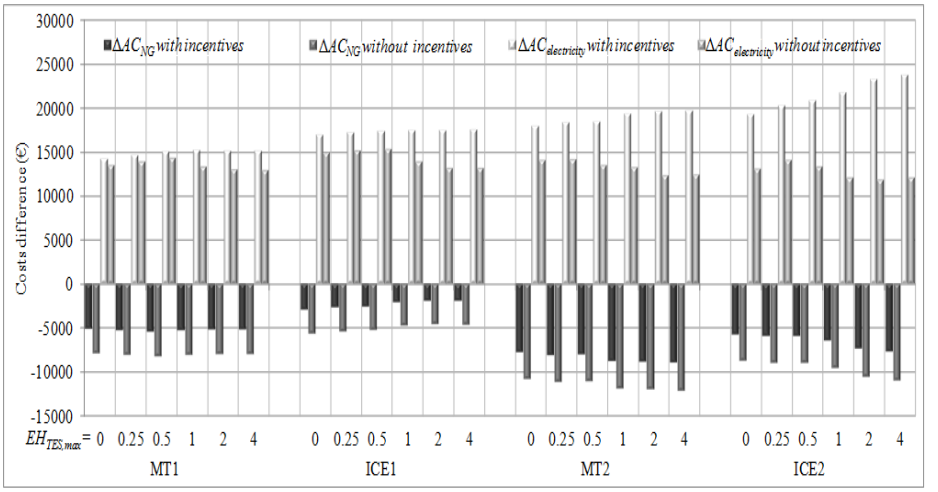

Figure 3.21. Difference between the natural gas annual cost in separate generation and the one in combined generation, and between the electricity annual cost in separate generation and the one in combined generation, with and without incentives, relative to *operation 2* with η_{AB}=0.95.

3.5.3. Economic analysis

The market price of a micro-CHP system depends mainly on the prime mover technology and size. Furthermore, even for a given technology and a certain size, in the Italian context it is very likely to get very different offers by different suppliers, due to the absence, at the moment in Italy, of a well-established market for micro-cogeneration systems. Conversely, for DHW storage tanks it is possible to obtain a reliable market price, as hot water storage represents an old technology widespread in many applications. For the above reasons, in order to identify for each prime mover the best size of the heat storage system from the economical point of view, the economic analysis is based on the evaluation in each case of the feasible investment cost for the purchase and the maintenance of the micro-CHP system net of the cost of the heat storage system, for two fixed pay-back periods.

Figure 3.22 shows a sketch of the hot water thermal energy storage system. In each analyzed case, the storage system is considered composed of an insulated cylindrical steel tank with aspect ratio 2, filled with water, and coil heat exchangers. The volume of the hot water inside the tank V_{HW} is estimated as follows:

$$V_{HW} = \frac{C_{TES,max}}{\rho_w c_{p,w} \left(T_{h,TES} - T_{c,TES}\right)} \tag{3.9}$$

where $T_{h,TES}$ is the hot water temperature with the storage tank fully charged, $T_{c,TES}$ is the reference cold water temperature relative to the heat storage tank, ρ_w and $c_{p,w}$ are the water density and specific heat at constant pressure, respectively, both calculated at the hot water temperature, and $C_{TES,max}$ is expressed in Joule. In all the

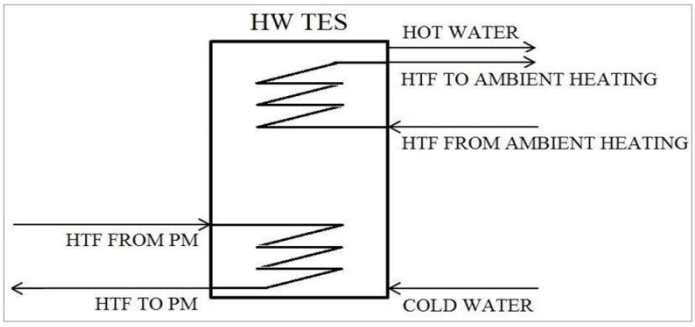

Figure 3.22. Sketch of the hot water thermal energy storage system.

analyzed cases, $T_{h,TES}$ is considered equal to 70°C, while $T_{c,TES}$ is fixed to 30°C. This last value represents the weighted average between the temperature of water entering the tank when the stored heat is used to feed the hot water utilities, namely the mains water at 10°C, and the temperature of the Heat Transfer Fluid (HTF) returning to the tank from the ambient heating system, that is supposed to be constant and equal to 35°C. The weight factors multiplying the above mains water temperature and HTF temperature are calculated as the ratio of the total thermal energy demand relative to domestic hot water, and of the total thermal energy relative to ambient heating to the total thermal demand, respectively. Table 3.5. reports the size of the DHW storage tanks of the micro-CHP systems for each value of the maximum TES equivalent hours.

The feasible investment cost of each micro-CHP system, that is returned over a given pay-back period, can be evaluated by means of the following relation:

$$NPV = -I + \sum_{i=1}^{N} AS_i /(1+r)^i = -(I^* + TC) + \sum_{i=1}^{N} AS_i /(1+r)^i \qquad (3.10)$$

where NPV is the net present value, AS_i represents the annual economic savings over the year i with respect to the separate generation, considered to be constant and equal to the ones reported in the previous sections, r is the discount rate, I is the investment cost relative to the purchase and the maintenance of the micro-CHP system, I^* is the above investment cost net of the cost of the heat storage system (TC). The cost of the boiler is not included in the investment cost since it is also present in separate generation. In each analyzed case, the cost of the heat storage system is evaluated by means of second order interpolation or extrapolation considering as base data the average costs of commercial hot water tanks relative to

Table 3.5. Sizes of the DHW storage tanks.

Prime mover	$EH_{TES,max}$	**0.25**	**0.5**	**1**	**2**	**4**
MT1	V_{HW} (m^3)	0.200	0.401	0.802	1.605	3.210
ICE1		0.257	0.515	1.030	2.060	4.120
MT2		0.325	0.650	1.301	2.602	5.205
ICE2		0.542	1.084	2.169	4.337	8.675

various sizes, derived from the offers by four different Italian suppliers shown in Figure 3.23. The values in Figure 3.23 refer to the costs of DHW storage tanks with two fixed serpentine heat exchangers, with the tanks made of steel with vitrification treatment, and insulated with a polyurethane layer of 50 mm, while the serpentine heat exchangers are made of stainless steel.

Figures 3.24 and 3.25 show I^*, expressed in €/kW$_{el}$, relative to the cases with conventional boiler, for a fixed pay-back period of 5 and 10 years, at which the net present value is assumed null, respectively. It can be seen that the prime movers with lower power present higher value of I^* than the ones with higher power, but this does not mean that they certainly are more economically convenient, since also their costs per electric kilowatt is expected to be higher. Differently from the economic savings, for all micro-CHP systems and for both operation strategies the maximum values of I^* are not obtained at the maximum storage sizes.

Considering the results relative to *operation 1*, for all the micro-CHP systems and for both the pay-back periods, the best choice from the economical point of view for the heat storage tank size is the one relative to $EH_{TES,max}$ equal to 2, and this is because for all systems the difference between the economic savings at $EH_{TES,max}$ equal to 2 and those relative to smaller values of $EH_{TES,max}$ is enough high to compensate the higher cost of the TES system, and also because the economic savings at $EH_{TES,max}$ equal to 4, that involve higher costs of the TES systems, are slightly higher than the ones at $EH_{TES,max}$ equal to 2.

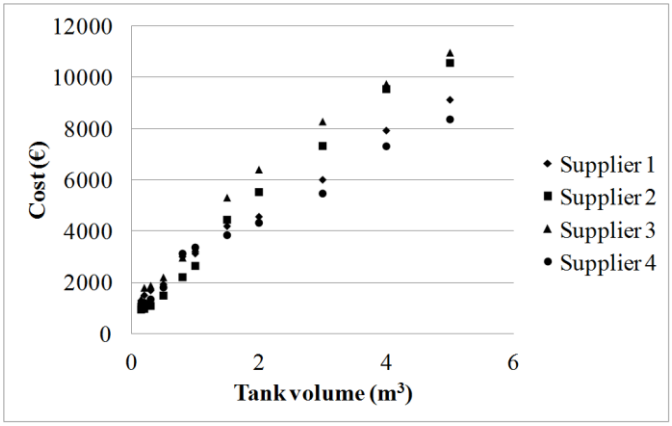

Figure 3.23. Cost of DHW heat storage tanks with two fixed serpentine heat exchangers.

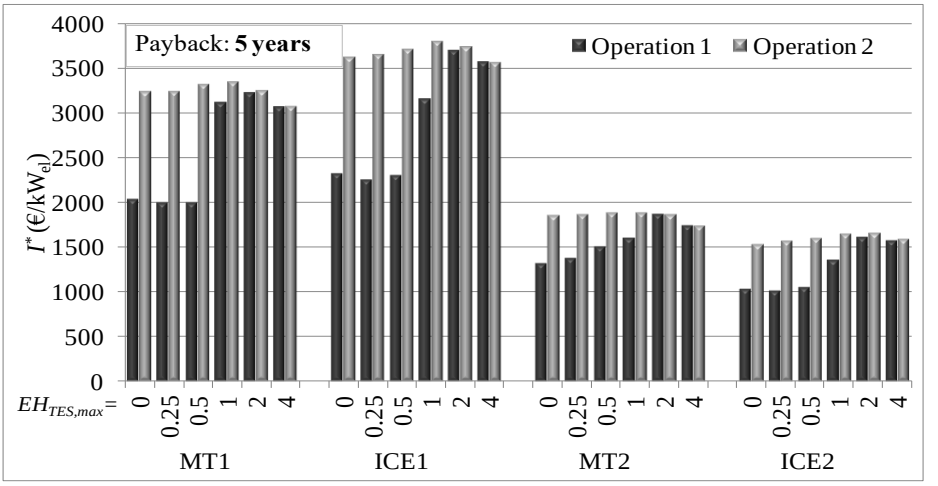

Figure 3.24. Feasible investment costs for a pay-back period of 5 years (η_{AB}=0.8).

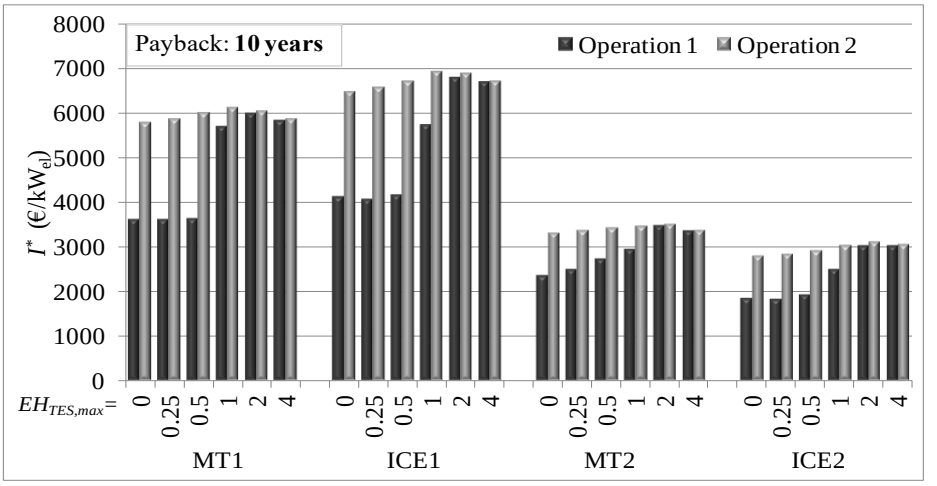

Figure 3.25. Feasible investment costs for a pay-back period of 10 years (η_{AB}=0.8).

As regards the results relative to *operation 2*, namely the operation strategy with heat dumping, it can be observed that for each micro-CHP system the maximum values of I^* are slightly higher than the corresponding ones relative to *operation 1*. For the micro-CHP systems relative to MT1 and ICE1, for both pay-back periods the maximum values of I^* are obtained at a lower storage size with respect to *operation 1*, i.e. at $EH_{TES,max}$ equal to 1, while for the ones relative to MT2 and

ICE2 the storage size corresponding to the maximum values of I^* depend on the pay-back period. In fact, for both systems the maximum I^* is at $EH_{TES,max}$ equal to 1 with the pay-back period of 5 years, while it is at $EH_{TES,max}$ equal to 2 with the pay-back period equal to 10. However, in the cases with the pay-back period equal to 10, I^* at $EH_{TES,max}$ equal to 1 is very close the one at $EH_{TES,max}$ equal to 2, so it can be assumed that the best choice of the heat storage size is the one relative to $EH_{TES,max}$ equal to 1 also for MT2 and ICE2, because it is much better in terms of encumbrance of the heat storage system. As a concluding observation, considering the above statements and that for all micro-CHP systems the values of I^* at the different heat storage sizes are very close to each other in *operation 2*, it can be assumed that in case of heat dumping for all systems the best choice for the heat storage size among the analyzed ones is the one relative to $EH_{TES,max}$ equal to 1, i.e. half compared to the case without dumping, as it can represent the right compromise between the necessity to maximize the feasible investment costs, the practical interest in limiting the encumbrance of the heat storage system, and the practical convenience of having a quite large thermal energy buffer.

Similar considerations can be made by analyzing Figures 3.26 and 3.27, showing I^*, relative to the cases with high efficiency boiler, for a fixed pay-back period of 5 and 10 years, respectively. As it was to be expected, the higher boilers efficiency involves in all cases a reduction of the feasible investment cost I^*.

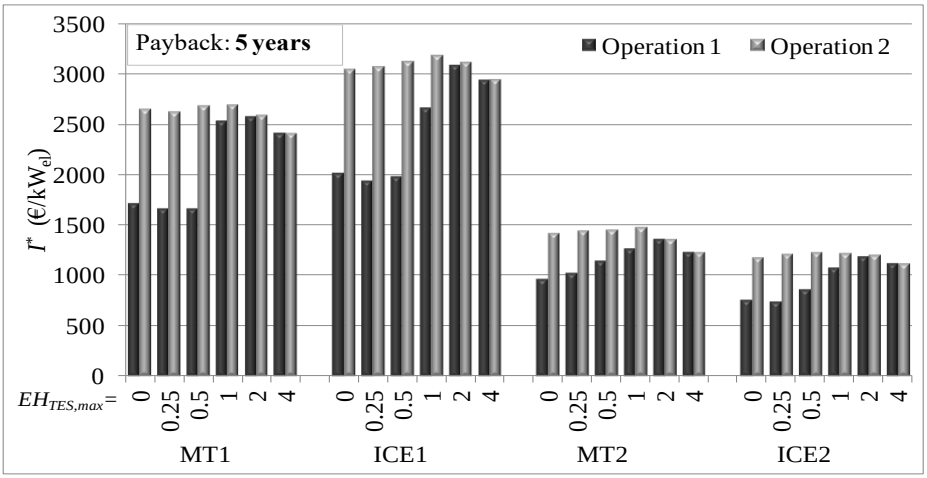

Figure 3.26. Feasible investment costs for a pay-back period of 5 years (η_{AB}=0.95).

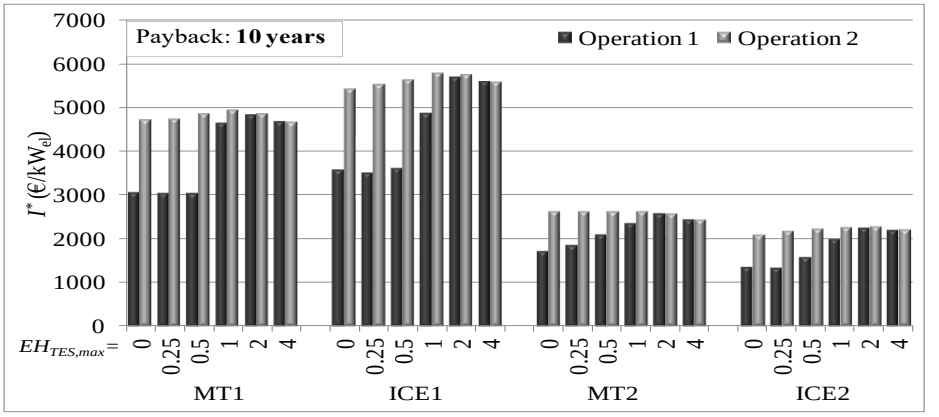

Figure 3.27. Feasible investment costs for a pay-back period of 10 years (η_{LAB}=0.95).

3.5.4. Pollutants emission

The annual global emissions of CO_2, evaluated by means of the approach described in Section 3.4.2, and relative to the cases with conventional boilers and the one relative to the cases with high efficiency boilers are reported in Tables 3.6 and 3.7, respectively. The annual local emissions of CO and NO_X, evaluated by means of the approach described in Section 3.4.2, and relative to the cases with conventional boilers and the one relative to the cases with high efficiency boilers are reported in Tables 3.8 and 3.9, and in Tables 3.10 and 3.11, respectively.

In Tables 3.6 and 3.7, the global CO_2 emissions relative to the micro-CHP systems, represented by the prime movers, also include the emissions relative to the auxiliary boilers and those relative to the electricity taken from the grid over the entire year, including the six months in which the prime mover is inactive. Differently, in Tables 3.8 and 3.9, and in Tables 3.10 and 3.11, which report annual emissions on local scale, the emissions relative to the electricity taken from the grid are not included in micro-CHP ones, as it is generated by centralized power plants that are usually located far away from residential districts. The tables also report the annual emissions due to the separate generation of heat and electricity in order to cover the heat and electricity demands of the user for both considered values of the auxiliary boilers efficiency, evaluated as described in Section 3.4.2.

The results reported in Tables 3.6 and 3.7 indicate that the annual global CO_2 emissions of the internal combustion engines are lower than the ones of the

microturbines, due essentially to their higher thermal and electrical efficiencies. However, the annual global CO_2 emissions of the micro-CHP systems are always well below the ones due to the separate generation, and this represents a very important result, since CO_2 emissions are one of the main responsible of the greenhouse effect in the Earth atmosphere.

The results reported in Tables 3.8 and 3.9 show that the annual local CO emissions of the micro-CHP systems are much higher than the ones due to separate generation, especially for the micro-CHP systems with an internal combustion engine as prime mover, because of their higher emission factors. The results reported in Table 3.10 and 3.11 show that the annual local NO_X emissions of the micro-CHP systems with microturbines as prime mover are lower than the ones of the separate generation, whereas the NO_X relative to the internal combustion engines are much higher than the ones of the separate generation.

Results also show that for each micro-CHP system the increase in annual global CO_2 emissions in *operation 2* with respect to *operation 1* are not marked, while the increase in annual local CO emissions in *operation 2* with respect to *operation 1* is very strong at low $EH_{TES,max}$, namely when there is a sensible heat dumping. As concerns the annual local NO_X emissions, it can be seen that for the internal combustion engines the emissions in *operation 2* are higher than the ones of *operation 1* especially at low $EH_{TES,max}$, whereas for microturbines the emissions relative to *operation 2* are lower than the ones of *operation 1*. Moreover, by increasing the storage size, the NO_X emissions of microturbines decrease. This is due to the fact that the NO_X emission factors of the two microturbines are lower than the corresponding one of the separate generation, for this reason by increasing the prime mover working hours, the NO_X emission decrease. Anyway, in case the comparison is made between the best configurations from the economical point of view, namely the ones relative to $EH_{TES,max}$ equal to 2 in *operation 1* and those relative to $EH_{TES,max}$ equal to 1 in *operation 2*, the differences between the two operation strategies are not significant. These results are a consequence of the fact that in *operation 2* at $EH_{TES,max}$ equal to 1 the total dumped heat represents a low percentage of the total thermal energy generated by the micro-CHP systems during the entire operation period.

Table 3.6. Annual CO_2 emissions released by the analyzed micro-CHP systems and by separate generation on a global scale for the cases in which η_{AB}=0.80.

Prime mover	$EH_{TES,max}$	**Annual global emission of CO_2 (kg)**		
		Operation 1 **(η_{AB}=0.80)**	***Operation 2*** **(η_{AB}=0.80)**	**SG (η_{AB}=0.80)**
MT1	0	1.045E+05	1.121E+05	1.925E+05
	0.25	1.045E+05	1.132E+05	
	0.5	1.046E+05	1.127E+05	
	1	1.096E+05	1.121E+05	
	2	1.114E+05	1.117E+05	
	4	1.117E+05	1.116E+05	
ICE1	0	1.021E+05	1.083E+05	
	0.25	1.014E+05	1.075E+05	
	0.5	1.014E+05	1.070E+05	
	1	1.028E+05	1.055E+05	
	2	1.047E+05	1.048E+05	
	4	1.048E+05	1.048E+05	
MT2	0	1.107E+05	1.246E+05	
	0.25	1.115E+05	1.238E+05	
	0.5	1.121E+05	1.227E+05	
	1	1.149E+05	1.259E+05	
	2	1.248E+05	1.255E+05	
	4	1.255E+05	1.255E+05	
ICE2	0	1.079E+05	1.223E+05	
	0.25	1.076E+05	1.216E+05	
	0.5	1.082E+05	1.220E+05	
	1	1.128E+05	1.223E+05	
	2	1.216E+05	1.238E+05	
	4	1.238E+05	1.241E+05	

Table 3.7. Annual CO_2 emissions released by the analyzed micro-CHP systems and by separate generation on a global scale for the cases in which η_{AB}=0.95.

Prime mover	$EH_{TES,max}$	**Annual global emission of CO_2 (kg)**		
		Operation 1 **(η_{AB}=0.95)**	***Operation 2*** **(η_{AB}=0.95)**	**SG (η_{AB}=0.95)**
MT1	0	0.898E+05	0.999E+05	1.326E+05
	0.25	0.899E+05	1.013E+05	
	0.5	0.899E+05	1.009E+05	
	1	0.973E+05	1.005E+05	
	2	0.987E+05	1.003E+05	
	4	1.00E+05	1.002E+05	
ICE1	0	0.891E+05	0.975E+05	
	0.25	0.875E+05	0.967E+05	
	0.5	0.875E+05	0.967E+05	
	1	0.906E+05	0.955E+05	
	2	0.947E+05	0.949E+05	
	4	0.949E+05	0.950E+05	
MT2	0	0.948E+05	1.103E+05	
	0.25	0.961E+05	1.116E+05	
	0.5	0.991E+05	1.110E+05	
	1	1.029E+05	1.141E+05	
	2	1.137E+05	1.144E+05	
	4	1.144E+05	1.144E+05	
ICE2	0	0.932E+05	1.091E+05	
	0.25	0.931E+05	1.108E+05	
	0.5	0.957E+05	1.113E+05	
	1	1.031E+05	1.139E+05	
	2	1.162E+05	1.182E+05	
	4	1.195E+05	1.196E+05	

Table 3.8. Annual CO emissions released by the analyzed micro-CHP systems and by separate generation on a local scale for the cases in which η_{AB}=0.80.

Prime mover	$EH_{TES,max}$	**Annual local emission of CO (kg)**		
		Operation 1 **(η_{AB}=0.80)**	***Operation 2*** **(η_{AB}=0.80)**	**SG (η_{AB}=0.80)**
MT1	0	23.41	35.41	12.46
	0.25	23.46	36.74	
	0.5	23.46	36.88	
	1	33.18	37.06	
	2	36.58	37.02	
	4	37.01	36.97	
ICE1	0	40.44	76.39	
	0.25	43.19	76.89	
	0.5	43.58	77.73	
	1	57.59	77.90	
	2	76.61	77.77	
	4	78.00	78.09	
MT2	0	34.58	56.19	
	0.25	36.09	56.12	
	0.5	37.22	56.90	
	1	42.43	61.32	
	2	60.88	62.12	
	4	62.26	62.30	
ICE2	0	65.80	129.22	
	0.25	65.69	130.47	
	0.5	69.12	135.77	
	1	95.72	144.03	
	2	146.31	157.11	
	4	159.55	160.82	

Table 3.9. Annual CO emissions released by the analyzed micro-CHP systems and by separate generation on a local scale for the cases in which η_{AB}=0.95.

Prime mover	$EH_{TES,max}$	**Annual local emission of CO (kg)**		
		Operation 1 **(η_{AB}=0.95)**	***Operation 2*** **(η_{AB}=0.95)**	**SG (η_{AB}=0.95)**
MT1	0	20.29	32.84	8.31
	0.25	20.34	34.23	
	0.5	20.34	34.40	
	1	30.56	34.63	
	2	34.14	34.60	
	4	34.59	34.54	
ICE1	0	37.69	74.15	
	0.25	40.26	116.43	
	0.5	40.66	117.67	
	1	55.02	75.82	
	2	74.53	75.71	
	4	75.96	76.05	
MT2	0	28.41	49.22	
	0.25	29.98	51.28	
	0.5	34.24	51.02	
	1	39.88	55.44	
	2	55.44	56.41	
	4	56.47	56.53	
ICE2	0	55.47	110.16	
	0.25	55.32	118.70	
	0.5	65.35	123.15	
	1	93.76	133.36	
	2	144.07	150.81	
	4	156.69	157.22	

Table 3.10. Annual NO_X emissions released by the analyzed micro-CHP systems and by separate generation on a local scale for the cases in which η_{AB}=0.80.

Prime mover	$EH_{TES,max}$	**Annual local emission of NO_X (kg)**		
		Operation 1 **(η_{AB}=0.80)**	***Operation 2*** **(η_{AB}=0.80)**	**SG (η_{AB}=0.80)**
MT1	0	61.92	53.78	78.95
	0.25	61.88	53.08	
	0.5	61.88	52.44	
	1	54.35	51.68	
	2	51.72	51.44	
	4	51.39	51.42	
ICE1	0	105.00	147.00	
	0.25	107.00	147.20	
	0.5	107.80	148.77	
	1	123.65	147.00	
	2	145.12	146.45	
	4	146.69	146.80	
MT2	0	58.00	47.70	
	0.25	57.14	47.09	
	0.5	56.49	46.37	
	1	53.52	43.51	
	2	42.98	42.32	
	4	42.13	42.13	
ICE2	0	136.44	214.22	
	0.25	136.48	215.11	
	0.5	140.27	221.14	
	1	171.96	230.24	
	2	232.83	245.37	
	4	248.01	249.55	

Table 3.11. Annual NO_X emissions released by the analyzed micro-CHP systems and by separate generation on a local scale for the cases in which η_{AB}=0.95.

Prime mover	$EH_{TES,max}$	**Annual local emission of NO_X (kg)**		
		Operation 1 **(η_{AB}=0.95)**	***Operation 2*** **(η_{AB}=0.95)**	**SG (η_{AB}=0.95)**
MT1	0	18.17	17.87	20.78
	0.25	18.17	17.88	
	0.5	18.17	17.75	
	1	17.70	17.59	
	2	17.53	17.52	
	4	17.51	17.51	
ICE1	0	66.00	116	
	0.25	66.26	74.69	
	0.5	66.83	75.58	
	1	87.67	117.89	
	2	115.96	117.68	
	4	118.03	118.17	
MT2	0	18.77	19.01	
	0.25	18.77	18.97	
	0.5	18.77	18.84	
	1	18.77	18.88	
	2	18.77	18.78	
	4	18.77	18.77	
ICE2	0	88.73	168.65	
	0.25	88.89	181.04	
	0.5	103.12	187.48	
	1	144.56	202.36	
	2	217.92	227.79	
	4	236.33	237.10	

Figures 3.28, 3.29 and 3.30 show a graphical representation of CO_2, CO and NO_X emissions relative to the cases with conventional auxiliary boilers, respectively.

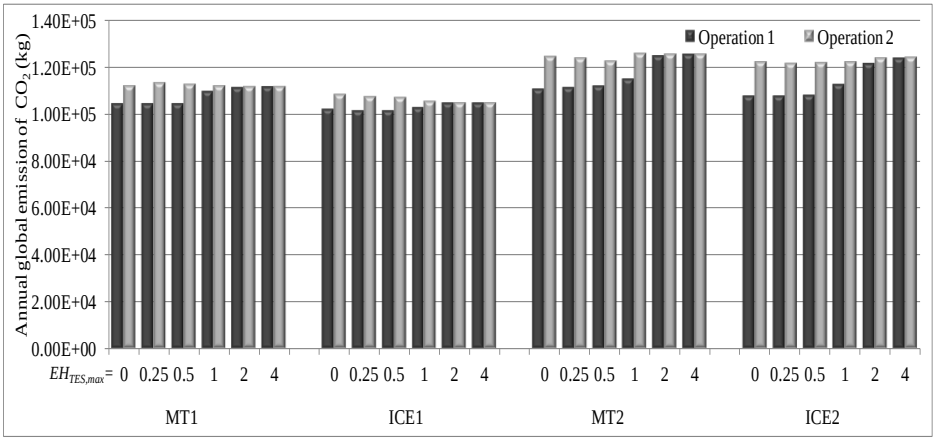

Figure 3.28. Annual global emission of CO_2 for micro-CHP systems with conventional boilers.

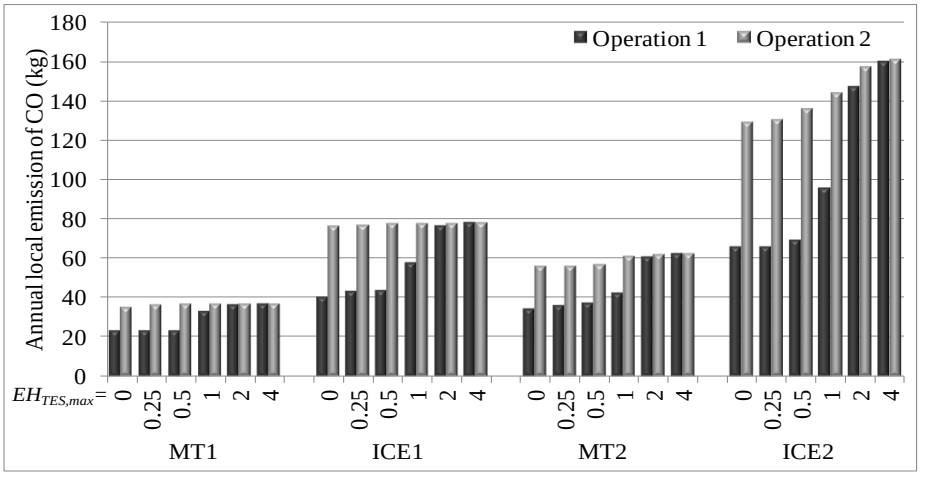

Figure 3.29. Annual local emission of CO for micro-CHP systems with conventional boilers.

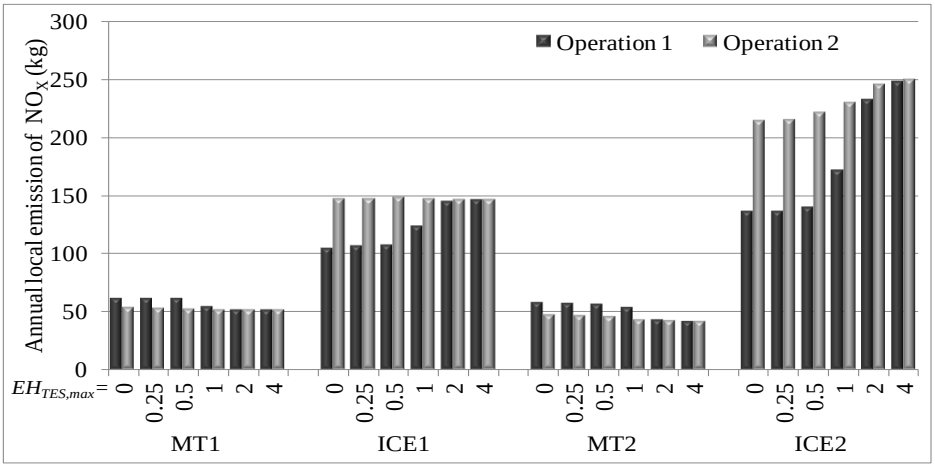

Figure 3.30. Annual local emission of NO_X for micro-CHP systems with conventional boilers.

References

[1] E.S. Barbieri, F. Melino, M. Morini. Influence of the thermal energy storage on the profitability of micro_CHP systems for residential building applications. Applied Energy. Volume 97 (2012), pp. 714–722.

[2] G. Streckiene, V. Martinaitis, A.N. Andersen, J. Katz. Feasibility of CHP-plants with thermal stores in the German spot market. Applied Energy. Volume 86 (2009), pp. 2308-2316.

[3] M. Bianchi, A. De Pascale, P.R. Spina. Guidelines for residential micro-CHP systems design. Applied Energy. Volume 97 (2012), pp. 673–685.

[4] A. Canova, G. Chicco, G. Genon, P. Mancarella. Emission characterization and evaluation of natural gas-fueled cogeneration microturbines and internal combustion engines. Energy Conversion and Management. Volume 49 (2008), pp. 2900-2909.

[5] P. Mancarella, G. Chicco. Global and local emission impact assessment of distributed cogeneration systems with partial-load models. Applied Energy. Volume 86 (2009), pp. 2096–2106.

[6] EPBD buildings platform. Country reports; 2008. [ISBN 2-930471-29-8].

[7] Italian D.M. 22/11/2012, Gazzetta Ufficiale n. 290 (2012).

[8] http://www.autorita.energia.it/it/inglese/index.htm.

[9] Italian law 44/12, Gazzetta Ufficiale n. 99 (2012).

[10] Resolution ARG/elt 74/08 (2008), http://www.autorita.energia.it/it/docs/08/074-08arg.htm.

[11] Directive 2004/8/EC of the European Parliament and of the Council, Official Journal of the European Union, 11 February 2004, pp. 50-60.

[12] Italian D.lgs 20/07, Gazzetta Ufficiale n. 54 (2007).

[13] Italian D.M. 04/08/2011, Gazzetta Ufficiale n. 218 (2011).

[14] Italian D.M. 05/09/2011, Gazzetta Ufficiale n. 218 (2011).

"There is no such thing as steady-state, the world is always changing"

Chapter 4. Dynamic simulation of a micro-CHP system operating according to the operation strategy with heat dumping

4.1. Introduction

In this chapter, the dynamic simulation of a residential micro-CHP system operating according to the heat dumping and no-dumping full-load operation strategies, introduced in Chapter 3, is presented to demonstrate the practical feasibility of the two above operation strategies, and the effectiveness of the heat dumping.

In detail, the dynamic simulation of two cases optimized in the previous chapter, one for each operation strategy, that present nearly the same operation hours and economic savings is carried out by using the commercial software TRNSYS 17, and the choice of the two configurations is made by considering a compromise between the economic savings and the size of the storage tank.

The micro-CHP system under consideration is the one presented in Chapter 3 with ICE1 as prime mover, since it presents the highest value of the feasible investment cost for both fixed values of the payback period, and the selected configurations are relative to the one with $EH_{TES,max}$ equal to 2 in the case without heat dumping (*operation 1*), and the one with $EH_{TES,max}$ equal to 1 in the case with heat dumping (*operation 2*), as they present almost the same value of the economic savings and of the working hours. The user is the same considered for the economic

optimization conducted in Chapter 3, and is represented by a residential block of flats with 50 apartments situated in the Italian climatic zone E.

In the following, the case study, or rather the details of the energetic system, and of the user are presented in Section 4.2. The main results of the economic optimization of the micro-CHP system with ICE1 as prime mover, obtained with the analysis conducted in Chapter 3, are presented in Section 4.3, to clarify how the two configurations are selected. Then, the TRNSYS dynamic simulation of the system for both operation strategies is presented in Section 4.4, whereas the main results are presented and discussed in Section 4.5.

4.2. Case study

Figure 4.1 shows a simplified layout of the micro-CHP plant. According to it, the prime mover is interconnected with the external electrical grid, the internal electric network relative to the user, and the thermal energy storage system (TES). In turn, it is connected with the heat distribution network of the user, and an auxiliary boiler (AB) fed by natural gas.

The TES system allows to accumulate thermal energy for a later use when the instantaneous thermal demand is lower than the micro-CHP prime mover heat generation.

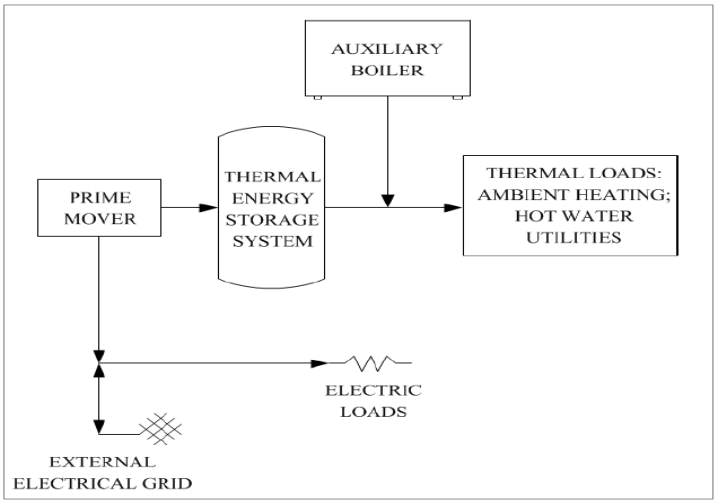

Figure 4.1. Layout of the micro-CHP plant.

The electrical energy generated by the prime mover is sent either to the users, or to the external electrical grid in the case of zero electric energy consumption, or to both of them in the case of a surplus of generation with respect to the instantaneous electricity demand. Otherwise, if the instantaneous electricity demand is higher than the electric power provided by the prime mover, electricity is taken from the external grid.

The prime mover is considered to be the internal combustion engine ICE1, presented in the previous chapter, whose main characteristics are shown in Table 4.1, since the economic results of the optimization process, conducted in Chapter 3, relative to the operation optimization of the micro-CHP system with ICE1 as prime mover, present the highest feasible investment cost for both fixed values of the payback period, as shown in Figures 3.24, 3.25, and 3.26, 3.27 showing the maximum feasible investment cost relative to the purchase of the micro-CHP systems in the cases in which the auxiliary boiler efficiency is equal to 0.8 and 0.95, respectively.

As to the user, it is represented by a residential block of flats with 50 apartments located in the Italian climatic zone E, whose main characteristics are shown in Table 4.2. Its thermal and electrical demand, and the hourly load profile relative to the ambient heating, domestic hot water, electrical appliances, and air conditioning demands are evaluated as in the previous chapter with reference to [1-3].

4.3. Main results of the micro-CHP system economic optimization

The economic optimization of the micro-CHP system operating according to the two operation strategies, or rather the one without heat dumping (*operation 1*), and the one with heat dumping (*operation 2*) are carried out as in Chapter 3, considering the tariffs and the incentives reported in [4-7]. As presented in Chapter 3, the micro-CHP system operation is analyzed by considering six values of the thermal energy storage system equivalent hours, ranging from the limit case without storage to 4.

Table 4.1. Prime mover characteristics.

Prime mover	P_{el} **(kW)**	P_{th} **(kW)**	η_{el} **(%)**	η_{th} **(%)**
ICE1	20	47.5	28.6	67.9

Table 4.2. Main characteristics of the user.

Total floor area (m^2)	5000
Shape factor S/V (m^{-1})	0.5
Yearly thermal energy demand for ambient heating ($kWh/m^2/yr$)	68
Yearly thermal demand for the hot water utilities ($kWh/m^2/yr$)	15
Yearly electric energy demand for electric appliances ($kWh/m^2/yr$)	18
Yearly electric energy demand for air conditioning ($kWh/m^2/yr$)	7

In the following the main results of the economic optimization of the system are reported in terms of the prime mover working hours, the percentage of the heat dumped, the primary energy savings obtained with respect to the separate generation of electricity and heat, and the economic savings to explain how the two configurations to be dynamically simulated are chosen.

Figure 4.2 shows for both operation strategies the total operation hours of the prime mover as a function of the maximum TES equivalent hours. In the case of *operation 1*, the prime mover operation hours increase with the increase in the maximum TES equivalent hours, especially at low values of $EH_{TES,max}$, whereas in the case of *operation 2*, it presents in general a low variation of the total operation hours. From this figure it can be noticed that, in the case of *operation 1* with $EH_{TES,max}$ equal to 2 and in the case of *operation 2* with $EH_{TES,max}$ equal to 1, the prime mover presents almost the same values of the working hours, being equal to 3512, and 3588, respectively. As already widely said in Chapter 3, the main effect of heat dumping on the prime mover operation is the increasing of its working hours that, in some cases, can be substantial with respect to the values obtained when the prime mover operates according to the no-dumping operation strategy. However, in the case with ICE1 as prime mover, the percentage of heat dumping is always quite low as compared to the total thermal energy generated by the prime mover. Figure 4.3 shows the percentage of the annual heat dumped from the micro-

CHP system, represented by the prime mover, for each value of $EH_{TES,max}$ relative to *operation 2*. The dumped heat is higher at low $EH_{TES,max}$ and approaches zero at larger heat storage system, being at most equal to about 9% of thermal generation, and equal to 4.2% for $EH_{TES,max}$ equal to 1.

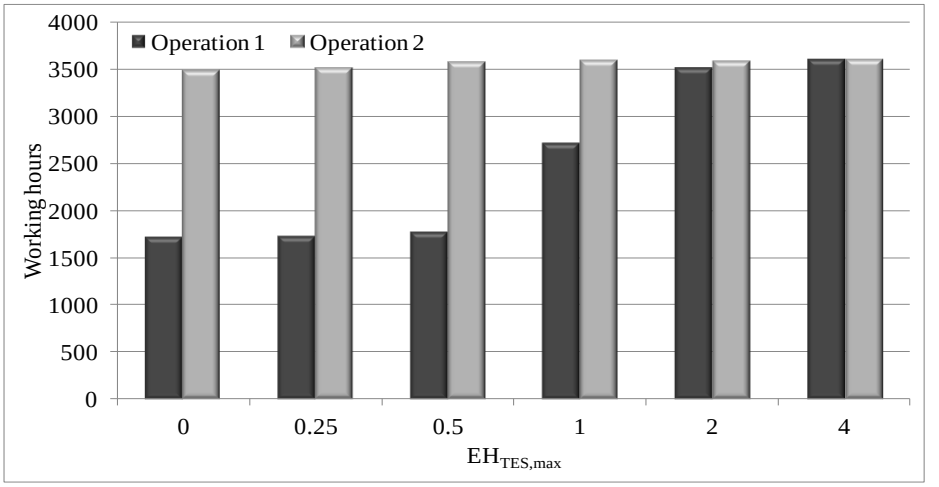

Figure 4.2. Total operation hours of the prime mover as a function of the maximum TES equivalent hours for both operation strategies.

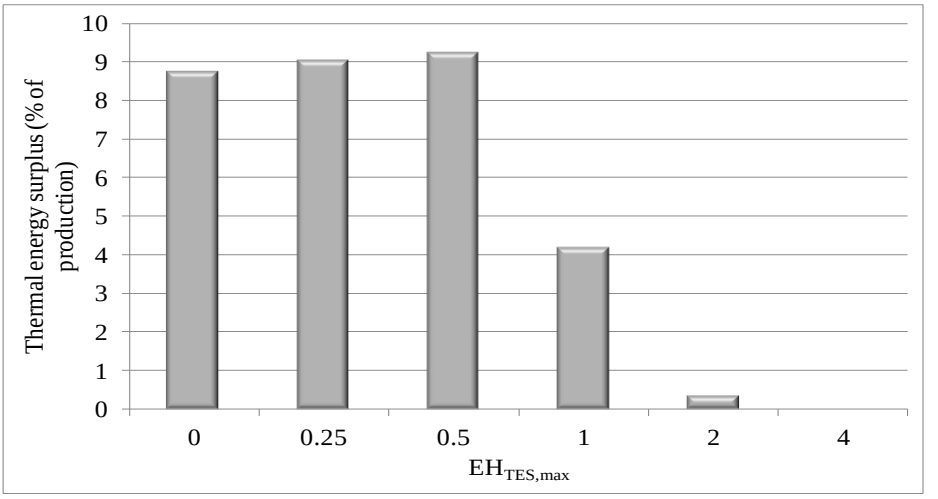

Figure 4.3. Percentage of the annual heat dumped from the prime mover as a function of the maximum TES equivalent hours for *operation 2*.

Figure 4.4 shows the primary energy savings evaluated according to [8,9], and relative to the micro-CHP system for both operation strategies and for all values of $EH_{TES,max}$, whereas Figure 4.5 shows for both operation strategies and for all values of $EH_{TES,max}$, the annual economic savings obtained by the micro-CHP system with respect to the separate generation of electricity and heat. From Figure 4.4, it can be seen that the heat dumping in *operation 2* permits to obtain higher primary energy savings than those relative to *operation 1*, and from Figure 4.5 that at low $EH_{TES,max}$ the economic savings relative to *operation 2* are much higher than the ones relative to *operation 1*, due essentially to the much higher total operation hours of prime movers that occur when the heat dumping is allowed. From this figure, it can also be notice that the economic savings obtained in the case of *operation 1* with $EH_{TES,max}$ equal to 2 are almost the same of those obtained in the case of *operation 2* with $EH_{TES,max}$ equal to 1, being equal to 18,264 €, and 18,269 €, respectively.

As consequence of this, it is clear that in the case of *operation 1* the best choice for the heat storage tank size could be the one relative to $EH_{TES,max}$ equal to 2, because there is a sensible difference between the economic savings at $EH_{TES,max}$ equal to 2 and those relative to smaller values of $EH_{TES,max}$, and also because the economic savings at $EH_{TES,max}$ equal to 4, that would involve higher investment costs for the TES systems, are slightly higher than the ones at $EH_{TES,max}$ equal to 2.

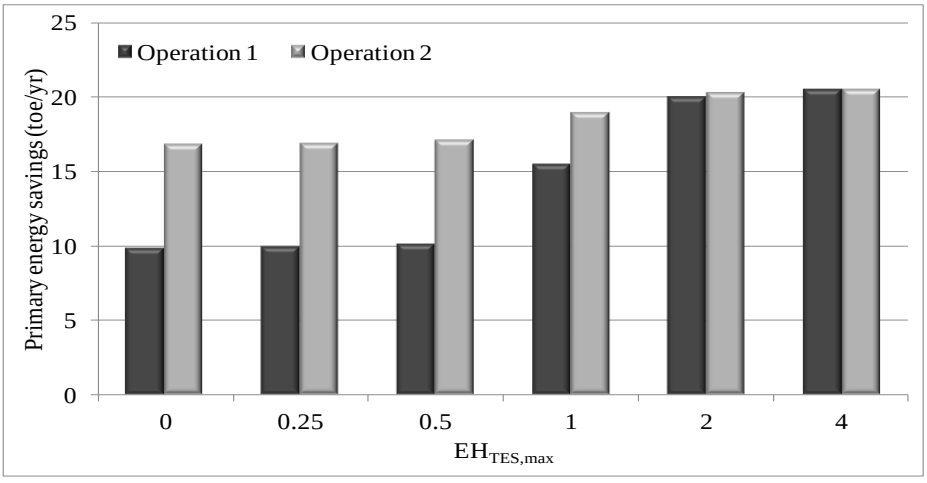

Figure 4.4. Primary energy savings relative to the micro-CHP system as a function of the maximum TES equivalent hours.

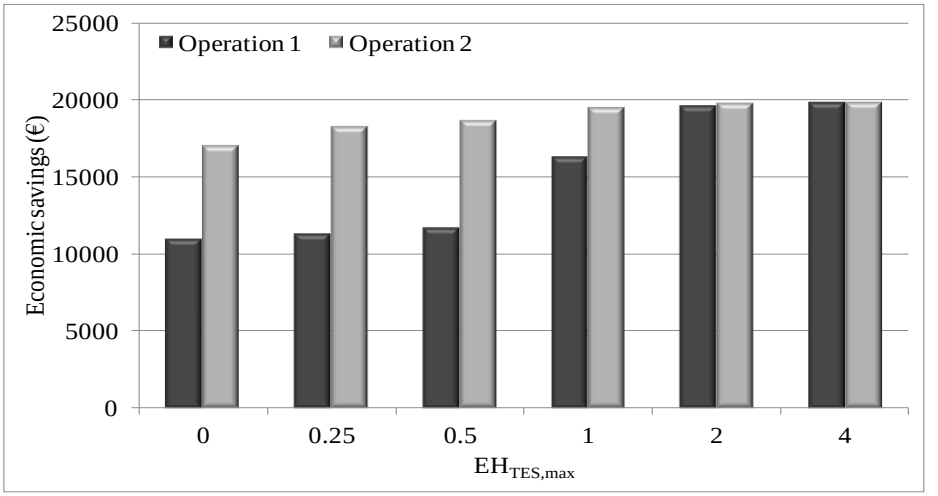

Figure 4.5. Annual economic savings relative to the micro-CHP system as a function of the maximum TES equivalent hours.

As to the results relative to *operation 2*, the same economic savings obtained in *operation 1* at $EH_{TES,max}$ equal to 2 are achieved at $EH_{TES,max}$ equal to 1, with slightly lower primary energy savings, implying lower investment costs for the TES system.

For the above reasons, the two configurations selected for the purpose of the dynamic simulation of the prime mover operating according to the two operation strategies are, the one relative to $EH_{TES,max}$ equal to 2 in the case without heat dumping, and the one relative to $EH_{TES,max}$ equal to 1 in the case with heat dumping.

4.4. TRNSYS simulation

The commercial software TRNSYS 17 is used to demonstrate the effectiveness of heat dumping. For this purpose, the simulation of two optimized cases, one for each operation strategy, that present nearly the same operation hours and economic savings are carried out. The choice of the two configuration is made considering a compromise between the economic savings and the size of the tank. In particular, according to the results shown in Section 4.3, the two selected configurations are the one relative to $EH_{TES,max}$ equal to 2 in the case without heat dumping, and the one relative to $EH_{TES,max}$ equal to 1 in the case with heat dumping.

In the following the thermal energy storage system characteristics are presented in Section 4.4.1, whereas the dynamic simulation of the system operating according to the operation strategy without heat dumping, and to the one with heat dumping are presented in Sections 4.4.2, and 4.4.3, respectively.

4.4.1. Thermal energy storage system

Figure 4.6 presents the scheme of the thermal energy storage system. It consists in a vertical cylindrical tank for hot water storage, with aspect ratio equal to 2, and two immersed coiled tube heat exchangers, and it is considered divided into 50 isothermal nodes.

In order to conduct the dynamic simulation of the storage system, in both cases, or rather in the case of *operation 1* (no-dumping), and in the case of *operation 2* (with heat dumping), the TRNSYS *Type 60* is used. This TRNSYS component represents the most detailed tank model available in the standard TRNSYS library, and models a stratified fluid storage tank with optional internal heaters and optional internal heat exchangers, which makes it suitable to model many commercially available domestic hot water tanks [10].

In each case, the tank volume is evaluated so that the maximum equivalent hours relative to the heat storage system correspond to a decrease of the tank mean temperature of 20°C, since the maximum temperature of the water inside the tank is assumed equal to 60°C, and the temperature of water entering the tank is evaluated as the weighted average between the temperature of the public water supply, namely 10°C, and the Heat Transfer Fluid (HTF) temperature of the ambient heating coming from the user at 45°C. In detail, in the case of *operation 1*, the volume tank is equal to 4.17 m^3, in the case of *operation 2*, it is equal to the half of the one of *operation 1*, or rather 2.08 m^3. In the case without heat dumping, the storage system is considered composed of one inflow/outflow duct for the water in order to receive/send the water from/to the user; in the case with heat dumping, it is composed of two inflow/outflow ducts in order to receive/send the water from/to the user, and to perform the heat dumping. The tank main characteristics are shown in Table 4.3.

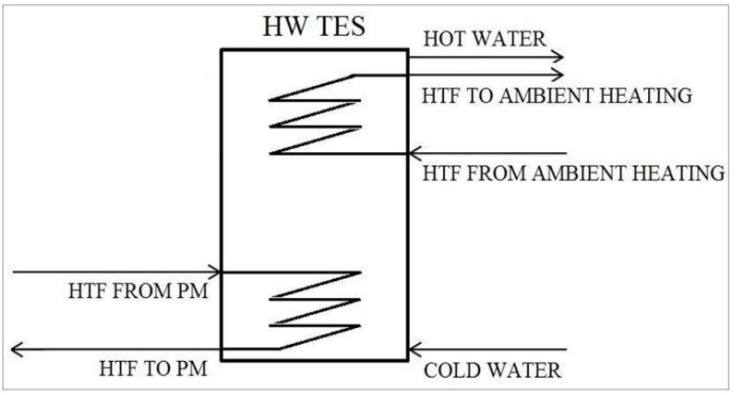

Figure 4.6. Scheme of the considered TES system.

As concerns the heat exchangers, the one at the bottom side of the tank (HX_1) is used to warm up the water in the tank by means of the HTF flowing through the prime mover, while the one at the top side (HX_2) is used to transfer heat from the hot water in the tank to the HTF of the ambient heating network. The heat exchangers are the same for both cases, and their dimensions are fixed so that the mean exchanged power through each of them is equal to the prime mover thermal power. HX_1 is considered the same since the same prime mover is used, whereas to establish the size of HX_2 several tests are conducted. The results show that the for both cases, or rather for both sizes of the tank, the mean exchanged power is the same, and equal to the prime mover thermal power, and the increase of the maximum power is negligible. Table 4.4 shows the main characteristics of the heat exchangers for both analyzed cases.

Table 4.3. Main characteristics of the tanks.

		Operation 1	**Operation 2**
Tank	TRNSYS Type	60 (d)	60 (f)
	N° of water inlet/outlet	1	2
	Volume (m^3)	4.17	2.08
	Height (m)	2.77	2.20

Table 4.4. Main characteristics of the heat exchangers.

	HX_1	HX_2
Inside diameter (m)	0.025	0.047
Outside diameter (m)	0.027	0.049
Heat exchange surface (m^2)	6.5	3.8
Length (m)	80	25.9
Mass flow rate (l/s)	1.1	2.85

4.4.2. Dynamic simulation of the system in No-dumping case

Figure 4.7 shows the TRNSYS diagram of the case without heat dumping relative to $EH_{TES,max}$ equal to 2.

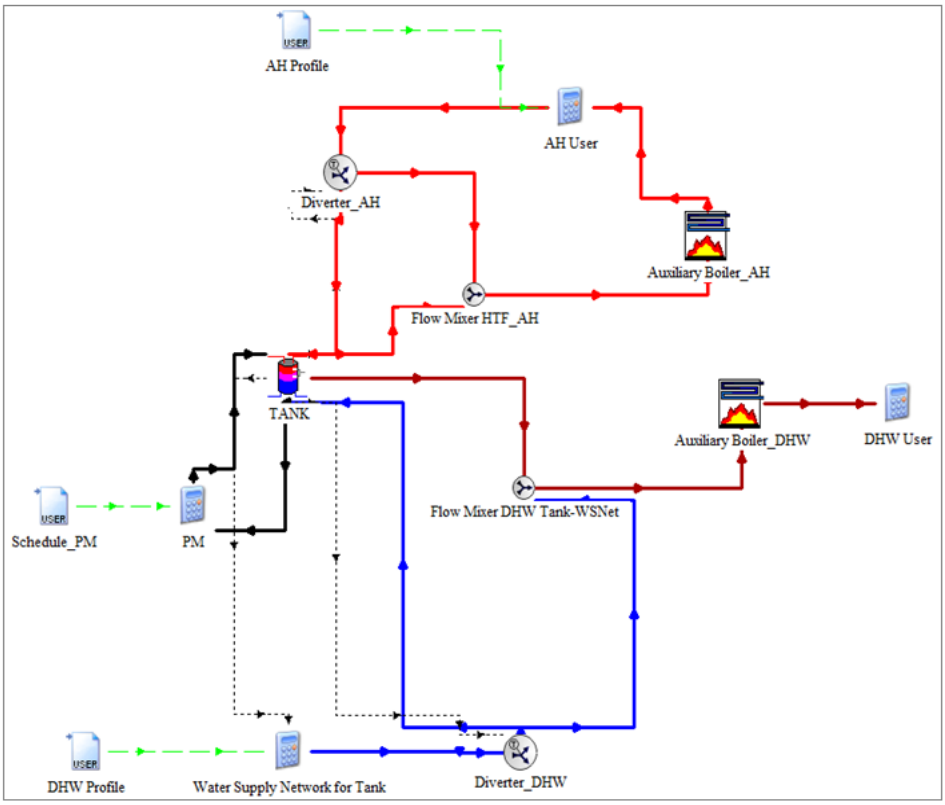

Figure 4.7. TRNSYS diagram for the case of *operation 1*.

To perform the dynamic simulation of the operation strategy without heat dumping, the prime mover hourly schedule, indicated as *Schedule_PM* in Figure 4.7, is fixed, and the schedule resulting from the optimized Matlab *operation 1* is used.

The loads for domestic hot water (*DWH User*) and ambient heating (*AH User*) are assigned so that the temperature of hot water flowing to the user is constant and equal to 55°C, and the temperature of the heat transfer fluid to the user is constant and equal to 50°C, respectively.

Two different diverters (*Diverter_DWH* and *Diverter_AH*) and auxiliary boilers (*Auxiliary Boiler_DWH* and *Auxiliary Boiler_AH*) are used in order to control and keep the above temperature values for hot water temperature and the HTF one. In practice, only one auxiliary boiler could be used.

4.4.3. Dynamic simulation of the system in Dumping case

Figure 4.8 shows the TRNSYS diagram relative to the case with heat dumping.

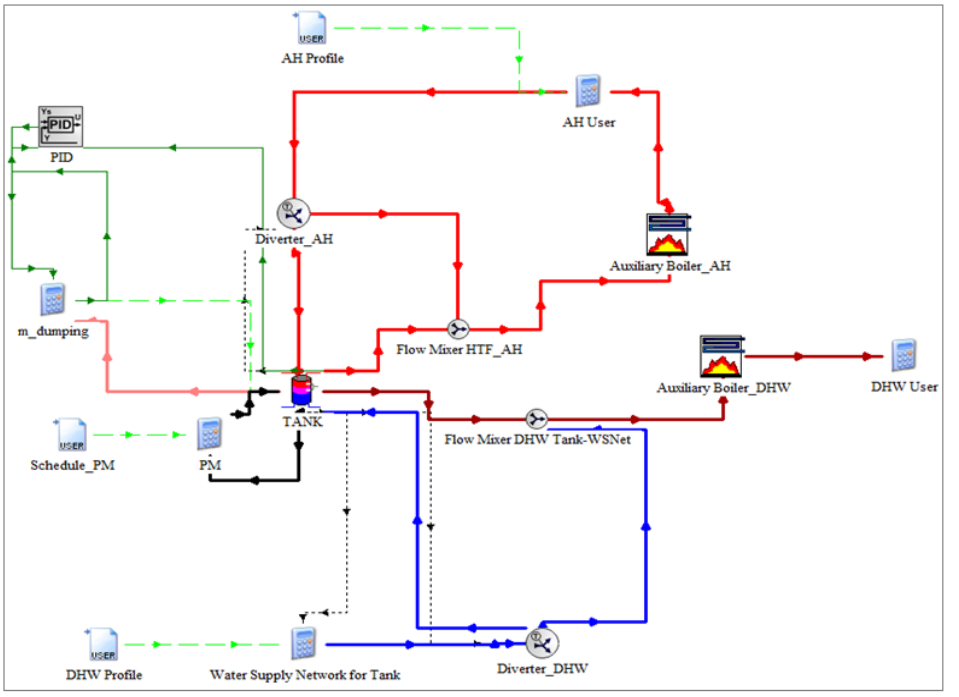

Figure 4.8. TRNSYS diagram for the case of *operation 2*.

In this case, the prime mover schedule resulting from the optimized Matlab *operation 2* with $EH_{TES,max}$ equal to 1 is used, and it can be noticed that heat dumping is performed by means of a PID controller. In particular, the heat dumping is realized by discharging hot water from the tank through a second outflow duct, and the controller calculates the mass flow rate of the hot water to be discharged to maintain the value of the controlled temperature that is represented by the temperature of the HTF entering the prime mover, lower than a set point one. The set point temperature is evaluated in order to obtain the same HTF mean temperature at the inlet and outlet of the HX_1 of the case without heat dumping, implying the equivalence of the prime mover operation in the two cases.

4.5. Results

The results are reported in terms of the comparison between the most representing temperatures of the water inside the tank, and of the HTF flowing in the two heat exchangers, obtained from the dynamic simulation of the system in the two cases and in the case in which the volume of the tank is the same used in the case with heat dumping, or rather 2.08m^3, but no heat dumping is applied. The latter test, indicated in the following as *operation 2**, is necessary to understand which values the above temperatures reach in the case in which the tank is too small and the dumping is not applied. Table 4.5 shows these results, obtained carrying out the dynamic simulation with a time step of 60 s.

It can be noticed that the mean temperatures at the inlet and outlet of HX_1, namely the heat exchanger connected to the prime mover, resulting from the simulation of the configuration relative to *operation 2* assume about the same value as in *operation 1*. The above result demonstrates the equivalence between the two configurations, and it is obtained by imposing a set point temperature for the PID controller in *operation 2* equal to 75°C, generating a percentage of dumped heat of 4.2%, precisely the same resulting from the optimization problem resolution. Moreover, from Table 4.5, it can be seen that the configuration *operation 2** in which the TES size is the same as in *operation 2*, but no heat dumping is applied, the relevant temperatures are quite higher than the corresponding ones in the other

Table 4.5. Comparison between the most representing temperatures resulting from the dynamic simulation.

		Operation 1	**Operation 2**	**Operation 2***
Tank	T_{max} (°C)	73.3	72.5	91.8
	T_{mean} (°C)	59.6	58.1	60.7
HX₁	$T_{HTF,max}$ (°C)	90.6	86.9	109.4
	$T_{in,mean}$ (°C)	72.9	72.4	75.2
	$T_{out,mean}$ (°C)	64.0	63.3	66.2
HX₂	$T_{HTF,max}$ (°C)	68.0	73.8	86.7
	$T_{in,mean}$ (°C)	43.1	43.1	43.1
	$T_{out,mean}$ (°C)	47.6	47.6	49.4

cases, especially the maximum temperature of the storage tank water, and the maximum temperature of the HTF for both heat exchangers.

References

[1] EPBD buildings platform. Country reports, [ISBN 2-930471-29-8], 2008.

[2] E.S. Barbieri, F.Melino, M.Morini. Influence of the thermal energy storage on the profitability of micro-CHP systems for residential building applications. Applied Energy. Volume 97 (2012), pp. 714–722.

[3] A.D.Smith, P.J.Mago, N.Fumo. Benefits of thermal energy storage option combined with CHP system for different commercial building types. Sustainable Energy Technologies and Assessments. Volume 1 (2013), pp. 3-12.

[4] Directive 2004/8/EC of the European Parliament and of the Council, Official Journal of the European Union, pp. 50-60, 11 February 2004.

[5] Italian D.lgs 20/07, Gazzetta Ufficiale n. 54, 2007.

[6] Italian D.M. 04/08/2011, Gazzetta Ufficiale n. 218, 2011.

[7] Italian Regulatory Authority for Electricity Gas and Water, website: http://www.autorita.energia.it/it/prezzi.htm, access date: December 2014.

[8] Italian D.M. 04/08/2011, Gazzetta Ufficiale n. 218 (2011).

[9] Italian D.M. 05/09/11. Gazzetta Ufficiale n. 218 (2011).

[10] TRNSYS 17, Volume 4, Mathematical Reference. Available at: http://web.mit.edu/parmstr/Public/TRNSYS/04-athematicalReference.pdf

"A fact in itself is nothing. It is valuable only for the idea attached to it, or for the proof which it furnishes"

Chapter 5. Comparison between two CHP systems operation strategies: heat dumping vs. load-partialization

5.1. Introduction

In this chapter, the optimized results relative to a residential natural gas-fired CHP system operating according to the novel operation strategy with heat dumping are compared with the ones relative to the case in which the CHP system operates following a heat-driven strategy allowing load partialization, in order to generalize the effectiveness of the novel operation strategy for heat-driven residential natural gas-fired CHP systems.

The CHP system under consideration is composed of a natural gas-fired microturbines as prime mover, a thermal energy storage system, and auxiliary boiler, supplying electricity and heat to two Italian residential buildings. Also in this case, the effects of the variation of the size of the thermal energy storage system on the optimization results are investigated, and the simulation of the two different operation strategies is realized by using a numerical code written in Matlab environment. The heuristic algorithm patternsearch is used to perform the economic optimization of the operation relative to both implemented strategies, aimed at maximizing the economic savings obtained by the CHP system with respect to the separate generation of electricity and heat. Moreover, the pollutants emission of the system operating according to the two operation strategies are evaluated.

From the economic point of view, the results show that the difference between the best CHP system configuration in the case with heat dumping and the one relative to the case with load partialization is minimal, with the latter presenting a slightly higher economic performance. As concerns pollutants emissions, results show that the impact of load partialization on a local scale is much higher, with CO emissions that can be up to three times the ones relative to conventional systems for the separate generation of electricity and heat.

Moreover, in this chapter an analysis about conditions in which heat dumping could yield higher economic performances than load partialization is presented.

In the following, the analyzed case is presented in Section 5.2, whereas the operation strategies are presented in Section 5.3. The methodologies used to evaluate the prime mover optimal scheduling, and the pollutants emission of the CHP system and of the separate generation system are presented in Section 5.4. Lastly, the analyses results are presented and discussed in Section 5.5.

5.2. Analyzed case

In the following, the details of the energetic system, and of the user are presented in Sections 5.2.1, and 5.2.2, respectively.

5.2.1. Energetic system

Figure 5.1 shows the layout of the CHP system. According to it, during the CHP system operation, if the user instantaneous electricity demand is null, the prime mover electricity generation is sent to the external electrical grid, whereas in case the user instantaneous electric power demand is not null, and it is lower than the electric power generated by the prime mover, part of the electricity generated by the prime mover is used to fill the user demand, and the generation surplus is sent to the external electrical grid. All the prime mover electricity generation is absorbed by the user in case it equals the instantaneous demand, otherwise, if the electric power generated by the prime mover is lower than the instantaneous demand, then part of the demand is filled with electricity from the grid.

When thermal power generated by the prime mover is higher than the instantaneous thermal demand, the thermal energy surplus is accumulated in the

thermal energy storage system for a later use, whereas the auxiliary boiler, fed by natural gas (NG), is used to integrate the prime mover and the thermal energy storage system heat supply.

Table 5.1 reports the nominal electrical and thermal power of the commercial natural gas fuelled microturbine (MT) used as prime mover, and its efficiencies at three different electrical loading levels [1].

As concerns the thermal energy storage system, different sizes are analyzed: calculating the maximum heat storage equivalent hours ($EH_{TES,max}$) as the ratio between the maximum heat storage capacity and the thermal power generated by the prime mover, six values of $EH_{TES,max}$ are considered, from the limit case without heat storage ($EH_{TES,max}$=0), to four. Lastly, the auxiliary boiler efficiency is fixed to 0.8, representing the efficiency of the average available technologies.

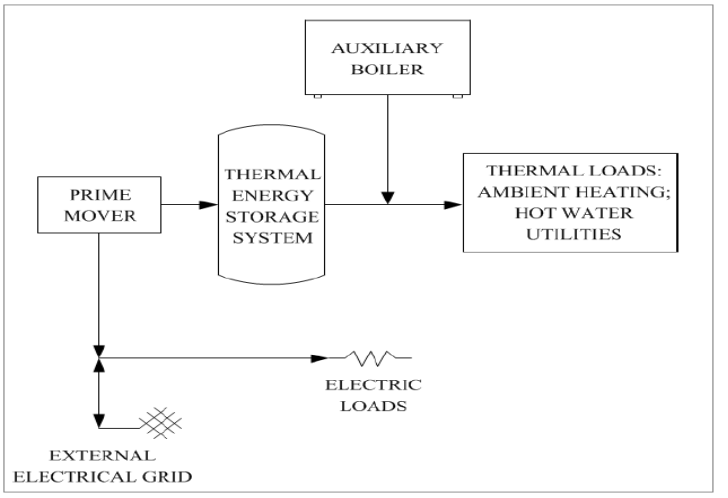

Figure 5.1. Layout of the CHP plant.

Table 5.1. Prime mover characteristics.

Prime mover	P_{el} (kW)	P_{th} (kW)	Electrical loading level (%)	η_{el} (%)	η_{th} (%)
MT	60	120	50.0	20.0	57.0
			75.0	24.0	56.0
			100.0	26.0	52.0

5.2.2. User

The user is represented by two equal residential buildings located in the north-west of Italy (climatic zone E), and is characterized by 2611 Heating-degree-days [2]. Each building includes 50 apartments, and is characterized by a total surface area equal to 5000 m^2 and a shape factor *S/V* of 0.5 m^{-1}. For the ambient heating, the annual total thermal energy demand, calculated using the Italian limits for the energy performance of buildings [2], is equal to 68 $kWh/m^2/yr$, while the annual total thermal energy demand due to hot water utilities is fixed to 15 $kWh/m^2/yr$ [3].

The user annual total electric energy demand for electrical devices, excluding the ones for air conditioning in the warm season, is equal to 18 $kWh/m^2/yr$, while an electricity demand of 7 $kWh/m^2/yr$ is considered for the air conditioning during the warm season [4].

The hourly profiles both for the thermal and electrical demand are evaluated according to the works of Barbieri et al. [4] and Bianchi et al. [5]. Figure 5.2 shows the non-dimensional distribution of the annual total thermal energy demand among the months relative to the cold season, whereas, Figures 5.3 and 5.4 show the non-dimensional hourly profile relative to the thermal energy demand for ambient heating in the cold season and for domestic hot water, respectively, this last assumed to be the same all over the year.

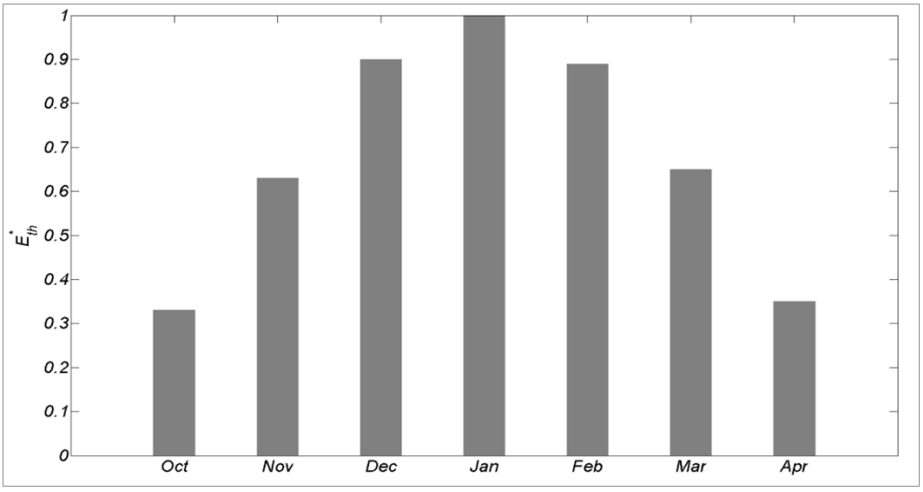

Figure 5.2. Non-dimensional monthly total thermal energy demand in the cold season.

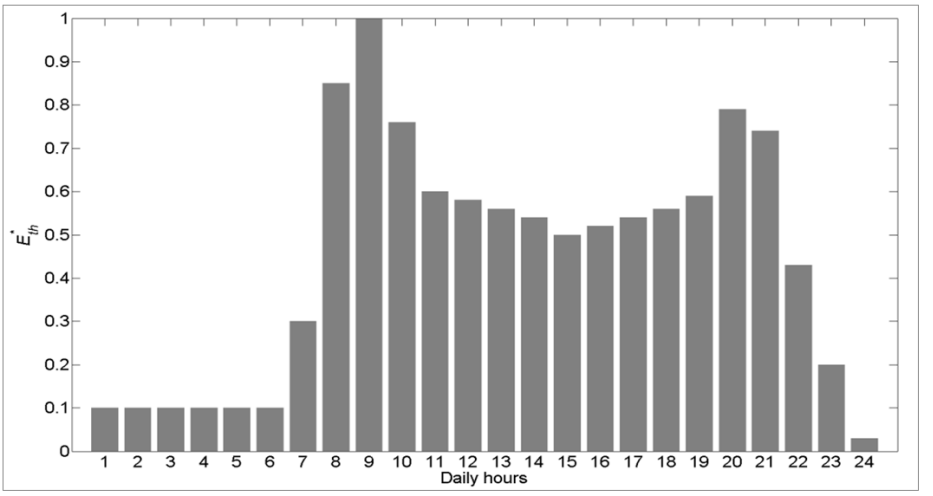

Figure 5.3. Non-dimensional hourly thermal demand for ambient heating in the cold season.

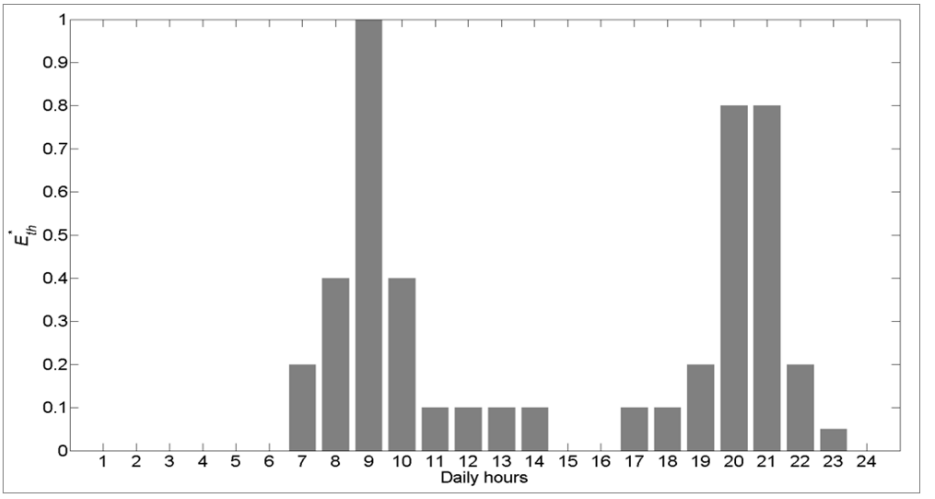

Figure 5.4. Non-dimensional hourly thermal demand for domestic hot water.

Figures 5.5 and 5.6 show the non-dimensional hourly profiles relative to the electrical energy consumption of electrical appliances and for the air conditioning, respectively. The load profile relative to the electrical appliances is considered to be the same for each day of the year, whereas the electric loads relative to the air conditioning are considered only during the summer months of June, July and August.

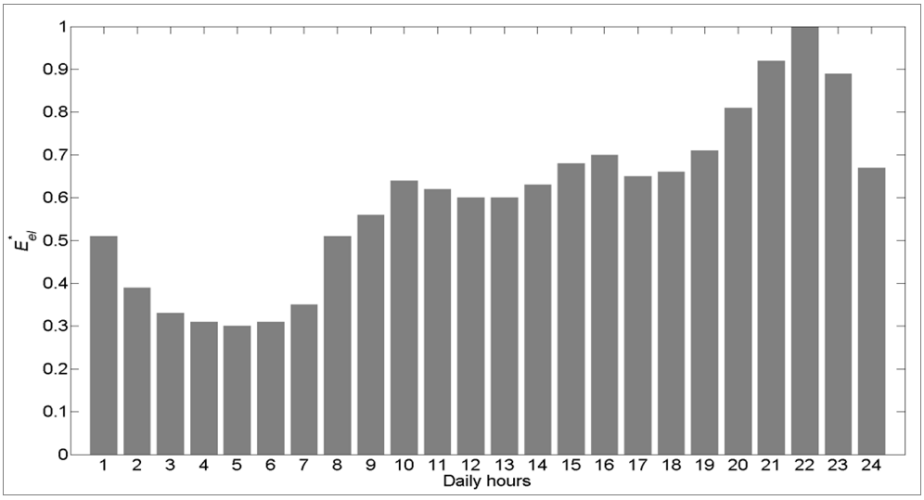

Figure 5.5. Non-dimensional hourly electric demand for the equipment.

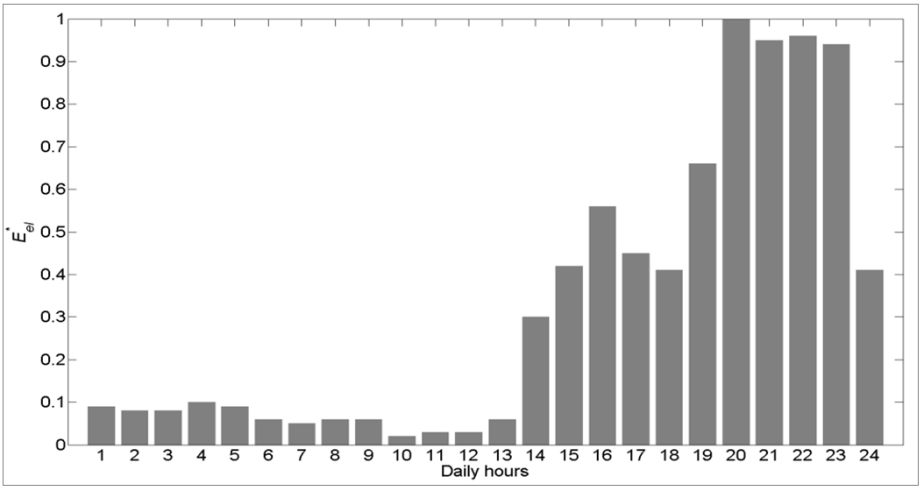

Figure 5.6. Non-dimensional hourly electric demand for air conditioning.

5.3. Operation strategies

The two implemented heat-driven operation strategies consist in the novel one with heat dumping, presented in Chapter 3, in which the prime mover can only operate at full-load and heat dumping is allowed, and in a partial-load operation strategy, in which no heat dumping is allowed.

For a given time-step of operation, in the operation strategy allowing heat dumping, part of the thermal energy generated by the prime mover can be dumped in order to match the sum of the energy demand of the user and the energy required to fill the thermal energy storage system (TES), this last equal to the difference between the maximum capacity and the current capacity of the TES. In this case, a maximum allowable value of the dumped thermal energy is imposed, equal to the 50% of the thermal energy generated by the prime mover, in order to limit the lowering of the primary energy savings involved by heat dumping.

As concerns the operation strategy allowing load partialization, the match between the thermal power generated by the prime mover and the sum of the user heat demand and the thermal energy needed to fulfill the TES is obtained by implementing partial-load operation. To limit the loss of primary energy savings due to the reduction of the prime mover electrical efficiency at partial-load operation, the prime mover minimum electric generation is fixed to 50% of the one generated at full-load.

Figures 5.7 and 5.8 show the block diagrams relative to the heat-driven operation strategies of the prime mover in the case with heat dumping and in the case with load partialization, respectively. The variables presented in such figures are evaluated considering a time-step of one hour. In detail, in Figure 5.7, $E_{th,PM,FL}$ represents the heat generated by the prime mover, $E_{th,user}$ the heat demand, and C_{TES} the current heat storage capacity, whereas in Figure 5.8, $E_{th,PM,PL}$ refers to the thermal energy generated by the prime mover at partial-load operation in one hour, and $E'_{th,PM,PL}$ is the thermal energy generated by the prime mover when the electric power generated by the prime mover is equal to the 50% of the one generated at full-load operation.

In the operation strategy with heat dumping, for each hour in which the prime mover is switched on, if the sum of the heat required to fill the heat storage system and the heat demand is lower than the heat generated by the prime mover operating at full load, then the surplus of heat generated by the prime mover is dumped. Differently, in the case relative to the operation strategy with load partialization, when the prime mover is switched on and the sum of the heat required to fill the heat demand and the heat storage system is lower than the heat generated by the

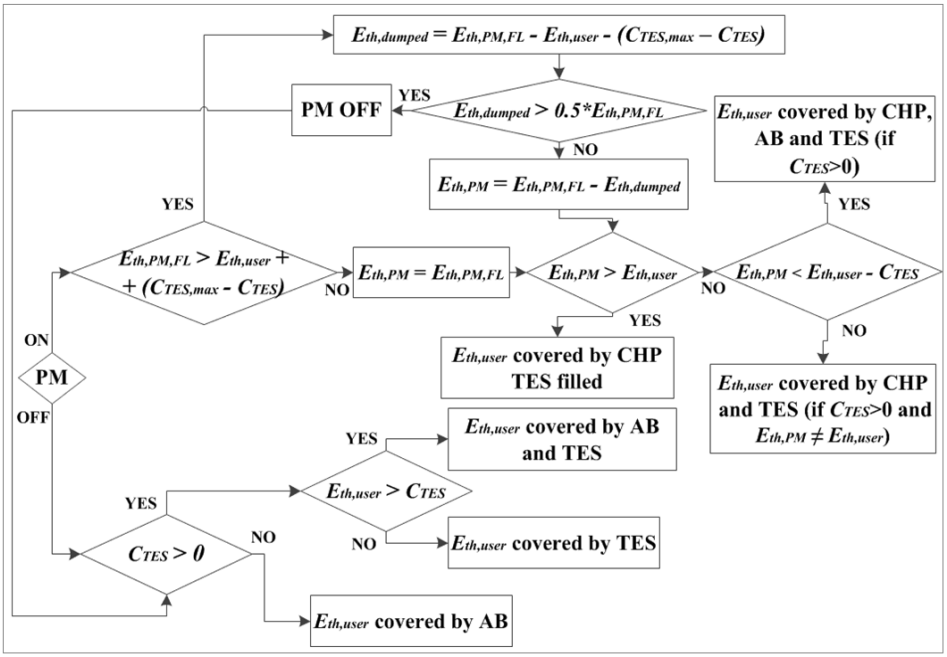

Figure 5.7. Block diagram relative to the prime mover operation strategy allowing heat dumping.

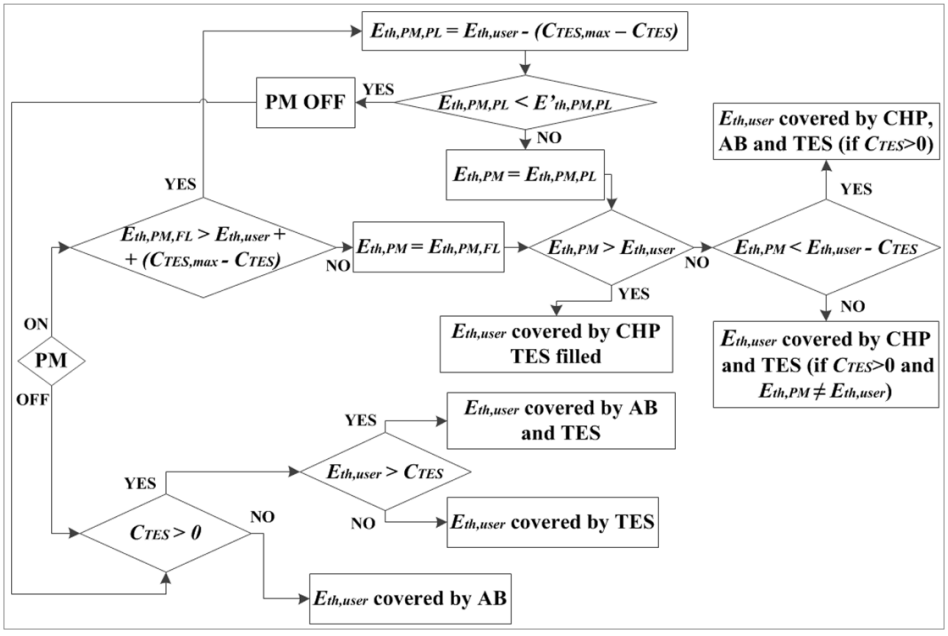

Figure 5.8. Block diagram relative to the prime mover operation strategy with load partialization.

prime mover operating at full load, then the above sum is matched by means of load partialization, as shown in Figure 5.8. To evaluate the electrical and thermal efficiencies in case of load partialization, a second order interpolation is performed by using the values reported in Table 5.1.

Finally, it is assumed that the prime mover can operate only in the cold season, namely from October 15th to April 15th, and that it can be switched on at most two times a day in order to limit the prime mover warm-up periods which limit its efficiency. The heat and electric demands for the rest of the year are fulfilled by separate generation using the auxiliary boiler and taking the electricity from the grid, respectively.

5.4. Methodologies

In the following, the methodologies used to evaluate the prime mover optimal scheduling, and the pollutants emission of the system operating according to the two operation strategies are presented in Sections 5.4.1, and 5.4.2, respectively.

5.4.1. Evaluation of prime mover optimal scheduling

The simulation of the two different operation strategies is realized by using a numerical code written in Matlab environment, and the patternsearch algorithm is used to perform the economic optimization of the prime mover operation schedules relative to the implemented strategies as compared to separate generation of electricity and heat. The economic optimization is conducted as in Chapter 3, by considering the Italian tariffs of electricity and natural gas [6,7], and the Italian incentives for cogeneration [8-13]. These last consist in a tax reduction on the natural gas used for the electricity generation, in benefits related to the possibility of releasing the electricity generated in cogeneration asset in the grid for a later use on a yearly basis, and in the possibility to gain a certain number of white certificates proportional to the energy savings obtained thanks to cogeneration. The objective function to be minimized in the optimization problem is given by:

$$FF = \Delta CF = -(\Delta AC_{NG} + \Delta AC_{electricity}) - R_{WC} \tag{5.1}$$

where ΔCF is the difference between the annual cash flow in case of separate generation and the one relative to combined generation, ΔAC_{NG} represents the

difference between the natural gas annual cost relative to separate generation and the annual cost of natural gas consumed in case of combined generation, this last including also the cost of the natural gas that is used to feed the auxiliary boiler, and that is not subject to tax reduction, $\Delta AC_{electricity}$ represents the difference between the electricity annual cost in case of separate generation and the one in case of cogeneration, and R_{WC} is the profit due to the white certificates. The evaluation of the costs differences and of the profit relative to the white certificates in equation (5.1) is made over an entire year.

The program main input data are the prime mover characteristics and the auxiliary boiler ones, the electrical and thermal demands of the user, the heat storage size, the tariffs of natural gas and electricity, and the initial operation schedule. The program main outputs are the optimized ON/OFF sequence for each day of operation, the hourly thermal and electrical generation of the prime mover, the dumped heat for each operation hour in case the operation allows heat dumping, the consumption and cost of natural gas and electricity from the grid both for cogeneration and separate generation, the primary energy savings, the incentives for cogeneration, and the global and local pollutants emission.

5.4.2. Evaluation of local and global pollutants emission

The difference between cogeneration and separate generation of electricity and heat, in terms of pollutants emission, are evaluated using the emission factors [1,14]. Considering a generic energy generator fed by a certain fuel, the mass of the generic pollutant p emitted for the generation of the generic energy vector X is calculated as:

$$m_p^X = \mu_p^X \cdot X \tag{5.2}$$

where μ_p^X is the emission factor expressed in g/kWh. For a generic pollutant, the emission factor mainly depends on the fuel type and on the generator characteristics and maintenance state.

The total emissions of the cogeneration system include the emissions of the prime mover, of the fraction of the electricity taken from the external grid by centralized power plants, and of the auxiliary boiler. In each of the analyzed cases,

the total emissions of the cogeneration system are compared to the emissions due to the separate generation of the same quantity of electricity and heat by centralized power stations and the auxiliary boiler, respectively. It is assumed that, in separate generation, the electricity is generated by a mix of conventional technologies representing the power system in Italy, and the heat by a conventional boiler fed by natural gas. Table 5.2 shows the emission factors used [1,14,15]. In each of the analyzed cases, the global emissions of the cogeneration system and those relative to the separate generation are evaluated, on a hourly basis, by means of equation (5.3) and equation (5.4), respectively.

$$m_p^{CHP} = \mu_p^{E_{el},PM} \cdot E_{el,PM} + \mu_p^{E_{th},SG} \cdot E_{th,AB} + \mu_p^{E_{el},SG} \cdot E_{el,taken} \quad (5.3)$$

$$m_p^{SG} = \mu_p^{E_{el},SG} \cdot E_{el,PM} + \mu_p^{E_{th},SG} \cdot E_{th,PM} + \mu_p^{E_{th},SG} \cdot E_{th,AB} + \mu_p^{E_{el},SG} \cdot E_{el,taken} \quad (5.4)$$

The local emissions, which do not include the emissions of centralized power stations that are usually located far enough from urban areas, are evaluated by means of equations (5.5) and (5.6).

$$m_p^{CHP} = \mu_p^{E_{el},PM} \cdot E_{el,PM} + \mu_p^{E_{th},SG} \cdot E_{th,AB} \quad (5.5)$$

$$m_p^{SG} = \mu_p^{E_{th},SG} \cdot E_{th,PM} + \mu_p^{E_{th},SG} \cdot E_{th,AB} \quad (5.6)$$

Table 5.2. Emission factors and energy production efficiencies.

Type of equipment	**Load (%)**	η_{el} **(%)**	η_{th} **(%)**	**NO_X (g/kWh)**	**CO (g/kWh)**	**CO_2 (g/kWh)**
Prime mover	50.0	20.0	57.0	0.121	10,251	1010
	75.0	24.0	56.0	0.078	2.204	842
	100.0	26.0	52.0	0.068	0.047	777
Separate generation of electricity	100.0	40.0	-	0.50	0.30	700
Separate generation of heat	100.0	-	80.0	0.19	0.03	253

5.5. Results

The optimized results are obtained considering the prime mover operating in the cold season, from October 15th 2013 to April 15th 2014. The results relative to the operation strategy allowing load partialization are referred to using *PL* (part-load operation), while the ones relative to the operation strategy with heat dumping using *D*.

In the following, the energetic results are presented in Section 5.5.1, whereas the economic ones are reported in Section 5.5.2. The global and local pollutants emission are presented in Section 5.5.3.

5.5.1. Energetic results

Figure 5.9 shows, for both operation strategies, the percentage of the annual electricity demand covered by the prime mover as a function of the maximum TES equivalent hours. For $EH_{TES,max}$ ranging from 0 to 2, for both operation strategies there is a sensible increase in the prime mover electricity generation with the increase in the maximum TES equivalent hours, because larger TES systems allow the prime mover to work for more hours, and consequently to generate more electricity, as it is possible to store more exceeding heat for a later use.

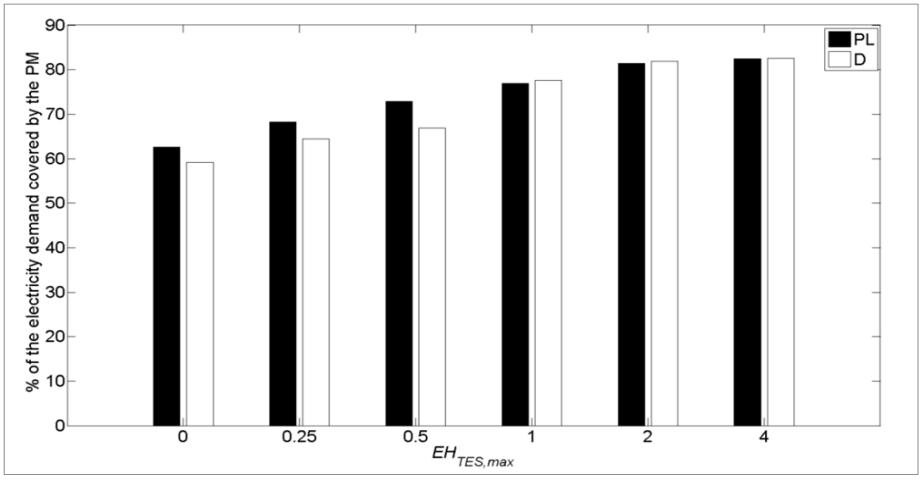

Figure 5.9. Percentage of the annual electricity demand covered by the prime mover as a function of the maximum TES equivalent hours for both operation strategies.

Relatively to the differences between the two operation strategies concerning the electrical energy generation at different storage sizes, Figure 5.9 shows that, at low storage sizes, the prime mover electricity generation relative to the partial-load operation strategy is higher than the corresponding one relative to the case with heat dumping, demonstrating the higher flexibility of partial-load operation. The *PL* strategy, despite the decrease of the electrical efficiency, permits to obtain an higher electricity generation than the one obtainable from the operation strategy with heat dumping, in case of relatively low thermal storage system sizes.

Figure 5.10 shows, for both operation strategies, the percentage of the annual total thermal demand, including ambient heating and domestic hot water, covered by the prime mover, for each value of $EH_{TES,max}$. In this figure, the values relative to the operation strategy with heat dumping do not include the corresponding dumped thermal energy, and this explains the different gaps between the values relative to the two operation strategies with respect to Figure 5.9. At large storage sizes, the electric and thermal power generated by the prime mover in the two different operation strategies approach the same asymptotic value, since the two operation strategies become equivalent to the classical heat-driven full-load operation mode, and the percentage of heat generated in partial-load conditions and the dumped heat

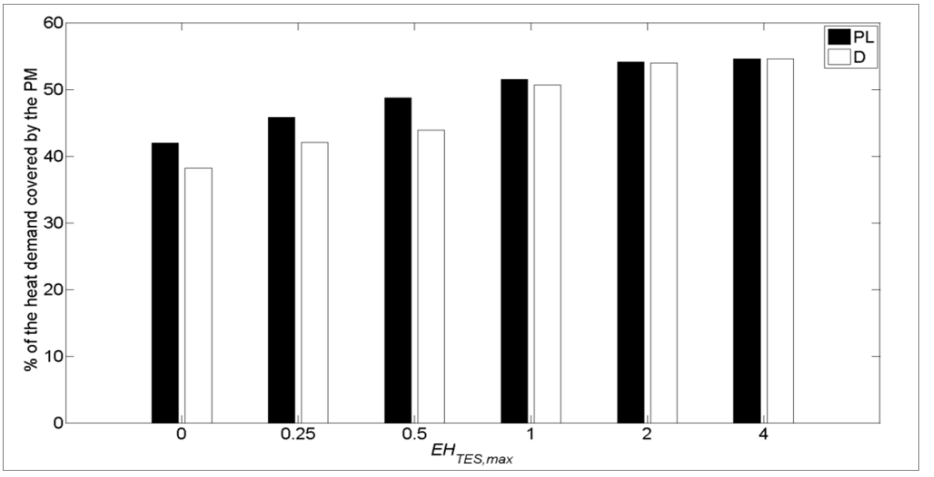

Figure 5.10. Percentage of the annual total heat demand (ambient heating + domestic hot water) covered by the prime mover as a function of the maximum TES equivalent hours for both operation strategies.

are very close to zero, as presented in Figure 5.11 showing the percentage of the heat generated in partial-load condition and the dumped heat with respect to the prime mover total thermal generation, for each value of $EH_{TES,max}$. Both the dumped heat and the partial-load heat generation are higher at low $EH_{TES,max}$, and approach zero at the largest heat storage size. Nevertheless, even when the storage size is low, they represent a relatively low percentage of the prime mover total thermal energy generation.

Taking into consideration the prime mover thermal power, the user thermal demand, and the period in which the prime mover can be active, it can be argued that the asymptotic value of thermal demand covered by the prime mover does not correspond to the maximum percentage of the thermal demand that the prime mover could cover. This because, in some hours, the electricity generated by the prime mover has a very low economic value and, consequently, buying electricity and using the auxiliary boiler for generating heat is more convenient.

This also is the reason for which the optimization effects in the case with load partialization and without the thermal storage are not null. In this case, the prime mover should follow the thermal demand, with the constraint represented by the minimum electricity generation indicated in Section 5.3, but in few hours, characterized by very low electricity export prices, the optimization algorithm chooses to buy electricity from the grid and to use the auxiliary boiler, rather than to use the prime mover. Nevertheless, in this case the optimization effects on the prime mover operation are negligible, and thus the results relative to this case can represent a benchmark for comparisons with the optimized results relative to the other analyzed cases.

Figure 5.12 shows, for both operation strategies, the annual natural gas consumption of the CHP system for each value of $EH_{TES,max}$. The annual natural gas consumption is equal to the sum of two contributions, namely the prime mover total natural gas consumption and the auxiliary boiler one, this last including also the natural gas consumption relative to the months in which the prime mover is inactive. For each operation strategy, for $EH_{TES,max}$ going from 0 to 2 the natural gas consumption increases slightly with the increase of the TES system size, due to the higher prime mover operation hours at large thermal storage sizes, and to the fact

that the prime mover thermal efficiency is well below the auxiliary boiler one. The same reason explains the differences between the natural gas consumptions relative to the two different operation strategies, for each the TES system sizes included in the above range.

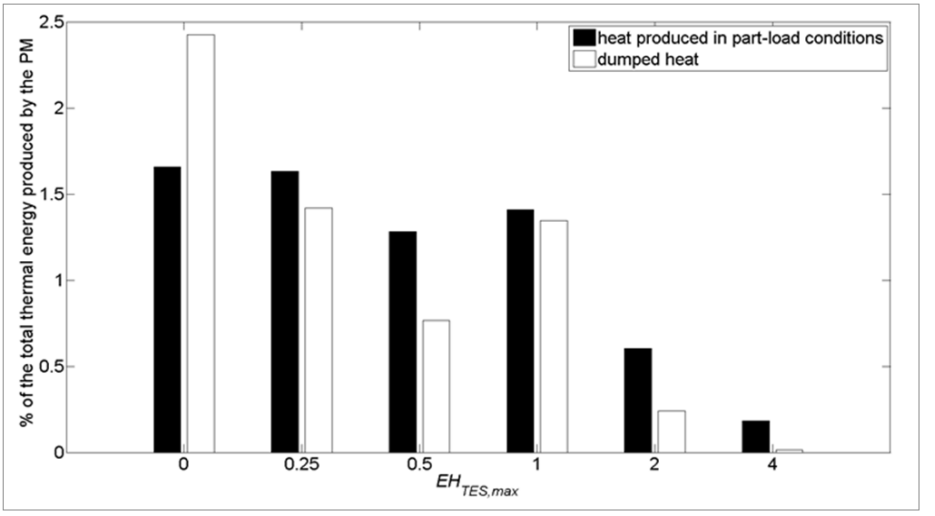

Figure 5.11. Heat generated in partial-load conditions and dumped heat.

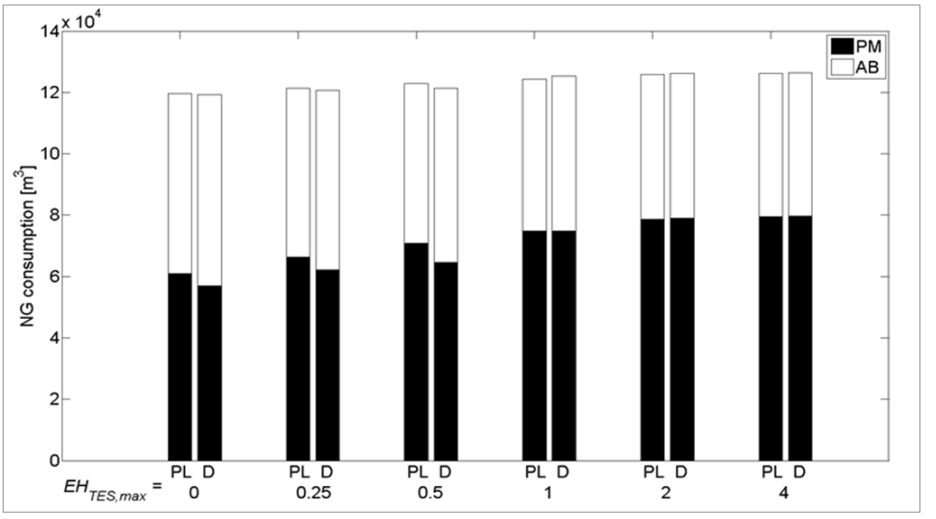

Figure 5.12. Natural gas annual consumption.

Figure 5.13 reports the primary energy savings relative to the CHP system for both operation strategies and for all values of $EH_{TES,max}$. The primary energy savings (PESs), expressed in equivalent oil tons per year, are evaluated as follows:

$$PES = \frac{E_{el,PM}}{\eta_{el,ref}} + \frac{\left(E_{th,PM} - E_{th,dumped}\right)}{\eta_{th,ref}} - E_f \tag{5.7}$$

where $E_{el,PM}$, and $E_{th,PM}$ represent the annual total electric and thermal energy generated by the prime mover, respectively, E_{dumped} is the total thermal energy dumped, E_f is the energy of the total natural gas consumed by the prime mover calculated using its lower heating value, and $\eta_{th,ref}$ and $\eta_{el,ref}$ are the Italian reference efficiencies for the separate generation of heat and electricity [12,13], respectively. Of course, the PES index, in the case with load partialization, are evaluated by means of the equation (5.7) considering the dumped thermal energy equal to zero.

As expected, for both operation strategies, the primary energy savings increase with the increase in the TES system size, as a consequence of the increased operation hours of the cogenerator. Moreover, for $EH_{TES,max}$ going from 0 to 0.5, the operation strategy with load partialitazion permits to obtain higher primary energy savings than those relative to the strategy with heat dumping, due to the higher prime mover working hours. Even at $EH_{TES,max}$ equal to 1, load partialization

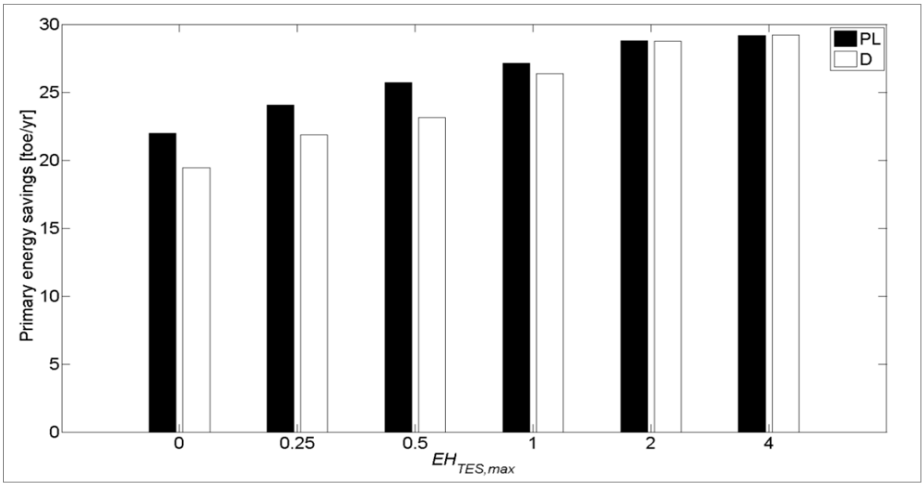

Figure 5.13. Primary energy savings for the two analyzed operation strategies at different TES system sizes.

generates higher PESs than the ones relative to the operation with heat dumping, and this is because, with this TES system size, the dumped heat is not yet negligible, while for larger TES system sizes, namely the ones with $EH_{TES,max}$ equal to 2 and 4, the PESs of the two different operation strategies assume practically the same values.

5.5.2 Economic results

The natural gas and electricity tariffs used for the costs evaluation and for the estimation of the incentives are relative to the period that goes from September 1st 2013 to August 31st 2014 [6,7]. In the present case, according to the Italian policy classifying the tariffs for natural gas and electricity by consumption brackets, the natural gas tariff and the tariff of the electricity taken from the grid depend on the annual total natural gas and electricity consumption, respectively. The electricity tariff also depends on the monthly consumptions, because the electricity tariff component relative to the excise is evaluated on a monthly basis. As concerns the natural gas tariff, the unitary cost (€/Sm^3) decreases passing from a consumption brackets to the subsequent higher one, whereas, on the contrary, for electricity, the unitary cost (€/kWh_{el}) increases at high consumption brackets. In the present case, relatively to the separate generation, the resulting cost of natural gas is equal to 0.848 €/m^3, while the cost of the electricity taken from the grid is equal to 0.190 €/kWh_{el}. The above electricity cost represents an average value, since, as stated before, the excise component of the electricity tariff is calculated on a monthly basis. The unitary cost of natural gas, electricity taken from the grid, and electricity sent to the grid, and thus not self-consumed, relative to the different CHP system configurations analyzed, are evaluated taking into account the incentives for cogeneration, and are shown in Table 5.3. Table 5.3 shows an average value also for the natural gas cost, because the natural gas consumed by the auxiliary boiler is not subject to the incentives. For both operation strategies, both the average unitary cost of natural gas and of the taken electricity decrease with the increase of the thermal energy storage size, due essentially to the higher amount of natural gas consumption in cogeneration regime at high storage sizes, and to the higher amount of taken electricity at low storage sizes, respectively. The unitary value of the

electricity sent to the grid varies on an hourly basis, and, in the present case, ranges from 0.02 €/kWh$_{el}$ to 0.15 €/kWh$_{el}$. The average unitary value of the sent electricity decreases with the increase of the thermal energy storage size. This is explained considering that the optimized results indicate that the higher is the storage size, the higher is the total amount of generated electricity and sent electricity. So, at high storage sizes, considering the limit relative to the hourly electricity generation represented by the prime mover maximum electric power, the optimization algorithm has less room for generating electricity when its economic value is high.

Figure 5.14 shows the annual economic savings due to cogeneration with respect to the separate generation of electricity and heat, for both operation strategies and for all values of $EH_{TES,max}$. The trends of the economic savings as a function of the

Table 5.3. Economic values of natural gas, electricity taken from the grid, and electricity sent to the grid relative to the different CHP system configurations analyzed.

Operation Strategy	$EH_{TES,max}$	**Average NG unitary cost (€/Sm^3)**	**Average unitary cost of electricity taken from the grid (€/kWh$_{el}$)**	**Average unitary value of electricity sent to the grid (€/kWh$_{el}$)**
D	0	0.773	0.170	0.089
	0.25	0.767	0.169	0.085
	0.50	0.765	0.169	0.084
	1	0.754	0.168	0.081
	2	0.750	0.168	0.080
	4	0.749	0.168	0.080
PL	0	0.769	0.169	0.086
	0.25	0.763	0.168	0.083
	0.50	0.759	0.168	0.081
	1	0.754	0.168	0.080
	2	0.750	0.168	0.080
	4	0.749	0.168	0.080

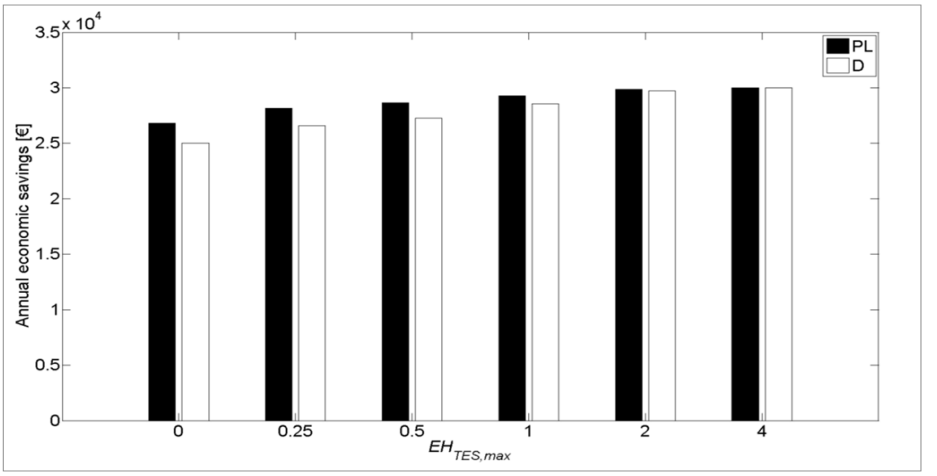

Figure 5.14. Annual economic savings for the two analyzed operation strategies at different TES system sizes.

TES system size are similar to the ones relative to the primary energy savings. Indeed, in general the economic savings increase with the increase of the TES system size, load partialization allows to have higher economic savings with respect to the strategy with heat dumping for $EH_{TES,max}$ from 0 to 1, while the strategies are equivalent at $EH_{TES,max}$ equal to 2 and 4.

In Italy it is quite hard to define a reliable market price for CHP systems, since to date there is not a well-established market for such systems, while this is not the case for the storage system, since hot water storage represents an old technology largely used in many applications. Thus, for both operation strategies analyzed, the most economically convenient configuration is found out by calculating the feasible investment cost for the CHP system net of the storage system, considering a fixed payback period. For each analyzed configuration of the CHP system, the feasible investment cost, that is returned over a given pay-back period, is evaluated as follows:

$$NPV = -I + \sum_{i=1}^{N} AS_i /(1+r)^i = -(I^* + TC) + \sum_{i=1}^{N} AS_i /(1+r)^i \qquad (5.8)$$

where NPV represents the net present value, I represents the investment cost for the CHP system purchase and maintenance, AS_i is the total economic savings with

respect to the separate generation over the year *i*, that correspond to the ones in Figure 5.14, *r* represents the discount rate, and I^* is the investment cost net of the storage system cost *TC*. The boiler cost is not present in the investment cost because this component is also included in separate generation. The size and cost of the thermal energy storage system, for each analyzed configuration including thermal energy storage, is evaluated as in Section 3.5.3, and are reported in Table 5.4.

Figure 5.15 shows the feasible investment cost I^* for all the analyzed cases, expressed in €/kW_{el}, for a fixed pay-back period of 5, at which the net present value is assumed null. For both operation strategies, the values of I^* at the different heat storage sizes are very close to each other. For the operation strategy with heat dumping, the best choice from the economical point of view for the heat storage size, among the analyzed ones, is the one relative to $EH_{TES,max}$ equal to 2, while in the case with load partialization the best one is that with $EH_{TES,max}$ equal to 1.

By comparing the best values of the feasible investment cost relative to the two investigated operation strategies, it is clear that the most economically convenient operation strategy for the CHP system is the one with load partialization, although the difference in terms of feasible investment cost between the best configurations is low, i.e. about 2% of the best feasible investment cost with load partialization. Moreover, the difference between the feasible investment costs relative to the cases with heat dumping characterized by $EH_{TES,max}$ equal to 1 and 2 is minimal. Indeed, the difference between the configuration with heat dumping and the one with load partialization, both characterized by $EH_{TES,max}$ equal to 1, in terms of feasible investment cost, is about 3%.

Table 5.4. Size and cost of thermal energy storage systems.

$EH_{TES,max}$	Size (m^3)	Cost (€)
0.25	0.65	2,55
0.5	1.3	4,72
1	2.6	6,14
2	5.2	10,15
4	10.4	16,45

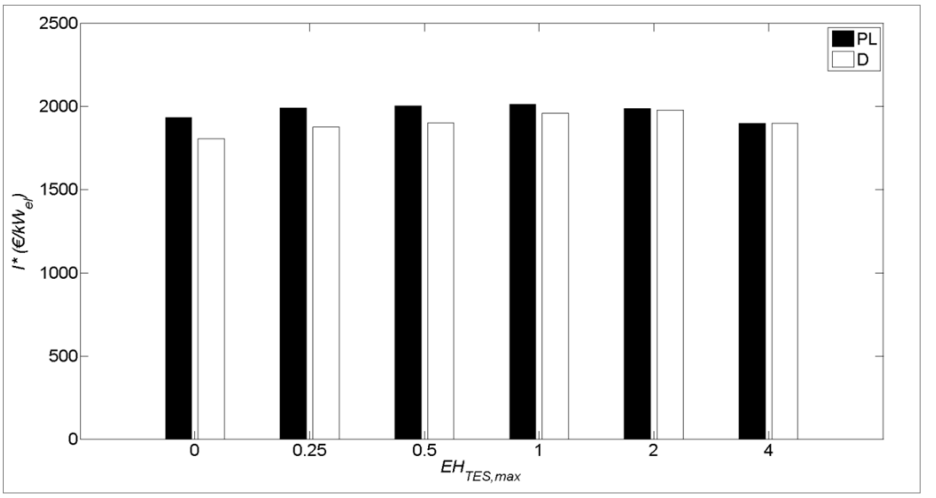

Figure 5.15. Feasible investment costs for a pay-back period of 5 years.

Finally, the best size for the heat storage system, for both operation strategies, can be assumed to be the one corresponding to $EH_{TES,max}$ equal to 1, since it is a good compromise between the necessity to have a high feasible investment cost, a low encumbrance, and a relatively large buffer of thermal energy.

5.5.2.1. Further insights on economic results

The results reported in the previous section show that, for the present case study, the operation strategy with load partialization is slightly more economically convenient than the one with heat dumping. This is essentially because, in the operation strategy with heat dumping, the positive effects associated with the electricity generation at full load, and thus at maximum electrical efficiency, are not sufficient to cope with the negative ones associated to the dumped surplus of thermal energy, or equivalently to the surplus of the natural gas consumed, in order to overcome partial-load operation.

In this section, a detailed evaluation of the difference between the cash flow relative to the operation strategy with heat dumping and the one relative to the operation strategy with load partialization is made in order to get further insights on the difference between the two above operation strategies from the economical point of view. The analysis presented in this section is made considering the electric

power required by the user ranging from 0 to P_{el}, this last being the electric power generated by the prime mover at full load. The difference between the cash flows of the two operation strategies in case the electric power demand is higher than P_{el} can be easily derived from the results reported in the following.

Considering the prime mover operating at the operation mode with load partialization, for a generic operation hour, the cash flow can be expressed as:

$$CF_{PL} = -\frac{P_{th,PL}}{\eta_{th,PL}} \cdot CST_{NG} - max(P_{el,user} - P_{el,PL}, 0) \cdot TV + max(P_{el,PL} - P_{el,user}, 0) \cdot SV \quad (5.9)$$

where $P_{el,PL}$ and $P_{th,PL}$ represent the electric and thermal power generated by the prime mover operating at partial load, respectively, $P_{el,user}$ is the electric power required by the user, $\eta_{th,PL}$ represents the prime mover thermal efficiency at partial load, CST_{NG} represents the natural gas cost expressed in €/kWh, and TV and SV are the economic value of the electricity taken from the grid and sent to the grid both expressed in €/kWh$_{el}$, respectively. For the same hour, the cash flow in the case with heat dumping is:

$$CF_D = -\frac{P_{th}}{\eta_{th,FL}} \cdot CST_{NG} + (P_{el} - P_{el,user}) \cdot SV \quad (5.10)$$

where $\eta_{th,FL}$ represents the prime mover thermal efficiency at full load. In the case with heat dumping, and under the above limitation relative to the electric power required by the user, $P_{el,user}$ always corresponds to the electric power generated by the prime mover that is self-consumed, and the term in parenthesis in equation (5.10) represents the electric power generated by the prime mover and sent to the external grid. Consequently, indicating with f_{SC} the fraction of the electric power generated by the prime mover in the case with heat dumping and self-consumed, equation (5.10) can be written as:

$$CF_D = -\frac{P_{th}}{\eta_{th,FL}} \cdot CST_{NG} + P_{el} \cdot (1 - f_{SC}) \cdot SV \quad (5.11)$$

and equation (5.9) as:

$$CF_{PL} = -\frac{P_{th,PL}}{\eta_{th,PL}} \cdot CST_{NG} - max(P_{el} \cdot f_{SC} - P_{el,PL}, 0) \cdot TV + max(P_{el,PL} - P_{el} \cdot f_{SC}, 0) \cdot SV \quad (5.12)$$

Considering equations 5.11 and 5.12, the difference between the cash flows relative to the two different operation strategies can be expressed as:

$$\Delta CF = CF_{PL} - CF_D = \left(\frac{P_{th}}{\eta_{th,FL}} - \frac{P_{th,PL}}{\eta_{th,PL}} \right) \cdot CST_{NG} + P_{el} \cdot (f_{SC} - 1) \cdot SV - max(P_{el} \cdot f_{SC} - P_{el,PL}, 0) \cdot TV + \\ + max(P_{el,PL} - P_{el} \cdot f_{SC}, 0) \cdot SV \quad (5.13)$$

Thus, the operation strategy with load partialization is more convenient from the economical point of view than the one with heat dumping if the difference between cash flows, defined in equation (5.13), is positive. For a given partialization of the electric power generated by the prime mover, the corresponding thermal power generated by the prime mover can be expressed as:

$$P_{th,PL} = P_{th} \cdot TPR \quad (5.14)$$

where *TPR* represents the ratio between the thermal power generated at partial load and the one generated at full load. Consequently, equation (5.13) can be written as:

$$\Delta CF = P_{th} \cdot \left(\frac{1}{\eta_{th,FL}} - \frac{TPR}{\eta_{th,PL}} \right) \cdot CST_{NG} + P_{el} \cdot (f_{SC} - 1) \cdot SV - max(P_{el} \cdot f_{SC} - P_{el,PL}, 0) \cdot TV + \\ + max(P_{el,PL} - P_{el} \cdot f_{SC}, 0) \cdot SV \quad (5.15)$$

Defining the electric power ratio (*EPR*) as the ratio between the electric power generated at partial load and the electric power generated at full load, two different cases can be distinguished: the first one is the case in which:

$$P_{el} \cdot f_{SC} \geq P_{el,PL} \rightarrow f_{SC} \geq EPR \quad (5.16)$$

while the second one is the case in which:

$$P_{el} \cdot f_{SC} < P_{el,PL} \rightarrow f_{SC} < EPR \quad (5.17)$$

For a given electrical load partialization, the electric power ratio and the thermal one do not assume the same value, due to the different trends that characterize the electrical and thermal efficiencies of prime mover at different load partialization levels. Figure 5.16 shows the behavior of the thermal power ratio as a function of the electric power one.

In the first case, i.e. the case in which the electric power demand relative to the user is higher than or equal to the electric power generated by the prime mover in

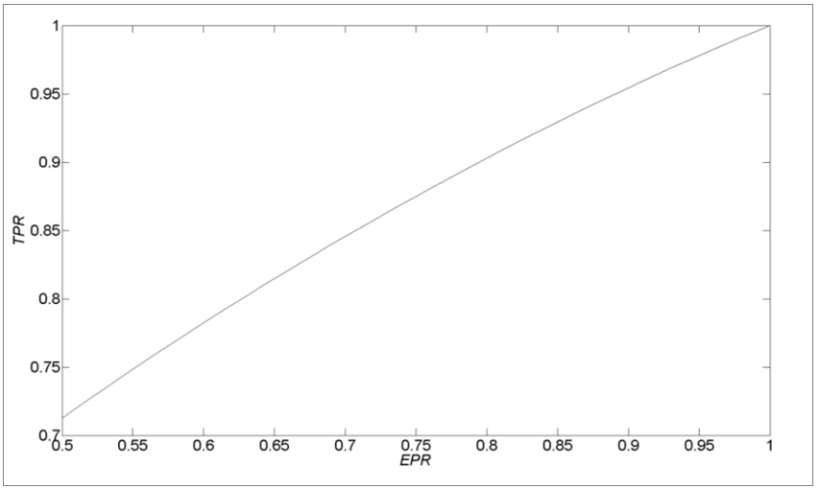

Figure 5.16. Thermal power ratio vs. electric power ratio.

case of load partialization, equation (5.15) can be rewritten in the following forms:

$$\Delta CF = P_{th} \cdot \left(\frac{1}{\eta_{th,FL}} - \frac{TPR}{\eta_{th,PL}} \right) \cdot CST_{NG} + P_{el} \cdot (f_{SC} - 1) \cdot SV - (P_{el} \cdot f_{SC} - P_{el,PL}) \cdot TV \quad (5.18)$$

$$\Delta CF = P_{th} \cdot \left(\frac{1}{\eta_{th,FL}} - \frac{TPR}{\eta_{th,PL}} \right) \cdot CST_{NG} + P_{el} \cdot (f_{SC} - 1) \cdot SV + P_{el} \cdot (EPR - f_{SC}) \cdot TV \quad (5.19)$$

Equation (5.19) shows that the difference between the cash flows is equal to the sum of three contributions. The first one is proportional to the natural gas cost, and it can be either positive, i.e. favorable to the operation mode with load partialization, or null. It embodies the disadvantages relative to heat dumping operation strategy, namely the surplus of gas consumption. As it was to be expected, this factor tends to zero with the increasing of the thermal power ratio. The second contribution is proportional to the economic value of the electricity sent to the external grid. It is null when the fraction of the electric power generated by the prime mover in the case with heat dumping and self-consumed is equal to 1, otherwise it is negative and favorable to heat dumping. The third contribution is proportional to the economic value of the electricity taken from the external grid, and it can be either negative, namely favorable to heat dumping, or null, since in this case equation (5.16) holds.

In the second case, i.e. the case in which the electric power demand relative to the user is lower than the electric power generated by the prime mover in case of load partialization, equation (5.15) can be rewritten in the following form:

$$\Delta CF = P_{th} \cdot \left(\frac{1}{\eta_{th,FL}} - \frac{TPR}{\eta_{th,PL}} \right) \cdot CST_{NG} + P_{el} \cdot (f_{SC} - 1) \cdot SV + (P_{el,PL} - P_{el} \cdot f_{SC}) \cdot SV \quad (5.20)$$

that, after some passages, becomes:

$$\Delta CF = P_{th} \cdot \left(\frac{1}{\eta_{th,FL}} - \frac{TPR}{\eta_{th,PL}} \right) \cdot CST_{NG} + P_{el} \cdot (EPR - 1) \cdot SV \quad (5.21)$$

Thus, in this case, the difference between the cash flows does not depend on the fraction of electric power self-consumed in the case with heat dumping, and it is equal to the sum of two contributions. The first contribution is equal to the first one in equation (5.19). The second one can be either negative and thus favorable to heat dumping, or null, depending on the value of *EPR*.

Figure 5.17 shows a graphical representation of the difference between the cash flow relative to the operation with load partialization and the one with heat dumping for two hours, as a function of the electrical load partialization and the fraction of the electricity generated in the case with heat dumping that is self-consumed.

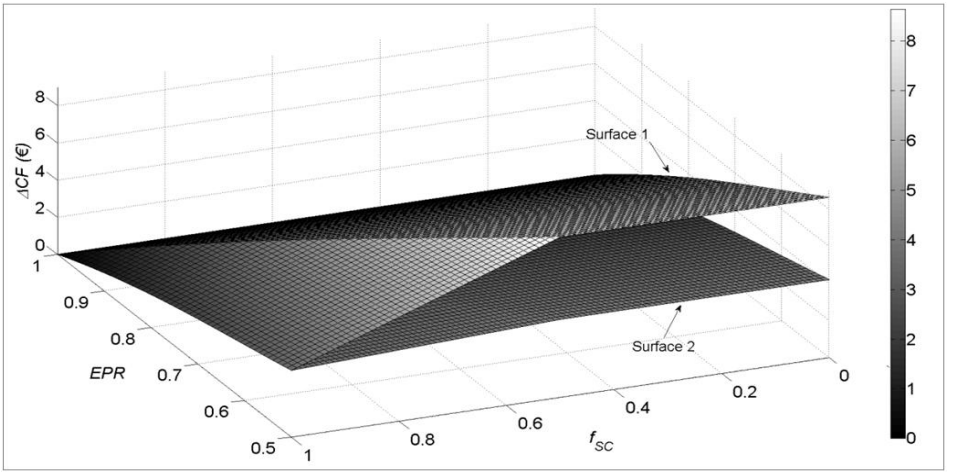

Figure5.17. Difference between the cash flow relative to the operation with dumping and the one with load partialization: Surface 1 refers to the case in which the electricity sent to the external grid is paid at its minimum economic value, while Surface 2 at its maximum economic value.

For both the considered economic values of the sent electricity, the difference between cash flows is always positive, except in the case relative to full load operation in which it is null, and this confirms that the operation strategy with load partialization is more economically convenient than the one with heat dumping. It can be also noticed that the difference between the cash flows relative to the minimum economic value of the sent electricity is always higher than the corresponding one relative to the maximum economic value of the sent electricity, except, of course, for the cases in which the fraction of self-consumed electricity is equal to 1. Indeed, the curve representing the intersection of the two surfaces lies in the plane f_{SC}=1. Figure 5.17 also shows that, for both surfaces, ΔCF always decreases with the increase in the percentage of the electric power ratio, and this result, that in the present investigation can be extended to any economic value of the sent electricity, is a consequence of the fact that load partialization is always more economically convenient than heat dumping.

Furthermore, Figure 5.17 also shows that, as prescribed by equation (5.21), for both economic values of the sent electricity, the difference between cash flows does not vary with f_{SC} when the electric power demand relative to the user is lower than the electric power generated by the prime mover in the case of part-load operation. On the other hand, when the electric power demand relative to the user is higher than the electric power generated by the prime mover in the case of load partialization, for each value of *EPR* (and *TPR*), its behavior, at different f_{SC}, depends on the economic values of the sent and taken electricity, as it is prescribed by equation (5.19). In particular, the difference of cash flows increases with the increase of f_{SC} when the economic value of the sent electricity is higher than the one of the electricity taken from the grid, meaning that, in this case, the higher is the fraction of self-consumed electricity, the higher is the economic convenience of load partialization with respect to heat dumping. Conversely, when the economic value of the sent electricity is lower than the one of the electricity taken from the grid, as always verifies in the present investigation, the difference of cash flows decreases with the increase of f_{SC}.

Finally, it has to be considered that, when the economic value of the electricity sent to the external grid is close to or equal to its maximum value, the difference of

cash flows between the operation with load partialization and the one with heat dumping is low as compared to the values of cash flows of both operation strategies (lower than 12%). In this conditions, that can verify in on-peak hours, and that represent the typical conditions in which residential cogenerators can maximize the economic value of the generated electricity, heat dumping could be more economically convenient than load partialization if prime movers fed with a cheaper fuel than natural gas are used, like for example a gas from gasification. Moreover, heat dumping could be more economically convenient in countries where there is a lower ratio between the natural gas price and the electricity price than the one in Italy. In such circumstances, a hybrid strategy could represent the most effective choice from the economic point of view.

5.5.3. Global and local pollutants emission

The annual global emissions of CO_2, and the annual local emissions of NO_X and CO, relative to the analyzed CHP system operating according to the two considered operation strategies, and evaluated by means of the approach described in Section 5.4.2, are reported in Figures 5.18, 5.19 and 5.20, respectively. In Figure 5.18, the annual global CO_2 emissions relative to the CHP system include the emissions relative to the prime mover, the auxiliary boiler and those relative to the electricity taken from the grid over the entire year, including the six months in which the prime mover is inactive. Differently, in Figures 5.19 and 5.20, which report annual emissions on a local scale, the emissions relative to the electricity taken from the grid are not included in CHP system ones, as it is produced by centralized power plants that are usually located far away from residential districts. Table 5.5 reports the annual emissions in case the annual heat and electricity demands of the user are covered by means of separate generation.

Figure 5.18 shows that the annual global CO_2 emissions of the CHP system relative to the analyzed configurations assume similar values, and that they are all lower than the ones due to the separate generation, and this important result is yet another demonstration of the effectiveness of cogeneration as a mean for reducing the annual CO_2 emissions, that are one of the main responsible of the greenhouse effect in the Earth atmosphere.

Relatively to the annual local NO_X emissions of the CHP system shown in Figure 5.19, for each of the TES systems size, the two different operation strategies present about the same emission levels. Furthermore, in all cases, the annual local NO_X emissions of the CHP system are well below the ones due to separate generation, with a reduction of about 50% if the NO_X emissions in separate generation are compared with the ones relative to the best configurations of the CHP system, namely the ones relative to the cases with $EH_{TES,max}$ equal to 1. This result is due to the very low emission factors characterizing the gas turbine considered as prime mover, even at part-load operation, as compared to the ones relative to separate generation.

Finally, Figure 5.20 shows the big difference between the two different operation strategies as regards the annual local CO emissions. The operation strategy allowing partial-load operation presents, in general, annual local CO emissions that are much higher than the ones relative to the operation strategy with heat dumping, these last being, in general, even slightly lower than the ones relative to separate generation. Furthermore, by comparing the CO annual local emissions relative to the assumed best configuration in case of load partialization, i.e. the ones with $EH_{TES,max}$ equal to 1, with the ones relative to separate generation, the operation strategy with load partialization produces about three times the emissions produced in the case of separate generation.

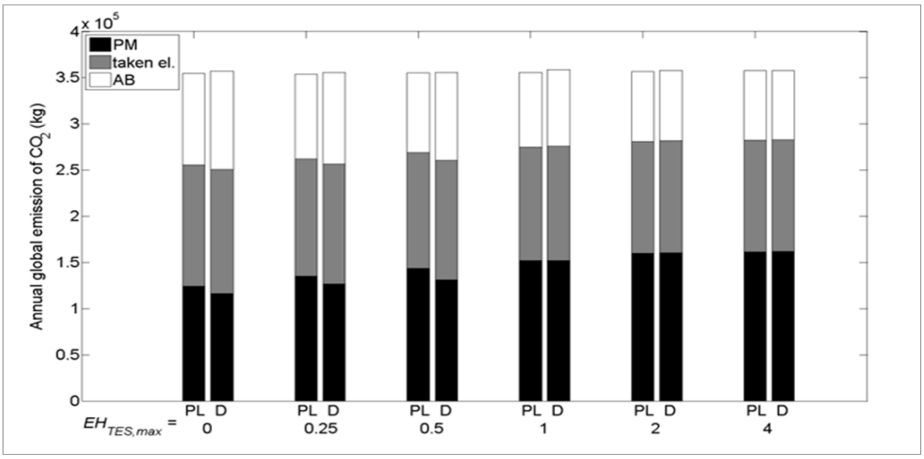

Figure 5.18. Annual global emission of CO_2.

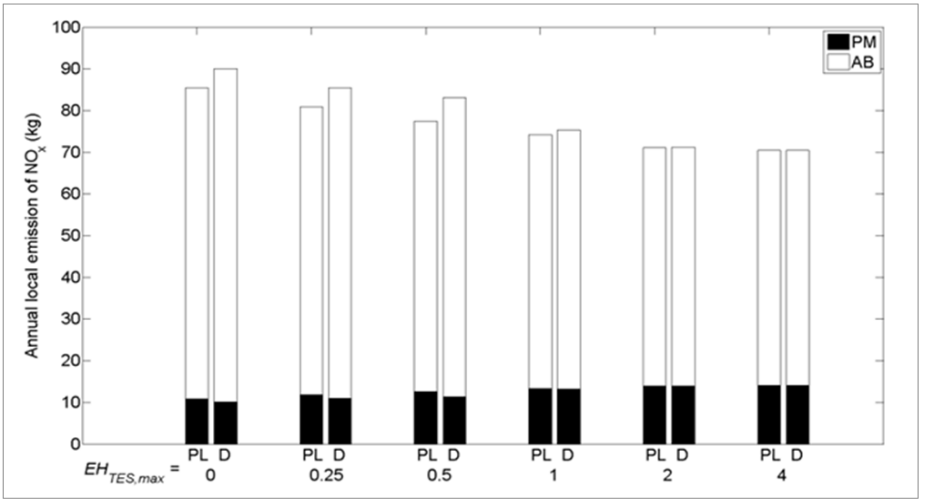

Figure 5.19. Annual local emission of NO_X.

These results poses a serious concern, and suggests that a dedicated analysis should be done in order to select adequate installation locations and exhaust systems for such residential CHP systems operating with load partialization, as CO emissions can be very dangerous for the human health.

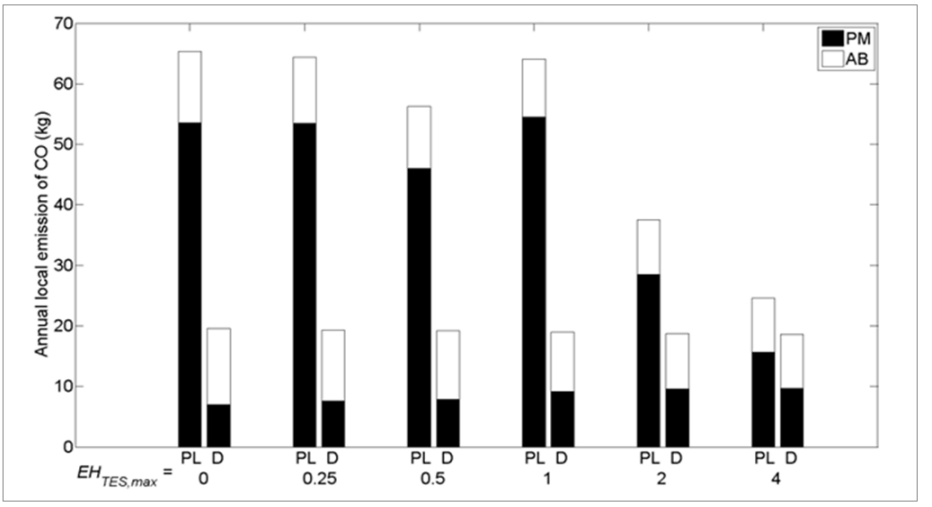

Figure 5.20. Annual local emission of CO.

Table 5.5. Annual emissions due to the separate generation of heat and electricity.

Annual global emission of CO_2 (kg)	**Annual local emission of NO_X (kg)**	**Annual local emission of CO (kg)**
3.7e+05	143.8	22.7

References

[1] A. Canova, G. Chicco, G. Genon, P. Mancarella. Emission characterization and evaluation of natural gas-fueled cogeneration microturbines and internal combustion engines. Energy Conversion and Management. Volume 49 (2008), pp. 2900-2009.

[2] EPBD buildings platform. Country reports; 2008. [ISBN 2-930471-29-8].

[3] Italian D.M. 22/11/2012, Gazzetta Ufficiale n. 290 (2012).

[4] E.S. Barbieri, F. Melino, M. Morini. Influence of the thermal energy storage on the profitability of micro_CHP systems for residential building applications. Applied Energy. Volume 97 (2012), pp. 714-722.

[5] M. Bianchi, A. De Pascale, P.R. Spina. Guidelines for residential micro-CHP systems design. Applied Energy. Volume 97 (2012), pp. 673-685.

[6] Italian Regulatory Authority for Electricity Gas and Water, website: www.autorita.energia.it, access done on December 2014.

[7] Gestore Mercati Energetici, website: www.mercatoelettrico.org, access done on December 2014.

[8] Italian law 44/12, Gazzetta Ufficiale n. 99 (2012).

[9] Resolution ARG/elt 74/08 (2008), http://www.autorita.energia.it/it/docs/08/074-08arg.htm.

[10] Directive 2004/8/EC of the European Parliament and of the Council, Official Journal of the European Union, 11 February 2004, pp. 50-60.

[11] Italian D.lgs 20/07, Gazzetta Ufficiale n. 54 (2007).

[12] Italian D.M. 04/08/2011, Gazzetta Ufficiale n. 218 (2011).

[13] Italian D.M. 05/09/2011, Gazzetta Ufficiale n. 218 (2011).

[14] P. Mancarella, G. Chicco. Global and local emission impact assessment of distributed cogeneration systems with partial-load models. Applied Energy. Volume 86 (2009), pp. 2096-2106.

[15] EDUCOGEN, Second Edition, December 2001.

Chapter 6. Conclusions

This thesis focuses on the optimal operation of cogeneration systems based on heat-driven operation modes. In detail, a novel approach for improving the operation of residential micro-Combined Heat and Power (CHP) systems from the economical point of view is proposed, based on the possibility to operate the prime movers of the CHP systems also when a heat dumping occurs.

The influence of such operation strategy with heat dumping is evaluated on the optimized operation of four residential micro-CHP systems, each composed of a prime mover generating electricity and heat, a thermal energy storage system, and an auxiliary boiler. The micro-CHP systems differ from one another on the prime mover technology, whereas the same multi-apartment housing located in Italy is considered as user. Four natural gas fuelled commercial prime mover are considered, or rather two internal combustion engines, and two microturbines, characterized by different electric and thermal powers. For each micro-CHP system, the novel operation strategy with heat dumping, and a classical full-load operation strategy without heat dumping are considered and implemented by means of a home-made numerical code developed in Matlab environment, and for both cases, the economic optimization of the prime movers operation is performed using the patternsearch algorithm. The effects on the optimization results of the variation of the thermal energy storage system maximum capacity are also investigated. Results demonstrate that a relatively low heat dumping allows a huge increase in the prime mover total operation hours at low storage sizes, with respect to the corresponding cases without heat dumping, and then by comparing the best configurations relative to the cases with heat dumping to the best ones relative to the cases without it, heat dumping involves a considerable reduction of the thermal energy storage size.

The effects on the CHP systems operation of the variation of the auxiliary boiler efficiency are also analyzed, considering two different values for the auxiliary

boiler efficiency, namely 0.8 and 0.95. Results show that, for both operation strategies, only the prime movers with higher power are sensitive to the cost reduction of heat in separate generation due to the use of high efficiency boilers. In this case, for all thermal storage sizes, the prime movers present lower operation hours than the corresponding ones relative to the use of conventional boilers.

The evaluation of the environmental impact due to both CHP systems operation strategies, and to both the separate generation systems is performed by means of a model based on emission factors. Results show that all the micro-CHP systems permit a remarkable reduction of annual CO_2 emission on global scale, and at the same time they involve a very marked augmentation of dangerous annual CO on local scale. The micro-CHP systems with microturbines as prime mover allow a reduction of the annual local NO_X emissions, especially in the case in which the microturbines operate according to the novel operation strategy. Results also show that, if the best configurations from the economical point of view are compared, the effects of heat dumping on micro-CHP systems pollutants emission are negligible with respect to the ones obtained when the strategy without heat dumping is considered.

The dynamic simulation of a residential micro-CHP system operating according to the heat dumping and no-dumping full-load operation strategies is presented. In detail, the dynamic simulation of two optimized cases, one for each operation strategy, that present nearly the same operation hours and economic savings is carried out by using the commercial software TRNSYS 17, and the choice of the two configurations is made by considering a compromise between the economic savings and the size of the storage tank. Results, in terms of comparison between the most representing temperatures obtained from the dynamic simulation of the two cases, demonstrate the equivalence between the two configurations, and the effectiveness of the novel operation strategy.

The novel approach effects are also compared to the ones obtained when CHP systems operate according to a classical heat-driven operation strategy with load partialization. The two operation strategies are implemented in a home-made numerical code written in Matlab, and the economic optimization of the prime mover operation is performed by means of the patternsearch algorithm. Economic

results show that the difference between the best CHP system configuration in the case with heat dumping and the one relative to the case with load partialization is minimal, with the latter presenting a slightly higher economic performance. Nevertheless, the economic analysis also shows that, for the considered application, heat dumping could yield higher economic performances than load partialization in on-peak hours, namely when the export price of the electric power is relatively high, in case a fuel cheaper than natural gas is used, for example a gas from gasification. Moreover, the economic results show that heat dumping could yield higher economic performances than load partialization in countries where there is a lower ratio between the natural gas price and the electricity price than the one in Italy. The environmental impact of both operation strategies is evaluated. Results show that both operation strategies permit a remarkable reduction of annual CO_2 emissions on global scale and of the NO_X emissions on local scale. As concerns CO emissions on local scale, results show that the impact of load partialization is much higher, with values that can be up three times the ones relative to conventional systems for separate generation.

In conclusion, the innovative operation strategy, presented in this thesis, may represent, in general, a good alternative choice to traditional operational strategies used in the field of cogeneration. In detail, the possibility offered by this approach, to halve the size of the thermal energy storage tanks, having equal economic savings with respect to a typical full-load operation strategy without heat dumping, makes it very interesting in residential contexts, in which the encumbrance issues can be very pressing and limiting. Moreover, such a strategy allows, in some cases, to significantly reduce certain pollutants emission on local scale, becoming, therefore, more environmental-friendly than the other analyzed strategies. The dynamic simulation has demonstrated the practical feasibility of such approach, for that, remaining issues, which will be object of future works, are relative to the experimental validation of such new presented approach, for the implementation of which an experimental prototype in laboratory scale will be realized.